

Title	駅前広場における微気候と屋外熱的快適性に適応した気候配慮による設計戦略
Author(s)	肖, 静
Citation	
Issue Date	2022-09
Type	Thesis or Dissertation
Text version	ETD
URL	http://hdl.handle.net/10119/18118
Rights	
Description	Supervisor:由井 隆也, 先端科学技術研究科, 博士

Doctoral Dissertation

**Climate-sensitive Design Strategies for Adapting the
Microclimate and Outdoor Thermal Comfort in the
Station Square Area**

XIAO JING

Supervisor: Takaya Yuizono

Graduate School of Advanced Science and Technology
Japan Advanced Institute of Science and Technology
Knowledge Science
September.2022

Abstract

With the challenges of climate change, heatwaves, and air quality problems, design schemes for public spaces are increasingly seeking climate-sensitive design to optimize climate regulation services. Numerical modeling has become a key tool for improving the reliability of urban planning and design decisions. Upgrading and improving the ENVI-met microclimate model has become one of the most popular software for assessing microclimate environment and thermal comfort. The thermal index continues to develop into a more specific assessment tool for thermal environment and mitigation strategies for different climate zones. In Japan, the Transit-Oriented Development (TOD) of urban planning is used to construct and manage cities systematically. In principle, the design and planning of station square areas in urban centers concern residents' living environment and quality of life. How to optimize the design strategies of the station square area to realize more environmental benefits and reduce urban energy consumption has become a major concern for designers within the TOD principle. Therefore, this study proposed the New Synergistic Strategy (NSs) in landscape design and the Urban Space Regulation Strategy (USRs) in urban building morphology to actively guide the rational configuration in the station square for achieving mitigation of microclimate conditions, thermal comfort, and air quality to address the severe challenges posed by the climate environment.

This study simulated the optimal design strategies in three small-scale square spaces (block, courtyard, and canyon) in Komatsu Station, Japan. It aims to obtain better aerodynamic effects, cooling effects, and the deposition of atmospheric particulate pollution. Firstly, the case study assessed the mitigation strategies (climate change, scale, and configuration) of the core area in the station square under extreme winter and summer weather conditions in the Hokuriku region as a holistic thermal environment using the NSs. The relationship between the building morphology and the green space configuration in the three small squares is explored under the USRs to regulate the three effects in a universal configuration for typical summer weather and thermal stress conditions. Secondly, greening indicators (tree configuration ratio, the ratio of number of deciduous and evergreen trees) were proposed in this study to analyze the mitigation and relevance to the thermal environment in two case studies. Finally, ENVI-met simulations validated and compared intervention scenarios with actual measured parameters to obtain more optimal planting patterns and configurations for urban station square areas.

The originality of this study lies in proposing the regulation of the thermal environment and exposure risk reduction in typical Japanese public spaces (Typology of station square orthogonally connected to the main parallel street) by greening indicators optimization strategy can be applied to 50% of the same typology of station squares in central cities within the Hokuriku region. Furthermore, the strategy studies (NSs and USRs) yielded the following results:

In the landscape design strategy of Chapter 4, the three types of landscape layouts are original in analogy to the peripheral, array, and scatter, and proposed co-adaptation responses for very cold and very hot climates. A comparison of the case studies showed that the tree configuration ratio (R_{DT}/R_{GT}) can regulate thermal comfort at night and during the day; the best mitigation performance of the three layout patterns is the array layout planted with trees. The large-scale tree configuration ratio is optimized for thermal comfort and microclimate conditions in winter and summer via scale regulation, alleviating extremely poor weather conditions in the central station square. Based on the results of the Komatsu station case study, it could be used as a reference to solve the problem of the tree type, number configuration, and vegetation structure in the urban center station of the Hokuriku region; and to solve the problem of local winter wind resistance and summer shade in the inner and outer ring spaces of the station.

In Chapter 5, the regulation strategy is innovative by comparing small-scale spaces: block, courtyard, and canyon types and simultaneously using building indicators of aspect ratio (H/W) and greening indicators (the ratio of number of deciduous to evergreen trees) to co-quantify the station square area. The results indicated that in typical hot weather in summer by the USRs, the composite layer structure (T3) is a universal greening pattern that optimizes microclimate, thermal comfort, and atmospheric $PM_{2.5}$ distribution; the cooling effect of the thermal environment depends on the ratio of number of deciduous and evergreen trees (R_g). Moreover, the canyon square downwind with a higher H/W has a more significant $PM_{2.5}$ removal.

These studies provide constructive references and decisions for the engineering analysis of the thermal environment in station squares and optimizing design schemes to provide important landscape design guidelines for developing Japan's TOD model and Sustainable Development Goals (SDGs). With the completion of the Komatsu City Master Urban Plan in 2040 and the Komatsu Hokuriku Shinkansen in 2023, the station square as the central urban renewal area is used as an example environmental simulation area to contribute to future urban construction (including landscape design, street maintenance, infrastructure renewal) to mitigate climate issues (extreme cold and hot, urban heat island effect, heat waves), air pollution issues (station square exhaust emissions of $PM_{2.5}$), with a particular focus on the overall station spatial structure and building morphology characteristics integrated tree types configuration for resilience improvement.

Keywords: Microclimate simulation, Thermal comfort, $PM_{2.5}$, Optimal design, Climate-sensitive design strategies

Acknowledgment

Upon completing this thesis, I am grateful to those who have offered me encouragement and support during my doctoral study.

Firstly, a special thanks to my eternal supervisor, Prof. Yuizono, whose patient guidance and constructive advice have been helpful to me. His kindness and concern have been crucial to my life and studies at JAIST over the past three years, and his efforts have contributed to my current academic achievements. In his daily work, I have felt a scholar and teacher's sense of responsibility and meticulousness, providing a good example for my future as an educational researcher.

Secondly, I am very grateful to my second supervisor Kim Sensei and my advisor Gokon Sensei for minor research, who give me a lot of advice and guidance from the school course's research discussion. I also would like to express my heartfelt gratitude to the school of knowledge science professors for understanding the relevance of the extensive knowledge to practical life and receiving innovative techniques and methods. Additionally, I am very thankful to my examiners- Prof. Saito Sensei, Prof. Yuizono Sensei, Prof. Kim Sensei, Prof. Gokon Sensei, and Prof. Huynh Sensei. I was honored to receive the examiner's guidance and review of my doctoral thesis to be present at the Ph.D. defense.

Then, thanks to my dearest parents for your constant tolerance, understanding, and support. It is a blessing to be your daughter! Thank you to all my family. You have helped me appreciate life's most important part: learning to be satisfied, forgiving, and keeping a progressive heart during this difficult journey.

Then, I also thank all my friends in Yuizono laboratory for their help in my life and study; this is the basis for a happy academic life.

Thank you to all. I hope all the effort will be delivered, and the next journey will follow.

Table of Contents

Abstract.....	i
Acknowledgment	iii
Chapter 1 Introduction	1
1.1 Research Background	1
1.1.1 Climate-sensitive Design	2
1.1.2 The Microclimate and Thermal comfort	3
1.1.3 Developing Trend in Climate-sensitive Design	5
1.1.4 Urban Renewal Plan and Developing Policy in Komatsu City and Station.....	6
1.2 Research Questions	7
1.3 Research Goals.....	7
1.4 Research Contributions	8
1.5 Thesis Structure.....	9
Chapter 2 Literature Review	11
2.1 Research on Microclimate and Thermal Comfort in Urban Square Area	11
2.2 Green and Building Space Adaptation from the Climate-Sensitive Design.....	13
2.3 Intersection of Theories.....	14
Chapter 3 Methodology	18
3.1 Research Methods and Workflow	18
3.1.1 Site Selection and Analysis	18
3.1.2 Measurement Methods	21
3.1.3 CFD-based Simulation Methods	22
3.1.4 Research Workflow	23
3.2 Quantitative and Qualitative Analysis Methods.....	25
3.2.1 Quantitative Methods in Urban Space	25
3.2.2 Qualitative Methods for Thermal Comfort Evaluation	26
Chapter 4 A New Synergistic Strategy (NSs) in Landscape Design	28
4.1 Landscape Design Theories	28
4.2 Greening Parameters and Indicators	28
4.3 Case Study of NSs at the Komatsu Station Square	29
4.3.1 Motivation.....	29
4.3.2 Study Area.....	29
4.3.3 Climatic Contexts.....	30
4.4 Methodologies for NSs	31
4.4.1 On-site Measurement and Investigation.....	32
4.4.2 Simulation Model with ENVI-met.....	35
4.4.3 Thermal Comfort Index-PMV.....	36
4.4.4 Greening Indicators.....	37
4.5 Landscape Design Scenarios on Microclimate and Thermal Comfort Regulation of Station Square	38
4.6 Results.....	41
4.6.1 Model validation	41
4.6.2 Variations in Winter Microclimate Parameters.....	42
4.6.3 Variations in Summer Microclimate Parameters.....	43
4.6.4 Thermal Environment Mitigation by Landscape Designs.....	47
4.6.5 The Optimized Scenarios and Thermal Conditions.....	50

4.6.6 The PMV Thermal Index Map	52
4.7 Discussion.....	53
4.7.1 Landscape Layout Pattern Improvement Effect.....	53
4.7.2 Effect of the Landscape Design Elements and Indictors.....	54
4.7.3 Effects of Seasonal Changes on Climate-adaptive Design.....	54
4.7.4 Regulation of Thermal Comfort at Different Scales	55
4.7.5 Limitations for the ENVI-met Simulation	55
4.8 Conclusions.....	56
Chapter 5 Urban Space Regulation Strategy (USRs).....	59
5.1 Urban Morphology Theories.....	59
5.2 Space Parameters and Indicators.....	61
5.2.1 Influencing Parameters and Indicators of Building Space	61
5.2.1 Influencing Parameters and Indicators of Green space	62
5.3 Case Study of USRs in Station Square Area.....	63
5.4 Motivation.....	63
5.5 Study Area.....	64
5.5.1 Overview of Komatsu City	64
5.5.2 Space Configuration.....	65
5.6 Methodologies for USRs.....	66
5.6.1 On-site Measurement	67
5.6.2 CFD Simulation Modeling-ENVI-met V5	68
5.6.3 Space Indicators	70
5.6.4 Thermal Index-PET	70
5.7 New Space Configurations in ENVI-met Scenarios	71
5.8 Results and Discussion.....	72
5.8.1 ENVI-met Validation of the Base Model	72
5.8.2 Microclimate Condition in Original Scenario.....	74
5.8.3 The Effect of Green Configuration	76
5.8.4 Effect of Building Morphology.....	77
5.8.5 Improvement of Thermal Comfort in Updated Scenarios.....	78
5.8.6 Mitigation in PM _{2.5} Deposition	81
5.9 Conclusions.....	84
Chapter 6 Discussion	87
6.1 Climate-sensitive Design Principles Achieved in NSs and USRs.....	87
6.2 The Challenges of Setting a Comfortable Station Square.....	88
6.3 New Implementations Effective for Station Square.....	89
6.3.1 Effective in NSs-A New Synergistic Strategy.....	90
6.3.2 Effective in USRs-Urban Space Regulation Strategy	91
6.4 How do you manage the gap between simulation and realistic scenarios?	92
6.4.1 Microclimate Model of ENVI-met Update	92
6.4.2 Progress of ENVI-met Software	93
6.5 Contributions to Knowledge Science.....	94
Chapter 7 Conclusion and Future Work.....	97
7.1 Conclusion	97
7.2 Future Work	98
Appendix A	100
Komatsu Station Square Area Developing Planning.....	100
Appendix B	102
Climate and Average Annual Weather Characteristics of Komatsu, Japan	102
Appendix C	104
Site Analysis.....	104

Appendix D	107
Survey on the Same Spatial Structure Pattern of Train Stations in the Hokuriku Region	107
Appendix E	109
Related Landscape (Green) Strategies Effect on Urban Square Microclimate and Thermal Comfort Studies.....	109
References.....	111
Publication	121
Papers Published and Submitted in Journals.....	121
International Conference Proceeding.....	121

List of Figures

Figure 1.1 Place factors in relation to weather and microclimate (Eliasson et al., 2007).	3
Figure 1.2 Description of heat and mass transfer in the urban canyon (Tumini, 2015).	4
Figure 1.3 Urban Heat Island processes at the microscale (Tumini, 2015).	4
Figure 1.4 A framework for a thermal comfort evaluation system (Liang Chen & Ng, 2012).	5
Figure 1.5 Komatsu urban renewal areas for the next 20 years (Source from: https://www.city.komatsu.lg.jp/material/files/group/18/03_keikakusyo_zentaikousou.pdf).	6
Figure 1.6 Landscape design area (From Komatsu City landscape plan) (Source from: https://www.city.komatsu.lg.jp/material/files/group/18/03_keikakusyo_zentaikousou.pdf).	7
Figure 2.1 The different scales of the urban climate effect (Adapted from Oke, 1997).	15
Figure 2.2 Urban microclimate in urban morphological structure, landscape, ground surface, and thermal exchange under anthropogenic activities (Sharifi & Lehmann, 2015).	16
Figure 2.3 This study intersects disciplines (I) with the main research contents (II) (Source from: https://www.theseus-fe.com/application-areas/automotive/passenger-comfort).	17
Figure 3.1 Japan climate zoon disruption from Köppen-Geiger climate classification (Rubel & Kottek, 2010).	19
Figure 3.2 Wind speed (WS) and air temperature (T_a) changes in Komatsu for August and February 2021 (Japan Meteorological Agency, 2007).	19
Figure 3.3 Changes in temperature and $PM_{2.5}$ from 2015 to 2019.	21
Figure 3.4 Typology of station squares' spatial structure (Adapted from Gehan et al., 2000).	21
Figure 3.5 Portable Weather & Environment meter (a) and $PM_{2.5}$ tester (b) were used for measuring the on-site areas.	22
Figure 3.6 ENVI-met simulation in five specific steps.	24
Figure 3.7 Thermal index calculation involves the setting of personal human parameters.	25
Figure 3.8 Universal outdoor thermal comfort evaluation of thermal index referencing standards (Asghari et al., 2019).	27
Figure 4.1 (I) Komatsu Station square location; (II) Google Earth map of study area divided to area A and area B scale, and the spaces include a square courtyard (1), a hotel (2), and the station canopy (3).	30
Figure 4.2 (I) The monthly maximum and minimum temperature (T_a); and (II) the daily maximum and minimum temperature (T_a), precipitation, and wind speed (WS) for Komatsu city from 2018 through 2021 recorded by JMA's weather station.	31
Figure 4.3 The research methods and workflow of a climate-adaptive landscape design in this study for mitigation of thermal conditions during extreme summer and winter days.	32
Figure 4.4 Komatsu Station Square (50m × 50m, 80m × 80m) configuration of building area, green area, hard pavement, and canopy structure.	34
Figure 4.5 Distribution of urban trees and utilization condition of Komatsu Station Square on winter and summer days.	34
Figure 4.6 Distribution of tree configurations for the original scenario L1-1 in ENVI-met with the receptor.	39
Figure 4.7 Validation results of coefficient of determination (R^2) and the root mean squared error (RMSE) by forcing simulated and measured air temperature (T_a) in a grid sensitivity analysis on February 27, 2021 (24 h).	41
Figure 4.8 Variations of winter simulation microclimate parameters (T_a , WS, RH, and T_{mrt}) for 10 scenarios compared to on-site measurements.	42
Figure 4.9 Variations of summer simulation microclimate parameters (T_a , WS, RH, and T_{mrt}) for 10 scenarios compared to on-site measurements.	47
Figure 4.10 PMV distribution (at 1.8 m height) of winter simulated scenarios at configuration conditions (a, b, c, and d).	48
Figure 4.11 PMV distribution (at 1.8 m height) of summer simulated scenarios at configuration conditions (a, b, c, and d).	49

Figure 4.12 PMV results of 24 h, and distribution of PMV error results (L2-2b and L2-2c scenarios against L1-1 scenario) at the co-optimum period (at 1.8 m height) in winter and summer.	50
Figure 4.13 Simulated T_a maps of winter (W) and summer (S) in the original L1-1 scenario and co-optimized scenarios (L2-2b and L2-2c) at 14:00 (at 1.8 m height).	51
Figure 4.14 Simulated T_{mrt} maps of winter (W) and summer (S) in the original L1-1 scenario and co-optimized scenarios (L2-2b and L2-2c) at 14:00 (at 1.8 m height).	52
Figure 4.15. Winter and summer PMV thermal index maps at 14:00 (at 1.8 m height) for landscape configuration conditions (a, b, c, and d).	58
Figure 5.1 Conceptual model of perceived environment.	60
Figure 5.2 Urban form combination system (Zhang et al., 2019).	60
Figure 5.3 The relationship between building types, typo-morphology, and urban form.	61
Figure 5.4 Major building parameters and indicators are influencing the outdoor thermal environment.	62
Figure 5.5 Major greening parameters and indicators influencing the outdoor thermal environment. ...	63
Figure 5.6 Locations of the major station square areas in Komatsu (QA: Doihara Bonnet Space; QB: Komatsu Station West Square, QC: Komatsu Station East Square).	64
Figure 5.7 Mean monthly precipitation and air temperature (T_a) and mean monthly maximum $PM_{2.5}$ in Komatsu city in 2017 to 2020.	65
Figure 5.8 Station square area with green space reconfiguration following the optimal design for microclimate, thermal comfort, and $PM_{2.5}$ mitigating effect.	67
Figure 5.9 Meteorological and air pollution monitoring points distributed as M1, M2, and M3 in QA, QB, and QC squares, respectively.	68
Figure 5.10 Updated ENVI-met models of typical tree species (TS) compositions and new green space configurations.	72
Figure 5.11 Fitting regressions between macro-monitored and on-site measured air temperatures against simulated air temperatures of ENVI-met at different sensitivity grids: $2 \times 2 \text{ m}^2$ (a), $4 \times 4 \text{ m}^2$ (b), and $5 \times 5 \text{ m}^2$ (c).	73
Figure 5.12 Distribution of microclimatic parameters (T_a , RH, WS, and T_{mrt}) in three small squares under the T0 scenario at 2.5 m height on August 27, 2021, 14:00 pm.	74
Figure 5.13 Microclimate condition variation under different green space configurations on August 27, 29, and 31, 2021.	76
Figure 5.14 PET distribution at 2.5 m height from 12:00 pm to 19:00 pm on August 27, 29, and 31, 2021, under updated building morphology integrated with green space configurations (a). PET distribution during the prime hottest hours (12:00 pm to 14:00 pm) (b).	79
Figure 5.15 PET distribution at 2.5 m height at 14:00 pm on August 27, 29, and 31, 2021, under updated integrated building morphology and green space configuration.	80
Figure 5.16 $PM_{2.5}$ distribution with green space configurations compared with on-site measurements in a homogeneous building context on August 27, 29, and 31, 2021.	82
Figure 5.17 $PM_{2.5}$ distribution 2.5 m height in a green configuration space under different wind directions ($150 \text{ m} \times 150 \text{ m}$ grid) in a heterogeneous building context on August 27, 29, and 31, 2021 (at 16:00 pm).	85
Figure 6.1 Transport-oriented development (TOD) of functional spatial cycles (Source from: https://www.nikken.co.jp/en/expertise/civil_engineering/planning_and_design_of_railway). ...	89
Figure 6.2 ENVI-met's tree models: (a) simple plants, (b) 3D plants, and (c) the model using the Lindenmayer-System in an ENVI-met V5 (Liu et al., 2021).	93
Figure 6.3 An integrated framework for organizational learning and knowledge creation (Brix, 2017).	95
Figure 6.4 The intersection of new strategies and urban climate knowledge.	96

List of Tables

Table 4.1 T_a , RH, WS, and T_g measured at Komatsu Station square on February 27 and August 4, 2021.	33
Table 4.2 Vegetation configuration around the measurement area.	35
Table 4.3 Fundamental parameter settings for the ENVI-met model simulation.	36
Table 4.4 Basic conditions of the new landscape design scenarios.	40
Table 4.5 Validation accuracy performance of air temperature (T_a) in ENVI-met model simulations for running four times with statistical indexes of the coefficient of determination (R^2) and the root mean squared error (RMSE).	41
Table 4.6 Maximum, minimum, and mean values of the winter simulation microclimate parameters (T_a , WS, RH, and T_{mrt}) relative to on-site measurements.	45
Table 4.7 Maximum, minimum, and mean values of the summer simulation microclimate parameters (T_a , WS, RH, and T_{mrt}) relative to on-site measurements.	46
Table 5.1 Vegetation configuration modes of different types of squares in station square area.	66
Table 5.2 Basic model initial settings in ENVI-met V5.	69
Table 5.3 Meteorological, soil, and cloud conditions settings in the simulation dates.	69
Table 5.4 Sensitivity grid analysis of the base model.	74
Table 5.5 Simulation results of microclimate parameters under different green space configurations on August 27 (a), 29 (b), and 31 (c), 2021.	75
Table 5.6 Variations in microclimatic conditions in updated scenarios under different receptors area on August 27, 29, and 31, 2021.	77
Table 5.7 Mean PET distribution at 2.5 m height from 12:00 pm to 19:00 pm on August 27, 29, and 31, 2021, under different green space configurations.	79
Table 5.8 Mean $PM_{2.5}$ distribution at 2.5 m height with different green configurations in a homogeneous building context on August 27, 29, and 31, 2021.	86

Chapter 1 Introduction

1.1 Research Background

Station squares play an exemplary role in the city's image of the urban landscape as a green space in urban public space. It provides an important cooling service to mitigate the urban heat island effect and regulates atmospheric pollution. The regulating effects of building and green spaces on microclimate, thermal comfort, and air quality have not yet been fully clarified. Environmental problems still have an important impact on urban thermal environments and human health.

1) Global climate change and urban climate problems significantly impact urban development and construction.

Urban sprawl, population concentration, and traffic pressures reduce urban green space and increase anthropogenic heat, combined with extreme weather events leading to a significant increase in discomfort thermal environment. According to the World Meteorological Organization survey, the 2015-2019 global average temperature is expected to be the warmest of any comparable period (Zhongming et al., 2019). CO₂ emissions reached 17.9% in 2016 from Japanese transportation. Japan Rail Transit (JR) accounted for 45.9% of passenger transportation. Traffic emissions are a major reason for the impact on the surrounding urban thermal environment and the health of urban inhabitants in their daily lives ("Transport and Environment in Japan," 2019). In the late 20th century, the Station Renaissance and Transit-oriented Development (TOD) were proposed to reconstruct the station space by greening systems of "Garden Roof" and "Green Wall" to set a high land-use model in Japanese railway stations (Kido, 2005). The TOD model was used for designing public places and transport in Japan. The country has been engaged in urban landscape planning centered on railway lines and stations since 1872 (Shinichi, 2021). Crucially, applying TOD policies ensures a compact urban form, which helps mitigate and adapt to climate change (Kidokoro, 2020). Accordingly, the high-quality square depends on the user's thermal perception and healthy environment, influenced by microclimatic conditions (air temperature, wind, related humidity, mean radiation temperature) and air pollution levels (Zeka, 2011).

Moreover, the combined effects of urbanization and global climate warming can deteriorate urban air quality and augment HUI intensity, amplifying the risk of exposing citizens to discomfort and health-related problems and increasing the energy demand for cooling (Moonen et al., 2012). Excessive greenhouse gas emissions from social activities in industries, transportation, businesses, and households are a major cause of global warming. Notably, traffic exhaust and air conditioning emissions significantly affect the urban thermal stress and the everyday health of urban residents (Transport and Environment in Japan, 2019). According to the Global Burden of Disease Study, at least 60,000 people die prematurely from air pollution in Japan each year (Cohen et al., 2017). Furthermore, PM_{2.5} is a crucial indicator of air pollution and the atmosphere's visibility derived from motor vehicle emissions (Japan Automobile Manufacturers Association (JAMA), 2011; Zhang et al., 2015). PM_{2.5} negatively affects human health. As such, an increase in PM_{2.5} of 10 µg/m³ increases mortality risk by 0.52% (Seposo et al., 2018). Therefore, reducing PM_{2.5} concentrations to improve air quality in urban areas has prompted extensive studies on the associations between the urban environment,

climate, and air pollution (Schaefer et al., 2021). In this light, urban station squares have gained much attention to the rise in urban population and traffic in recent decades (Xiao & Yuizono, 2022).

2) Outdoor public activities increased in cities, but space services lack climate resilience.

Through the early 20th century, trains became so thoroughly enmeshed with urban living in Japan that the major train stations. The train station's social and economic activities propelled became a metaphor for the modernizing city. They were closely woven into what it meant to live in the city. The station square has become Japan's most urbanized and densely populated activity place. Station squares have become an important link connecting the city center in megacities. More than 25 billion passengers were transported by rail in Japan in 2019 (Gorka, 2021). Densely populated station squares are particularly important outdoor activity areas that require more mitigation of thermal conditions during extreme weather. The traditional station square design focuses on the transport system and lacks the regulation of landscape services (e.g., climate change, scale, and element configuration).

3) Interdisciplinary research on urban climate issues requires complex analysis.

Very cold and hot urban climates significantly increase risks to their health (Koppe et al., 2004), especially in developed cities where the elderly are over-distributed. Importantly, the climate created by urban landscapes significantly affects human comfort, air quality, and energy consumption (Knaus & Haase, 2020). Therefore, improvement strategies attempt to contemplate mutually adaptive human and environmental engineering approaches from the perspectives of biometeorology, thermodynamics, aerodynamics, climatology, and planning design.

1.1.1 Climate-sensitive Design

The Climate- sensitive design must adapt to the climate, not against it, reducing the need to use heating and cooling systems to keep humans thermally comfortable. Designers must modify their designs according to the local climate in which climate zones. Climate-sensitive design can reduce the energy used for heating and cooling to almost zero. Moreover, designers must design outdoor public spaces that remain efficient in hotter or harsher climates as temperatures rise.

The climate-sensitive design combines climatology and urban design, also known as bioclimatic urban design or climate responsive design. The relationship between climate, the building environment, and people is a complicated but important concept for climate-sensitive design strategies. The interaction of the three can influence how, how long, where, and when people spend time in the outdoor public realm (Sanborn, 2017).

The main goal of the climate-sensitive urban design approach is to mitigate the thermal comfort of urban populations (i.e., residents, travelers, pedestrians). Urban comfort studies lag behind indoor thermal comfort studies because of the complexity of the outdoor thermal radiation balance, wind field variations, and the uncertainty of climate zones, weather, and design patterns (Tan et al., 2016). Outdoor comfort studies require complex analyses that consider numerous influencing factors.

1.1.2 The Microclimate and Thermal comfort

The relationship between thermal comfort and microclimate is strongly correlated. The microclimate conditions under different weather conditions determine the pedestrian's thermal perception and experiential feedback to the ambient environment and response to the rationality of the design decisions for the place (Figure 1.1).

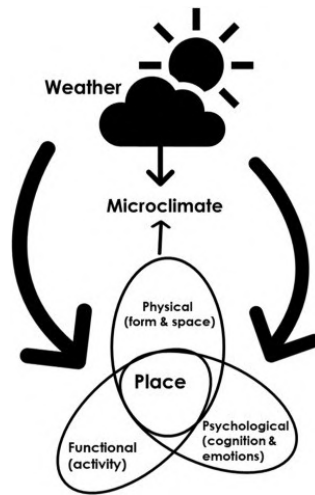


Figure 1.1 Place factors in relation to weather and microclimate (Eliasson et al., 2007).

How can we achieve energy balance for the human body in the urban context? Human thermal comfort originates from psychological and physiological responses, and different climatic characteristics, specific locations, and times affect the thermal environment created by heat transfer mechanisms (Figure 1.2). The fundamental parameter of the urban thermal environment is accomplished by transferring heat between the human body and the urban environment via convection, radiation, evaporation, and conduction (Fanger, 1970)

The urban thermal environment is studied in important places where people live and interact in everyday life (e.g., streets, squares, parks), mainly concerning urban design. The external urban spatial system consists of traffic, buildings, landscaping, and human activities. The external spaces are divided into two main types: (1) the sites within the neighborhood between the buildings and the buildings, and (2) the external streets and squares of the neighborhood parks. The design of streets and squares was discussed by academics as early as the 16th century (Palladio, 2002), and urban spaces were divided into streets and squares (Moughtin, 2007). Krier & Rowe (1979) has further classified urban streets and squares based on morphological characteristics. The heat island effect in micro-scale spaces can also be referred to as the local heat island effect, and we mean areas restricted to the community scale by micro-scale (buildings, streets, squares, gardens, etc.). The climate changes studied are those that occur on a small scale. Due to the atmosphere's interaction with urban elements, changes occur within several meters (Figure 1.3).

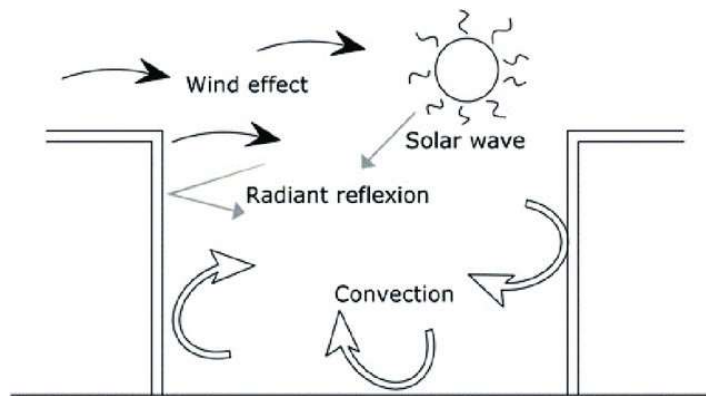


Figure 1.2 Description of heat and mass transfer in the urban canyon (Tumini, 2015).

MICROSCALE

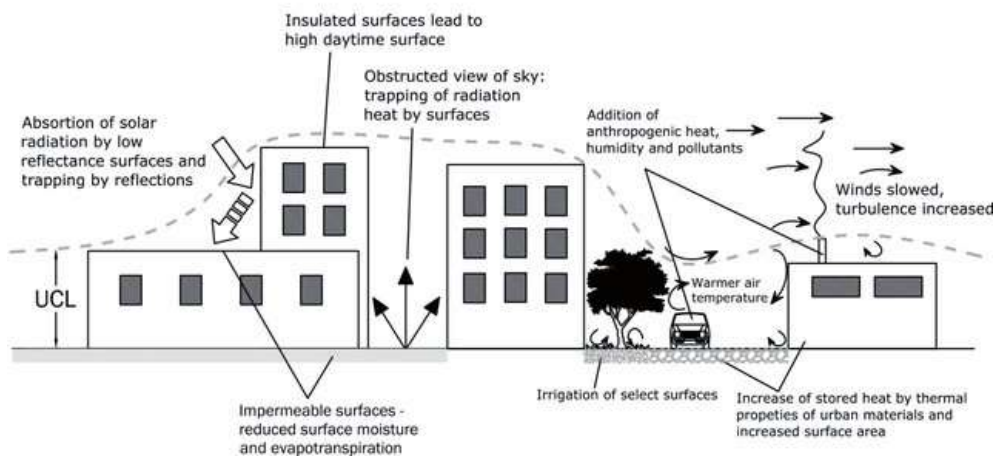


Figure 1.3 Urban Heat Island processes at the microscale (Tumini, 2015).

According to L. J. Battan (1973), microclimate is mainly from the ground to a dozen meters climate in 100m height. Page (1976) thinks microclimate refers to the part of the ground boundary layer whose temperature and humidity are influenced via the ground vegetation, soil, and terrain. In other words, it can be identified as a small-scale climate pattern, called a "microclimate," in which each location within a given region experiences deviations in climate over a few kilometers (Santamouris & Asimakopoulos, 1996). The urban microclimate is an important bridge between urban climatology and urban design. It not only provides architects with the expertise to explore the impact of different scales of urban building structures on microclimatic conditions but also to analyze the integration between microclimate and urban landscape elements (Erell et al., 2012).

The present study involves thermophysiology and human heat balance. Thermal comfort is the minimum ratio of neural signals from these receptors based on firing heat receptors in the skin and hypothalamus. Alternatively, thermal comfort is defined as a state of thermal comfort when the heat flow in the body is balanced, and the skin temperature and sweating rate are within the comfort range, which depends only on the metabolism (Höppe, 2002). The climate in different geographical regions affects thermal comfort and the

surrounding inhabitants' thermal behavior. Improving outdoor thermal comfort has attracted widespread attention to motivate pedestrians for outdoor activities and climate adaptation (Salata et al., 2017; Ouyang et al., 2020; Ghaffarianhoseini et al., 2015; Chatzidimitriou & Yannas, 2015). The external influences on the comfort level of the outdoor environment result from the microclimate environment. Its impact parameters include air temperature, relative humidity, wind speed, and mean radiation temperature (Liang Chen & Ng, 2012).

The framework of the thermal comfort evaluation system involves four major dimensions of impact parameters: physical, physiological, psychological, and social/behavioral (Figure 1.4). The four impact parameters corresponding to the different research approaches are divided into three categories: 1) measurement and modeling, 2) survey and interview, and 3) observation, interview, and prediction. Thermal comfort evaluation concerns microclimatic conditions and human perception in space and time. Static and objective aspects (i.e., physical and physiological characteristics) can be effectively measured and modeled to provide “climate knowledge of sensitivity.” In contrast, dynamic and subjective aspects (i.e., psychological and social/behavioral characteristics) require comprehensive field interviews and observations to provide “human knowledge ” (Liang Chen & Ng, 2012b). The subject of this research area relates to physical and physiological characteristics. It focuses on field measurements and modeling approaches for effective thermal comfort evaluation of site contexts.

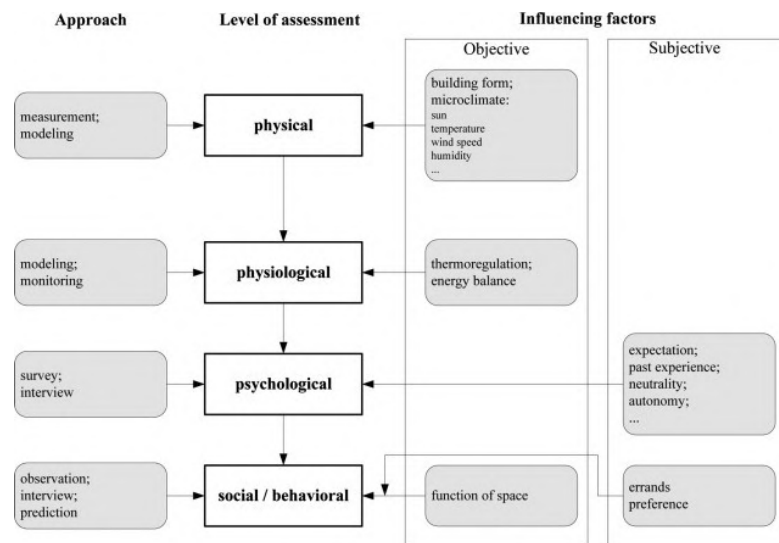


Figure 1.4 A framework for a thermal comfort evaluation system (Liang Chen & Ng, 2012).

1.1.3 Developing Trend in Climate-sensitive Design

With the maturation of outdoor thermal comfort and microclimate research at different spatial scales, the analysis of the mitigation effects of influencing parameters on the environment from simplicity is gradually carried out in a complex qualitative and quantitative manner. Gradually in these studies, a refined comparison of influencing parameters such as vegetation type, spatial combination in space, landscape layout, etc. Tree height, canopy layer, leaf area density, tree species, and other vegetation elements are compared to study the moderating effect on the thermal environment. The building space also compares the building floor height,

building aspect ratio, sky view factor, building volume ratio, and other building influence parameters. The optimization of the environment is assessed from the green or built environment alone to the intersection of building and green space. Climate-sensitive design is integrated into the microclimate and thermal comfort fields and the deposition effects of urban pollutants. The general trend is towards a gradual broadening of the research field and a more detailed analysis of the impact factors; the research methods are also diversifying beyond the traditional field measurements and wind tunnel experiments and remote sensing for data collection to an efficient method combining field measurements with computer numerical simulations.

1.1.4 Urban Renewal Plan and Developing Policy in Komatsu City and Station

With the emergence of climate change, environmental pollution, and socio-economic development issues, the construction of Sustainable Development Goals (SDGs), TOD, and climate-resilient cities are becoming mainstream urban area planning and renewal in the future. The SDGs and TOD focus on synergistic development in energy, climate, urbanization, transport, and the environment.

In 2019, Komatsu City declared an urban master plan framework to complete the urbanization and synergistic regional development of Komatsu City in 2040. The short-term goal for 2025 is to complete the opening of the Central Hokuriku Shinkansen at Komatsu Station to revitalize the city center and promote a convenient and comfortable urban environment. The urban planning area is divided into 10 districts. Moreover, the Komatsu Station area has been developed as a comprehensive urban infrastructure in the city's future construction plan located in the center of the urban planning area. This area is the central hub of an urban renewal plan that promotes learning, manufacturing, and traditional culture and creates a vibrant historic urban landscape (Figure 1.5).

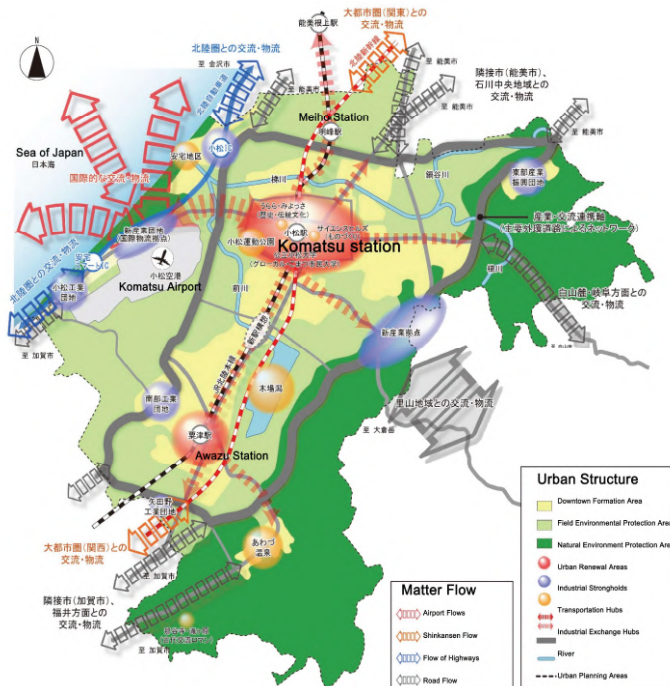


Figure 1.5 Komatsu urban renewal areas for the next 20 years (Source from: https://www.city.komatsu.lg.jp/material/files/group/18/03_keikakusyo_zentaikousou.pdf).

The implementation policy mainly involved: land application, urban development, transportation facilities development, parks and green areas, rivers and sewage treatment, landscape design, and urban disaster prevention. Among them, Komatsu Station is located in the inner part of the urban landscape renewal area with exemplary public places (Figure 1.6).

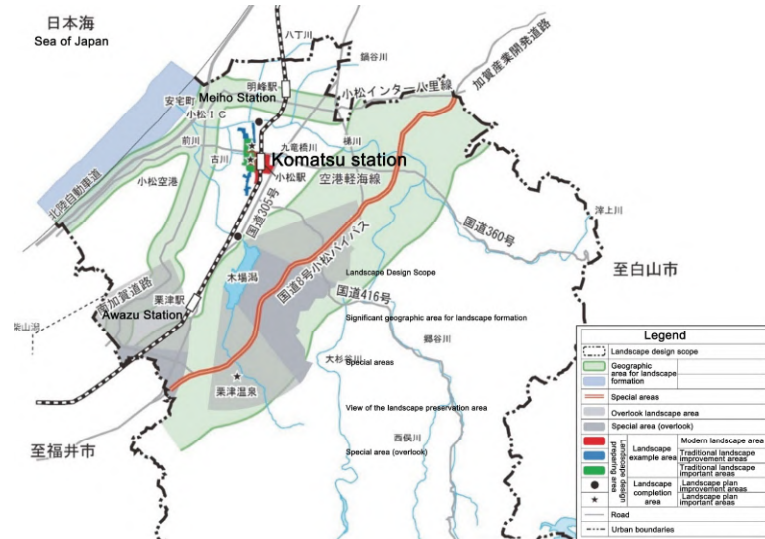


Figure 1.6 Landscape design area (From Komatsu City landscape plan) (Source from: https://www.city.komatsu.lg.jp/material/files/group/18/03_keikakusyo_zentaikousou.pdf).

1.2 Research Questions

Based on the previous sections on the important environmental benefits of climate-sensitive design in urban design for creating comfortable spaces, they positively guide people to outdoor activities, reducing energy consumption and pollution in cities. This research has proposed how can climate-sensitive design strategies be integrated into local Japanese station squares in a subtropical climate zone context. The main research question (MRQ) arises: how can climate-sensitive design strategies be integrated into local Japanese station square spaces in a subtropical climate zone context to achieve the best design contribution to environmental and social efficiency in a model of TOD urban planning?

To answer the climate-sensitive design strategies, we have divided them into two questions:

RQ1: How do designers integrate climate characteristics, scales, and seasonal changes through a landscape design approach to achieve a synergistic effect for optimizing and regulating station squares?

RQ2: How to achieve a strategy for the regulation of station squares in microclimatic conditions, thermal comfort, and air quality for multiple types of spaces, considering both the building and the green environment configuration?

1.3 Research Goals

This study investigates the mitigation of thermal stress and air pollution strategies that are more in line with the climatic characteristics, urban morphological features, and landscape configuration of the station square area in the Hokuriku Region, Japan. The main goal is to mitigate urban climate issues such as the urban heat

island effect, extreme weather, and air pollution to enhance the thermal comfort experience and sustainable design for outdoor station square areas.

Goal 1: This study proposes greening indicators (tree configuration ratio and the ratio of the number of deciduous and evergreen trees) for outdoor thermal comfort and microclimate regulation from a landscape design perspective. It implements a new synergistic effect in the landscape configuration for the multi-dimensional consideration of scale, seasonal change, and climatic characteristics.

Goal 2: In the complex texture of urban space, this study analyses the correlation and regulation of building morphology and green configuration that affect thermal comfort, microclimate, and air pollution concentrations at the multidisciplinary intersection of landscape design, urban morphology, and biometeorology.

1.4 Research Contributions

From the perspective of landscape design and urban morphology, this study investigates the joint influence of vegetation configuration on thermal comfort, microclimate, and air quality in station square areas in different morphological contexts. It derives a design strategy for the regulation of green and building environments.

Previous studies on the mitigation strategies of urban square typologies for microclimate and thermal comfort have mainly investigated public squares (Knez & Thorsson, 2006; Moser et al., 2017), urban squares (Rahman et al., 2017a; Stocco et al., 2021), intersecting multiple urban public spaces (squares, gardens, courtyards, streets, etc.) (I. Eliasson et al., 2007a). There is a lack of specificity in exploring the typology of squares and square space structure patterns. Compared to studies on the humid subtropical climate context of Japan (Knez & Thorsson, 2006; Thorsson et al., 2007), these studies only address the relevance of outdoor activities to the thermal environment and have limitations for proposing specific mitigation implementation.

Urban trees are a key urban design element in the mitigation of the thermal environment of urban squares by greening implementation approaches to optimize the thermal comfort of the environment (Moser et al., 2017; Gaspari et al., 2018; Rahman et al., 2018a; Zölch et al., 2019). These urban square studies mainly involve controlling factors such as layout, number of trees, structure, and greening indicators. While specific analyses of urban tree types on urban thermal mitigation performance have mainly involved deciduous and coniferous trees (Gaspari et al., 2018; Zölch et al., 2019), the optimal performance of evergreen trees in microclimate and thermal environments has not been analyzed in the context of humid subtropical climates.

With the spread of computers and thermal indexes (Oded Potchter et al., 2018), research methods have moved from traditional field measurements and questionnaires to a combination of numerical simulations and field measurements as the dominant research method, which can save time and construction costs in practice construction (Battista et al., 2019; Stocco et al., 2021). Numerical modeling studies provide a preliminary and reference opinion for assessing design options in pre-construction urban projects. Developing the microclimate model ENVI-met is intersectional and verifiable for environmental assessments such as urban climate, air pollution, and thermal comfort. For urban planning guided by urban Transit-oriented development in some Asian countries, it can efficiently validate the landscape design renewal pattern to solve urban heat

island and air pollution problems caused by peripheral exhaust emissions, which can promote the sustainability and resilience of the whole city (T. Kidokoro, 2019; Shinichi, 2021). The study of environmental mitigation strategies for urban station squares failed to fit well with the local urban master plan design goals in Appendix C, creating a better and more comfortable environment.

Accordingly, the main contribution of this study is to investigate the typology of station square orthogonally connected to the main parallel street (Gehan et al., 2000) in the Hokuriku region and to propose effective implementations for integrated urban mitigation. In the landscape design strategy, the tree configuration ratios in the greening indicators mainly mitigate the extreme cold and hot climatic conditions and simultaneously realize the cooling effect on the overall environment. The thermal index improvement performance along with adjustment of the evergreen and deciduous tree configuration ratios. The optimization mechanism of the landscape design strategy (landscape layout, vegetation structure, tree configuration ratio, seasonal variation, scale variation) achieved a synergistic optimization approach to the overall design elements and indicators. The fit of site measurements to the simulation further validates the performance of ENVI-met on the optimal performance of evergreen tree types in the urban station environment. The prominent contribution to the urban energy balance is blocking heat stress and evaporative cooling. Compared to other studies mitigating thermal comfort performance during the day (Zölch et al., 2019), the integrated large-scale evergreen to deciduous tree configuration ratio in an array layout resulted in a daytime and nighttime mitigation of the thermal environment in the winter and summer seasons, extending the duration of resilience to climate change.

The regulation (microclimate, thermal comfort, air quality) strategy expanded on more specific comparisons of building morphologies types and the effects of vegetation configuration than other square thermal comfort studies (Zölch et al., 2019; Gaspari et al., 2018). The greening indicator - the ratio of number of deciduous trees to evergreen trees is the same that has a minor effect on the improvement of the thermal environment. The analogy with the small spatial environment of the station square contributes to the improvement and processing of the relationship between the thermal and atmospheric environment in the overall station space of fine space (focusing on the green space configuration pattern, wind direction, tree type, tree canopy size, and tree height). The universal green space configuration pattern in planting Pagoda tree and grass help to address the impact of urban planning on microclimate environmental variables, contributing to reducing urban heat stress, energy consumption, and air pollution. Compared to other thermal comfort studies (Gaspari et al., 2018; Rui et al., 2019), the mitigation of pollution gas emissions from traffic vehicles in station square concurrently considered the harmonious relationship between microclimate and thermal environment.

1.5 Thesis Structure

This thesis consists of 7 chapters, as shown below:

Chapter 1 Introduction

This section deals with the background of the thesis and some of the main issues concerning station square spaces and the development trends in research on climate-sensitive design strategies. On this basis, the research directions are presented concerning the main subject areas and the definition of basic terms. Finally, we present the main questions, the research objectives, and this study's research contributions.

Chapter 2 Literature Review

This section reviews and summarizes the literature on climate-sensitive design strategies for urban squares in various climate zones. Furthermore, this study sorts out the intersection of the theoretical disciplines of this study and the scope of the research, especially for the building and landscape environment part of the urban design context.

Chapter 3 Methodology

This part focuses on the measurement methods adopted for this study, the urban microclimate simulation and modeling techniques, and the quantitative and qualitative analysis methods for the environmental impact factors of station squares, particularly the greening and building morphology indicators.

Chapter 4 A New Synergistic Strategy (NSs) in Landscape Design

This chapter introduces a synergistic and optimal approach to landscape design in enhancing the station square area design, realizing the typical design mechanisms for landscape design to comply with the principles of climate-sensitive design strategies and regulating the microclimatic and thermal environment of the station square. It also verifies the potential impact of greenery indicators, site scale, and seasonal changes on stations.

Chapter 5 Urban Space Regulation Strategy (USRs)

This chapter derives climate-sensitive design strategies that consider urban climate change while integrating the deposition effects of urban air pollution into urban design following a sustainable design strategy. In the case study evaluation, the microclimate, thermal environment, and atmospheric pollution in the station square area are regulated by the green space and building configuration.

Chapter 6 Discussion

This chapter examines the environmental contributions of optimal design strategic solutions to station squares (from Chapter 4 and Chapter 5), particularly how they can be realized in response to local problems of extreme climate, meteorological change, and air pollution. The next part is followed by a discussion of the specific contributions of this research to knowledge science, especially concerning the ecological, urban living, and residential well-being of environmental design strategies. The limitations describe the technical issues in urban microclimate simulation and the shortcomings of the research involvement. This section also illustrated the challenges and effectiveness of setting a more comfortable station square.

Chapter 7 Conclusion and Future Work

Finally, the study concludes with a review of the performance of scenario optimization design (NSs and USRs) via numerical simulations of the general environment of urban station squares, particularly for vegetation configurations in the thermal environment, and an outlook on future research directions.

Chapter 2 Literature Review

2.1 Research on Microclimate and Thermal Comfort in Urban Square Area

The urban landscape design has seen unprecedented development with high-density urban development and intensive construction. However, heat waves, the heat island effect, and extreme weather remain prevalent. These climate problems lead to discomfort and associated health risks for citizens (Moonen et al., 2012). Especially in developed cities where the elderly are over-distributed, very cold and very hot urban climates significantly increase their health risk (Koppe et al., 2004). The climate created by urban landscapes significantly affects human comfort, air quality, and energy consumption (Eliasson, 2000). Therefore, improvement strategies attempt to contemplate mutually adaptive human and environmental engineering approaches from the biometeorology and planning design perspectives.

A station square is a public place characterized by pedestrians and various vehicular traffic, in which surrounding landscape elements interact with the microclimate and thermal environment (Gómez et al., 2004). The TOD model was used for public places and transport in Japan. It compact urban form for mitigation of adaptation to climate change by applying TOD policies (Kidokoro, 2019).

In this context, the leading implementation tool for improving the urban climate to achieve sustainability is derived from vegetation (Kleerekoper et al., 2012; Erell et al., 2012b). Vegetation is a critical landscape element that actively cools the environment by evaporation and transpiration, and its shelter surfaces absorb shortwave radiation to provide shade (Kleerekoper et al., 2012; Dimoudi & Nikolopoulou, 2003). According to Rahman et al.'s study of the open green rectangular square compared to the circular paved square, urban trees planted in green squares are significantly cooler during the day (Rahman et al., 2017b). Vegetation's transpiration can also effectively enhance the microclimate (Rahman et al., 2017; Lindén et al., 2016; Rahman et al., 2018a; Gromke et al., 2015). Simultaneously, the selection of tree species is significant for the thermal environment (Rahman et al., 2018a; Moser et al., 2016). Zheng et al. found air temperature and thermal comfort at 1.5 m, trees > lawn > shrubs (Zheng et al., 2016). Coniferous trees are more effective than deciduous trees in reducing the predicted mean vote (PMV) by 0.5 in spring (Perini et al., 2018; El-Bardisy et al., 2016).

In addition, optimizing the landscape layout patterns positively impacts outdoor thermal comfort (Abdi et al., 2020a; Lin et al., 2008; Hong & Lin, 2015; Zhang et al., 2018; Zölch et al., 2019). Abdi et al. (2020a) verified that a rectangular planting of evergreen trees in the outer row and deciduous trees in the inner row perpendicular to the prevailing wind direction was the most effective method to improve outdoor thermal comfort. Lin et al. Hong & Lin (2015) showed that tree configurations around buildings existed in an optimal pattern with the lower standard effective temperature (SET) distribution. Zhang et al. (2018) found that evergreen tree species effectively reduced wind speed and blocked direct sunlight in winter. Consequently, many previous studies focused on the effect of vegetation on thermal comfort in public spaces, especially the role of trees on summer thermal comfort (Gromke et al., 2015; Zölch et al., 2019; Oliveira et al., 2011b; Srivanit & Hokao, 2013; Srivanit & Hokao, 2013; Salata et al., 2017; Rui et al., 2018). Furthermore, some studies have been focused on studying vegetation structure, leaf area index (LAI), and leaf area density (LAD) in landscape spaces (Morakinyo & Lam, 2016a; Rui et al., 2019). The greening indicator is beneficial to study

the pattern and microclimate of landscape space. Research has proved that urban vegetation is significant in mitigating the heat island effect and human health, especially the urban tree configuration relationship (Salata et al., 2017; Aboelata & Sodoudi, 2019; Ng et al., 2012; Shahidan et al., 2012; Zhang et al., 2017a; Ouyang et al., 2020b).

The regional climate affects thermal perception and thermal behavior. Improving outdoor thermal comfort has attracted widespread attention to motivate pedestrians to engage in outdoor activities and climate adaptation (Salata et al., 2017; Ouyang et al., 2020b; Ghaffarianhoseini et al., 2015b; Marçal et al., 2019; Nikolopoulou & Lykoudis, 2007b). The mainly external influences on thermal comfort result from the landscape microclimate parameter, which includes air temperature (T_a), relative humidity (RH), wind speed (WS), and mean radiation temperature (T_{mrt}) (Oliveira et al., 2011b). Previous studies have explored the parameters, evaluation indexes, and simulation models that influence outdoor thermal comfort in urban squares (Marçal et al., 2019; Nikolopoulou & Lykoudis, 2007b; Eliasson et al., 2007). Research on landscape space factors regulating thermal comfort in squares mainly involves urban trees, vegetation, landscape design elements, and urban green infrastructure (Gaspari et al., 2018; Robitu et al., 2006b; Kariminia & Ahmad, 2013). Zölch et al. (2019) used the ENVI-met microclimate simulation model to verify that the quantity and location of trees and the grass area configuration are important indicators characterizing thermal comfort. Moreover, they argued that the thermal comfort of public squares in the summer depends on the landscape design. Huang & Peng (2020a) proposed that landscape space enhances squares' winter thermal comfort. Some studies also found that T_a and T_{mrt} are essential climatic parameters influencing outdoor thermal comfort in winter (W. Liu et al., 2016).

The thermal comfort evaluation index is a crucial biometeorological index describing the level of outdoor and indoor thermal comfort impact. It primarily relates local microclimatic conditions to human thermal sensations. The indexes that have been used in the urban square are dominated by the physiological equivalent temperature (PET) (Gaspari et al., 2018) and PMV (Chatzidimitriou & Yannas, 2015). However, to the best of our knowledge, relatively few studies have used indexes such as wet bulb globe temperature (WBGT) (Gómez et al., 2004) and universal thermal climate index (UTCI) (Battista et al., 2019), SET*, etc. Among these indexes, PMV, PET, and UTCI are more suitable than others for the evaluation of outdoor thermal comfort in hot and cold conditions in humid subtropical climate zones. However, WBGT and SET* are not applied to cold climates (Oded Potchter et al., 2018). Here, PMV is selected as it is a more sensitive thermal index. Because PMV meets the overall considerations of indoor and outdoor environments, meteorological parameters, and personal factors. PMV's seven-point scale is early certified by the International Organization for Standardization (IOS) and has been applied in urban square thermal comfort studies combined with the computational fluid dynamic (CFD) model (d'Ambrosio Alfano et al., 2011). Finally, the PMV values have no impact on the correct numerical output during extreme weather (Rui et al., 2018); this is an important reason for choosing this thermal index in this study. The PMV thermal index is described in detail in the following sections.

2.2 Green and Building Space Adaptation from the Climate-Sensitive Design

A station square is part of the outdoor spatial environment and mainly involves transportation facilities and green infrastructure configurations in the surrounding space. It is a crucial image output of the city and an urban design component. At the end of the 20th century, “station renaissance” and “transit-oriented development” were proposed for reconstructing station spaces to pursue environmental sustainability and climate resilience. Concurrently, the green strategies of “garden roofs” and “green walls” have been adopted in landscaping, turning the Japanese railway stations into a highly regarded land model (KIDO, 2005; Zacharias et al., 2011). These squares' serviceability and environmental benefits focus on users' well-being, as affected by microclimatic conditions (Marcus & Francis, 1997; Nikolopoulou & Lykoudis, 2007; Zeka, 2011; Carmona, 2021). In these spaces, building layout and orientation affect the local thermal and wind environments. Furthermore, building geometry and shading are significant factors affecting the wind field on the building facade, which further influences the spatial distribution of particulate matter (Hong and Lin, 2015; Kariminia et al., 2015; Hong et al., 2017). Green spaces refer to the arrangement and composition of different land cover patterns with a specific amount of vegetation (Taylor & Hochuli, 2017). Vegetation reduces temperature and regulates microclimatic changes, contributing to the well-being and comfort of users (Honjo & Takakura, 1990; Robitu et al., 2006). In addition, vegetation plays a significant role in dust retention and noise reduction within different spatial elements. Previous studies on the effects of trees on particulate matter deposition have shown that tree species combinations significantly affect the deposition rate of particulate matter (Ould-Dada, 2002; Freer-Smith et al., 2005). Moreover, the dispersion of particulate matter is affected by canopy size, porosity, LAD, tree height, and tree planting distance (Salmond et al., 2013; Gallagher et al., 2015; Buccolieri et al., 2018; Ozdemir, 2019; Taleghani et al., 2020). Using CFD modeling, Amorim et al. (2013) confirmed that local air quality is closely linked to the synergy among meteorological conditions, the three-dimensional configuration of the street canyon, and vegetation. In another study, the ENVI-met microclimate model and wind tunnel experiments were applied to test the effects of vegetation structures along urban roads on PM_{2.5} deposition and composite tree-shrub structures were found to perform the best (Wu et al., 2021). Improving the configuration relationships of urban public spaces with one another reduced HUI intensity, building energy consumption, and health risks to pedestrians in high-density cities. Such mitigation strategies cleared air and noise pollution from traffic and production environments (Oliveira et al., 2011a).

Previous strategies for mitigating urban squares focused on thermal mitigation and microclimate effects; thermal comfort is the predominant concern field (Xiao & Yuizono, 2022). To the best of our knowledge, however, relatively few studies on the microclimate of station squares have integrated thermal comfort and air pollution level. Most studies focused on the thermal environment of urban squares based primarily on the physical environment and physio-psychological conditions (i.e., building green spaces, building materials, spatial behavior, perception). Building space is analyzed based on the aspect ratio (H/W), sky view factor (SVF), morphology, geometry, and orientation to regulate microclimate and thermal comfort. Kariminia et al. (2015) proposed a correlation between the PET index and H/W. They observed that T_a was reduced by 0.3 °C in the same building orientation at a H/W of 0.1, while T_a was reduced by 1.5 °C for a H/W of 0.1–0.3.

Typically, studies on green spaces involve plant type, number, canopy, shading, and evapotranspiration. Rahman et al. (2017) suggested that vegetation evapotranspiration integrated with street canyon yielded a stronger cooling effect at night; a hard square with 18% trees produced a stronger cooling effect than a green open circular square with 2% trees. Notably, shade is the most important influencing factor for microclimate and pedestrian thermal comfort. Robitu et al. (2006) found that pool altered the square microclimatic and comfort conditions by introducing vegetation, as trees reduced surface temperature and absorbed human heat radiation. Hence, green space reconfiguration positively affects the microclimate of urban square areas.

Investigating the thermal environment in public spaces involves urban green space planning of different site typologies on a large, moderate (i.e., parks, residences, squares, and campuses) or small (i.e., streets, blocks, canyons, and courtyards) scale. Green spaces produce a strong cooling effect on HUI and are affected by the building space characteristics (Thorsson et al., 2007; Aram et al., 2019). Ng et al. (2012) noted a cooling effect of trees up to 1.0 °C in 33% of high-density urban areas. Spangenberg et al. (2008) discovered that the park was 2.0 °C cooler than the square and the canyon in the same urban context. The effect of greenery on microclimate and thermal comfort is analyzed in terms of complex impact factors, including vegetation pattern, layout, structure, green quantity, and vegetation configuration in green spaces (Shahidan et al., 2012; Srivanit and Hokao, 2013; Gromke et al., 2015). Gromke et al. (2015) confirmed that street trees were the most effective in reducing the temperature in urban streets with integrated green strategies (i.e., street trees, green roofs, and green facades). Currently, the relevance of vegetation configuration to thermal effect in a tree design, vegetation structure, and LAI are critical quantitative research topics (Lin et al., 2008; Li & Song, 2019; Rui et al., 2019). Among these, green space configuration and vegetation type synergistically affect the efficiency of the cooling effect. The structure and number of vegetation affect air quality and urban microclimate, and these green indicators are useful for studying the effects of green space patterns on urban air quality.

2.3 Intersection of Theories

The study of climate-sensitive design strategies is based on the theory of urban climatology (UC), which is concerned with the regional climate impacts of cities and applies the new knowledge gained to better urban planning and design. The theory of UC is a great concern for the urban environment. It crosses various disciplines in meteorology, climatology, air pollution science, architecture, urban design, and biometeorology. According to the subject area of interest, researchers develop application tools and methods suitable for their interests (Mills, 2014).

The scientific basis for establishing UC started in the 1970s. UC can be traced back 200 years to Luke Howard's monitoring of changes in urban and rural meteorological differences (temperature, pressure, precipitation) and the publication of a research article on "London's Climate." It also developed into an interdisciplinary field combining local observational meteorology, physical geography, medical epidemiology, and building science (Howard, 1833). It is hypothesized that the main causes of the heat island phenomenon in densely urbanized areas are anthropogenic heat, multiple reflections, and airflow blockage.

UC has been divided into two main phases since 1900: descriptive and physical climatology. The early 20th

century concentrated urban climate research in Central Europe and focused on landscape and micro-scale climate studies. In 1981, Oke changed the previous use of the population as a variable for measuring urban form and function to introduce measures of urban geometry such as building height to street width ratio (H/W) and SVF as relevant variables for urban climate impact studies (Oke, 1981). The new approach to UC research commonly expresses the energy balance of the urban physical surface from the net radiation (Q^*), and the microscopic effects were integrated in 1990 to achieve an urban energy budget from the urban canopy layer (UCL) to the horizontal height of buildings in Eq. (1). UBL is defined as the lowest urban boundary layer. The urban boundary layer is divided into three scale effects (i.e., mesoscale, local, and microscale). The vertical atmosphere is divided into the rough surface sublayer, the surface layer, and the most external mixed layer (Figure 2.1). At the same time, different microclimatic phenomena occur in the urban canopy as a result of height changes in urban buildings and vegetation, which are closely related to urban design and human activities in the urban external space (Yang & Shi, 2019). The physically determining factors of temperature, airflow, precipitation, and humidity in the urban environment were explored via the development of thermodynamics and atmospheric dynamics in the 20th century. Furthermore, with the advancement of numerical simulations of urban environments, increasingly complex and detailed local-scale and micro-scale models have been developed to simulate urban heat island (UHI) and urban aerodynamic effects, including CFD and Energy Balance Models (EBM) (Mirzaei et al., 2010).

$$Q^* + Q_F = Q_H + Q_E + \Delta Q_S + \Delta Q_A \quad (1)$$

Where Q_F is described for anthropogenic heat flux, Q_H is atmospheric sensible heat exchange, Q_E is latent heat exchange, ΔQ_S is energy stored in the lower mat, and ΔQ_A is horizontal convective heat.

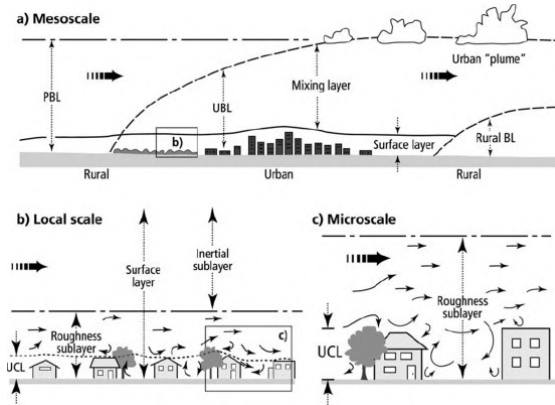


Figure 2.1 The different scales of the urban climate effect (Adapted from Oke, 1997).

Macroscales are suitable for describing weather phenomena associated with air masses and pressure systems, which are observed at a scale of 100 km. However, urban areas and the climate effects are identifiable at the mesoscale, which describes terrain on the order of 10 km. At the local scale, single kilometers or smaller resolutions reflect artificial targets, such as buildings and other urban structures. Microscale refers to this smallest domain where individual structures within trees cast shadows and deflect the flow of wind and where fine building elements alter sunlight reflection and the radiant temperatures to which people are most directly

exposed (Erell et al., 2012a).

The urban microclimate is a small area of urbanized land that has different atmospheric conditions than the surrounding area. The urban microclimate concerns the local climate effects in cities and towns. The main microclimate parameters affecting the environment are T_a , RH, T_{mrt} , WS, and wind direction. It mainly occurs from building to building, resulting in a thermal transformation in high-intensity buildings like the urban canyon effect. Anthropogenic influences cause changes in microclimatic conditions of urban outdoor spaces. The extensive hard paving materials, high-density buildings, and human activities in the city affect the thermal balance of the urban surface and influence the total albedo of this urban environment. In addition, the reduction of green space at the ground level affects the cooling effect of vegetation transpiration, and the area of water bodies affects the urban cooling capacity. Urban building morphology and vegetation configuration relate to the local environment's ventilation, humidification, and cooling effects, directly reflecting the local microclimate state. Climate change affects local weather conditions, and the local weather determines the latent heat exchange between the building and the environment. The thermal change in the outdoor space is completed by the primary processes (T. Hong et al., 2021):

- (1) Conductive and convective heat fluxes at urban surfaces.
- (2) Exchange of long-wave and short-wave radiation of the sun.
- (3) Latent and sensible heat transfer ventilation and permeability.

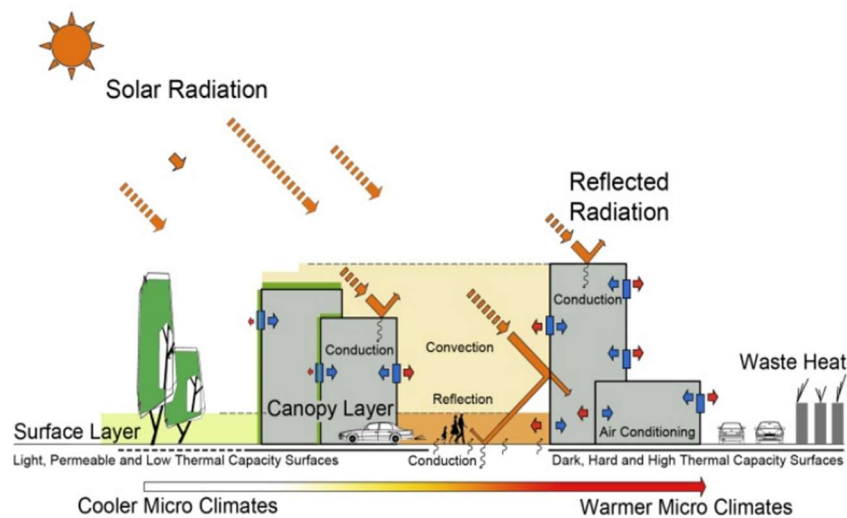


Figure 2.2 Urban microclimate in urban morphological structure, landscape, ground surface, and thermal exchange under anthropogenic activities (Sharifi & Lehmann, 2015).

Urban microclimates are strongly influenced by poor urban construction (such as dark, hard, high thermal capacity surface, urban trees too small, and excessive exhaust emissions), which are all important triggers for the exposure of cities to harsh climate and UHI, affecting the thermal benefits (body heat balance, metabolism, behavioral activities, thermal perception) of inhabitants and pedestrians (Figure 2.2). This study is based on the previous intersection of landscape design theory and urban morphology theory. The NSs is based on landscape design theory and urban climatology theory. The USRs focus on analogy-building morphologies and typologies in the same properties of the square space with climatology, urban morphology, and landscape

design theories. The climate-sensitive design strategies (NSs and USRs) are focused on space configuration to mitigate the thermal environment at the station square (Figure 2.3).

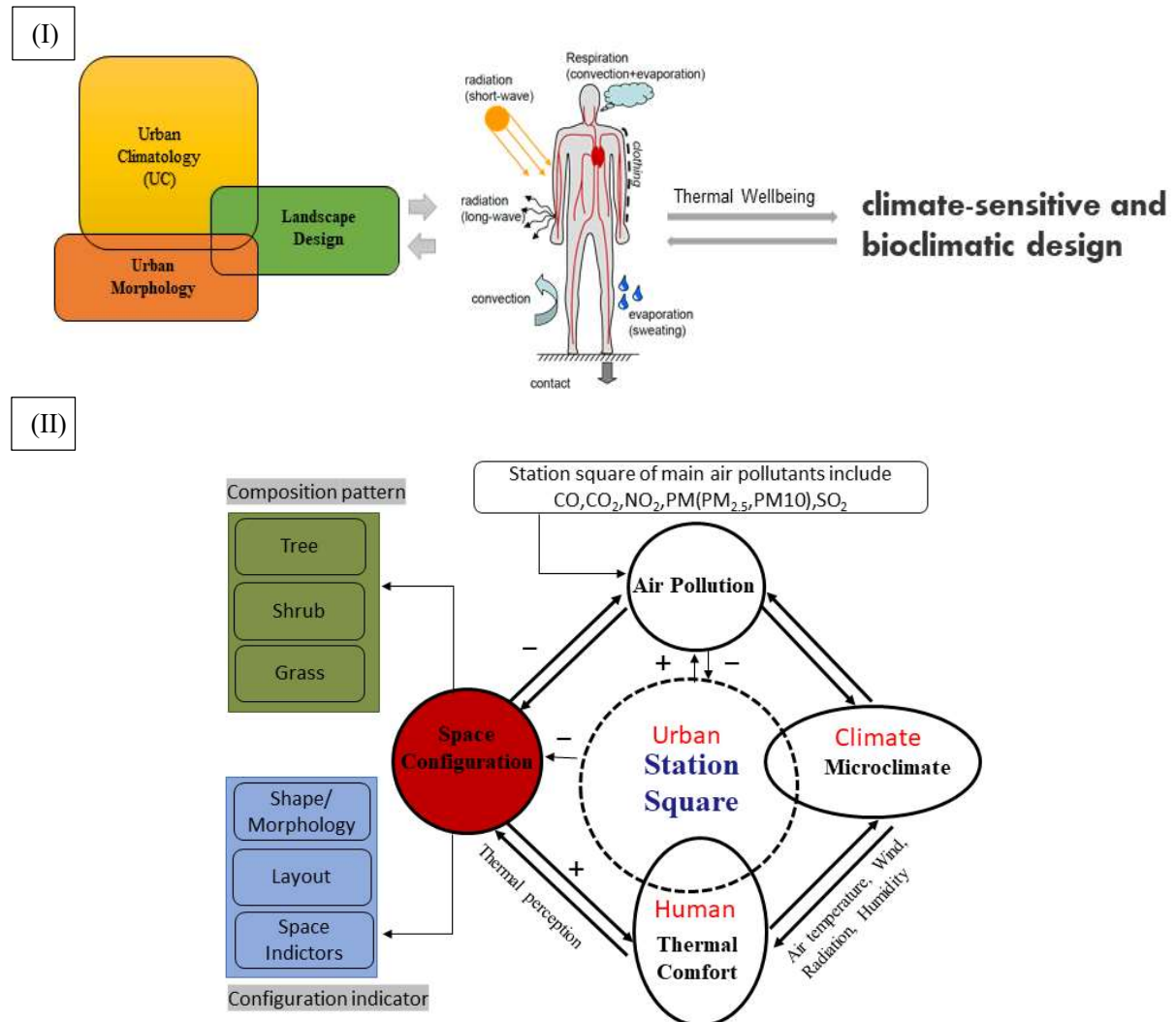


Figure 2.3 This study intersects disciplines (I) with the main research contents (II) (Source from: <https://www.theseus-fe.com/application-areas/automotive/passenger-comfort>).

Chapter 3 Methodology

3.1 Research Methods and Workflow

3.1.1 Site Selection and Analysis

Based on the current issues of Komatsu Station square and the city's development goals with urban plans, Komatsu Station square was selected as an example to investigate must the following these reasons:

(1) Consistency with the urban future development goals

Komatsu City has proposed a master plan for the city in the next 2040, aiming at urban renewal in the core area to promote urban vitality and accessibility (<https://www.city.komatsu.lg.jp>). An urban renewal and maintenance plan is located in the Komatsu station square's central area. The focus area is the district core planning from the east-west square of Komatsu station to integrate attractive commercial complexes by the improvement and protection of the urban environment in the station's front central area and infrastructure renewal in Appendix A. Adapting the landscape design, and infrastructure (traffic, green spaces, streets) makes the Komatsu station square more resilient and vitality.

Komatsu city is located in the southern part of Ishikawa Prefecture and belongs to the Hokuriku region of Japan. It is the third-largest city in Ishikawa, with a population of 107,023. The urban master plan covers an area of 371.05Km². The urban population has grown to be predominantly elderly. The aging of the population in the central region amounted to 27.6% in 2015 and is expected to reach 34.8% in 2040 for a population above 65 years. With significant climate change, there are concerns about the health of older people and children in hot conditions (e.g., Komatsu's protection against heat stroke). 60% of older people will be less well in 2021 due to extremely hot weather (<https://www.chunichi.co.jp>).

(2) Local climatic background characteristics.

Japan's predominant climatic distribution is characterized by a humid subtropical climate (Cfa), with this climate zone covering more than 50% of the urban climate in Japan (Rubel & Kottek, 2010) (Figure 3.1). The main center city of the Hokuriku region (36.40 °N, 137.19 °E) is Komatsu, characterized by hot and rainy summers followed by cold winds and thick snow in winter. In Appendix B, the hottest month is August in summer, and the coldest period in winter is February to March within this region. During the year, temperatures usually vary between 0 °C and 31 °C, rarely dropping below -3 °C or above 34 °C. The hottest periods are mainly between 12:00 - 16:00. Komatsu is often affected by cold Siberian air in winter with heavy snowfall and WS of up to 9m/s, and a minimum T_a of around -3 °C in 2021. Komatsu's summer T_a peak at around 34 °C with relatively steady winds in 2021 (Figure 3.2). The urban area's severe climate is predominantly spread over the winter and summer seasons, with the most significant discomfort responses to human thermal perceptions.

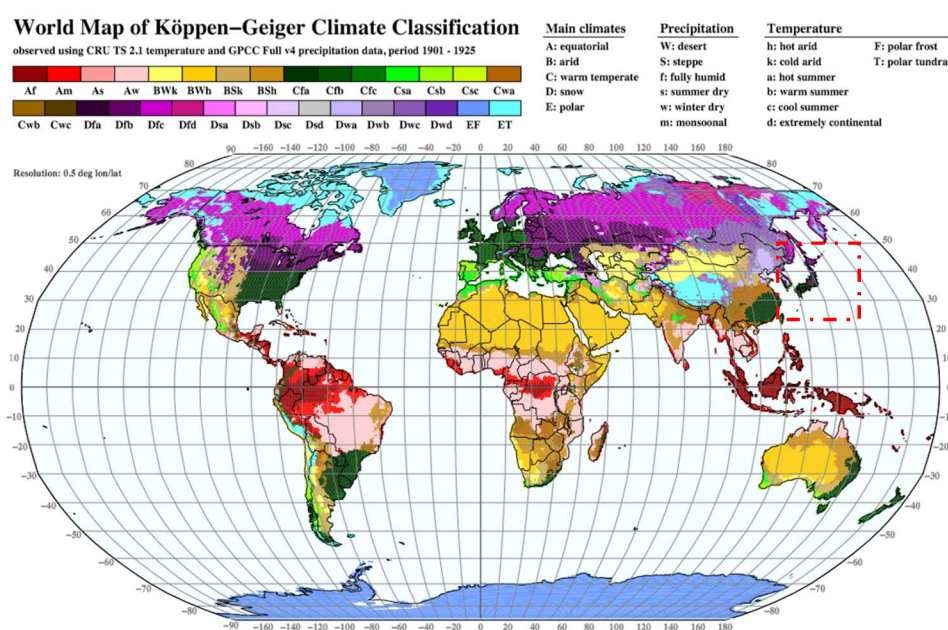


Figure 3.1 Japan climate zoon disruption from Köppen-Geiger climate classification (Rubel & Kottek, 2010).

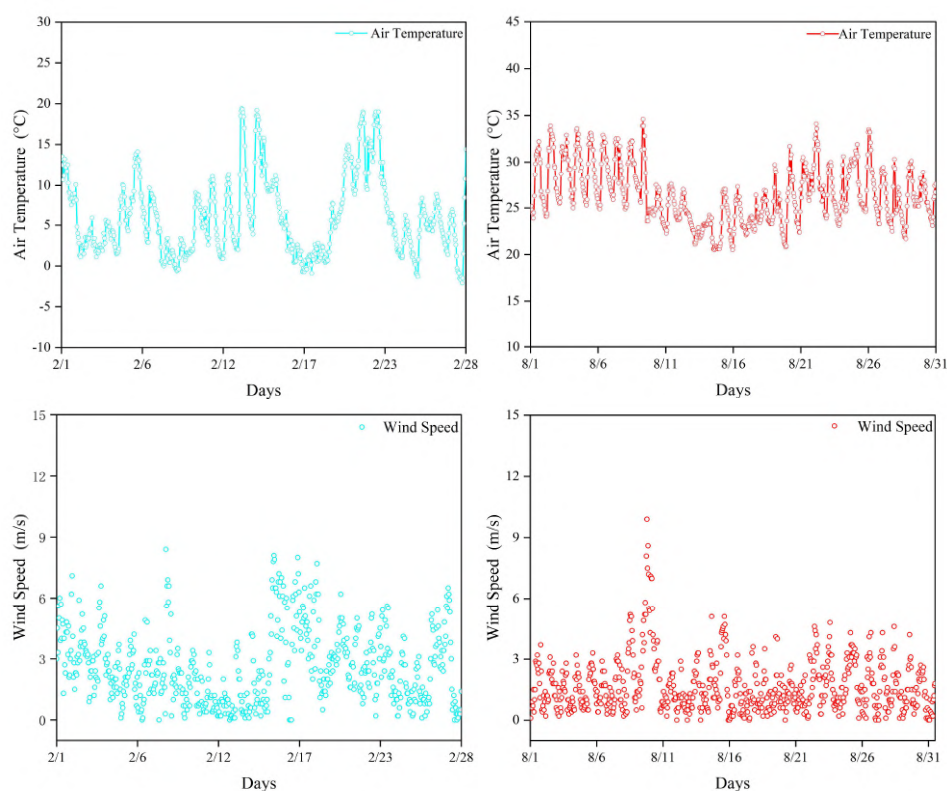


Figure 3.2 Wind speed (WS) and air temperature (T_a) changes in Komatsu for August and February 2021 (Japan Meteorological Agency, 2007).

(3) The lag in the landscape design of Komatsu Station square.

Komatsu Station square is relatively backward in infrastructure services compared to highly dense cities, especially concerning landscape configuration (Extensive distribution of hard pavement, urban street tree selection issues, imbalance in the configuration of evergreen and deciduous trees, and so on) in Appendix C and D. In Appendix C, according to the landscape environment analysis, there are the following problems:

- ① Grey infrastructure (481.2 km of railroad length) lacks softening in the urban landscape.
- ② *Cornus florida* is a small deciduous tree growing to 5 m high as mainly urban street trees. Its leaves do not develop well in windy areas, growth is stunted, and the risk of leaf spots is raised under strong winds in winter.
- ③ *Zelkova serrata* trees are not shade resistant and must be in full sun to grow better. It provides no good resistance to wind and shade.
- ④ The entrance tree planting array with dwarf *Magnolia denudate* (5m high) does not provide good shade.
- ⑤ Impermeable quartz bricks are used for the exterior square paving. This is not conducive to the infiltration of rainwater.
- ⑥ East square of Komatsu station renewed a small part of concrete permeable bricks.
- ⑦ Impermeable granite floor tiles are used for the internal square paving, and the sunken interior square is not conducive to stormwater drainage.
- ⑧ The parking lots are widely paved with concrete in the central area of Komatsu Station, exacerbating the UHI phenomenon and heatwave.
- ⑨ The sidewalk is dominated by horseshoe stones and locomotives in Doihara Bonnet Space. There is less space for activities.

In the transport environment, pollution from all types of motor vehicles (such as taxis, private cars, buses) and trains operating in the Komatsu station transport system. The quality of the surrounding greenery makes an important contribution to the reduction of noise, heat, dust, and the absorption of harmful particulate matter and gas emissions in the station square area. According to the Ministry of Land, Infrastructure, Transport, and Tourism (MLIT), motor vehicles emit important gases, including CO₂, CO, NO₂, PM (PM_{2.5}, PM₁₀), and SO₂. PM_{2.5} value of approximately 15 µg/m³ higher than the air quality standard (PM_{2.5} Annual Report, n.d.). The highest and lowest temperatures generally occurred in August, January, and February from 2015-2019 (Japan Meteorological Agency, 2007) (Figure 3.3).

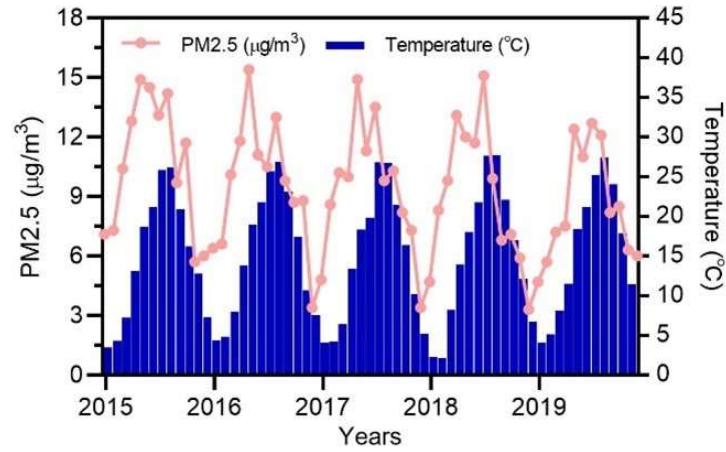


Figure 3.3 Changes in temperature and PM_{2.5} from 2015 to 2019.

(4) Homogeneity of the spatial structure at the station square.

The typology of station squares in some Japanese cities can be divided into relationships in which the station square is orthogonally connected to the main parallel street, as shown in Figure 3.4.

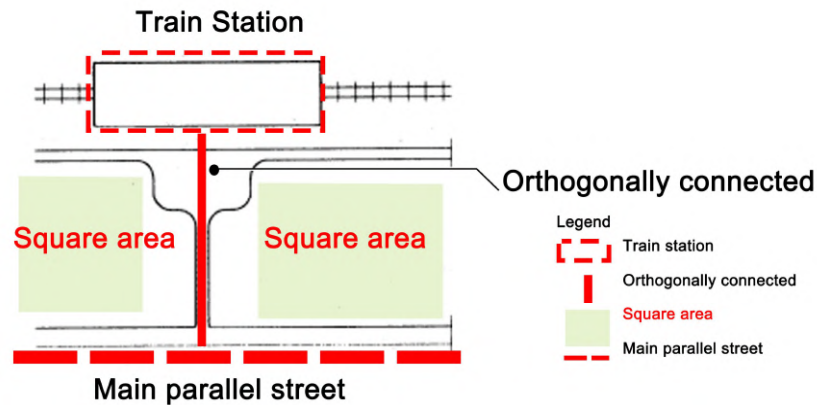


Figure 3.4 Typology of station squares' spatial structure (Adapted from Gehan et al., 2000).

This space type represents the typical Japanese spatial layout of station squares with orthogonal connections to major parallel street relationships accounting for 45% of station squares in Japan's central and suburban areas (Gehan et al., 2000).

Meanwhile, the spatial structure of station squares in major central cities (Kanazawa, Toyama, Fukui) of the Hokuriku region is the same as that of the Komatsu station square. In the Hokuriku region, the number of station squares with the same structure reached 50% in Appendix D. Therefore, the site selection of the Komatsu Station square is exemplary.

3.1.2 Measurement Methods

The macro-meteorological data for this study were obtained from macro-scale monitoring at the Komatsu City local weather station (<https://www.data.jma.go.jp>) and the Komatsu Airport weather station (<https://www.wunderground.com>) of the Japan Meteorological Agency, and meteorological parameters

including T_a , WS, wind direction (WD), humidity and cloudiness. Micrometeorological data is derived from on-site measurements using a portable Weather & Environment meter (Kestrel 5400 thermal stress tracker, NK Company, USA), which is placed on a tripod at the height of 2 m to monitor the meteorological parameters of T_a , RH, WS, and the globe temperature (T_g). The monitoring period is mainly during the hottest and coldest periods in the Hokuriku region of Japan, August and February 2021, respectively.

The soil analyzer measured the soil temperature and humidity at different local soil layer levels. The emission of urban air pollution concentrations is measured by the PM_{2.5} tester (Temtop, M2000 2nd, CNA) (Figure 3.5).

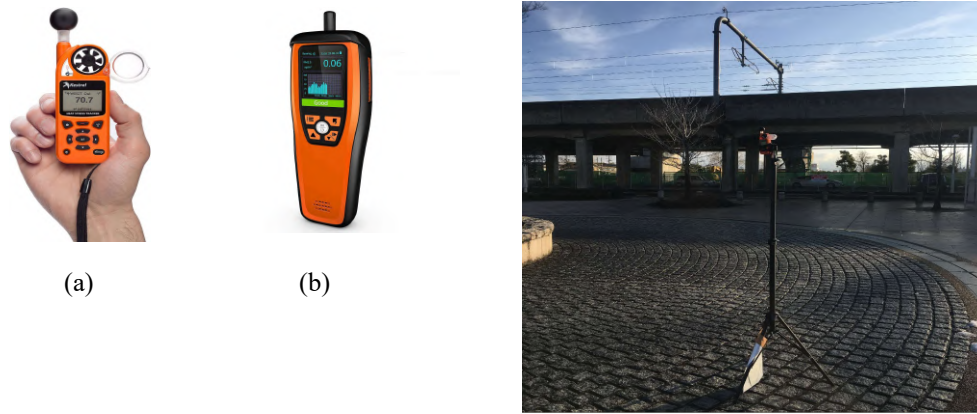


Figure 3.5 Portable Weather & Environment meter (a) and PM_{2.5} tester (b) were used for measuring the on-site areas.

3.1.3 CFD-based Simulation Methods

More and more architects and urban planners have become aware of the importance of the thermal environment in urban design. Wind tunnel experiments and CFD simulations are common methods used to evaluate the design scenarios (Jiaying Li et al., 2022). With the advances in information technology and the high consumption of on-site measurements, combined with the variability of uncontrollable influences, numerical modeling has become the most convenient scenario decision tool for urban landscape microclimate investigation studies in a complex urban environment. Common energy balance models include RayMan and SOLWEIG (to estimate radiant flux). CFD models include mainly Fluent (to assess the effect of vegetation on ventilation and canopies), SOLENE (to assess building energy consumption), and ENVI-met (to evaluate thermal comfort/microclimate/air quality) (Yang et al., 2019; Saito et al., 2017). Compared to the energy balance model, the main advantage of the CFD model is the high resolution in the coupled simulation mechanism, which allows for better reproduction of realistic scenarios and saves calculation time. Furthermore, ENVI-met in CFD models is widely applicable to the study of urban vegetation in microclimatic environments and outdoor thermal comfort, especially the cooling effects of trees, green space layout, and vegetation structure configuration (Zölch et al., 2019; Gaspari et al., 2018; Stocco et al., 2021). It is suitable for cross-simulation and comparative studies of complex vegetation structures and spatial layout patterns.

The numerical simulations of predicted scenarios were implemented by ENVI-met 4.4.5 and ENVI-met 5.0.1, which typically model the impact of urban planning on environmental variables and microclimate (Salata et al., 2016). ENVI-met is a three-dimensional microclimate model originally proposed by Bruse and Fleer's team at the University of Mainz, Germany, in 1998 (Huttner, 2009). The software model is based on CFD and thermodynamics. It can simulate the interaction processes between the ground, vegetation, buildings, and the atmosphere in a small-scale space. ENVI-met is mainly supported by the Biomet tool for calculating the thermal index and the Albero tool for creating a new vegetation model. With horizontal resolutions of 0.5–10 m and time steps of up to 10 s. Its simple force mode allows the model to force RH and T_a at 2 m height for 24 h. It is also particularly suitable for simulating microenvironments on medium and large scales. ENVI-met V4 implements the vegetation model from 1D to 3D, detailing the tree canopy geometry and LAD of vertical density, the root area density (RAD) distribution. It better demonstrates the leaf surface transpiration cooling of trees and the effect of tree shape on wind flow. ENVI-met has the unique advantage of providing a systematic classification of vegetation types, vegetation structures (trees, shrubs, grass), green roofs, and green walls in a vegetation database (Liu et al., 2021). Model performance is mainly related to setting basic parameters for spatial grid resolution, vegetation models, and building materials. The precise running performance determines the difference between the simulation and realistic scenarios. Studies have examined ENVI-met's modeling performance by combining statistical indexes with on-site measurements of meteorological conditions. Statistical indexes commonly used to verify the performance of the simulations include the coefficient of determination (R^2) and the root mean squared error (RMSE). A reliable model must tend to the following index values: $R^2 \rightarrow 1$ and $RMSE \rightarrow 0$ (Stocco et al., 2021). T_a was the most frequently evaluated meteorological variable in the literature with validation, followed by RH and T_{mrt} .

3.1.4 Research Workflow

A comparative study of numerical simulation prediction scenarios related to urban microclimate and thermal comfort proposes to comply with climate-sensitive design strategies. The process is divided into site measurement, numerical modeling, model validation, and environmental evaluation.

(1) Site measurements

Firstly, the general spatial measurements of the study area were carried out for the atmosphere, built environment, green environment, and ground surface. The atmospheric environment was mainly researched for the local climate zones and to investigate the main periods and seasons suitable to match the local occurrence of severe weather and climate change, including extreme heat and cold. At the same time, local meteorological parameters are monitored and obtained cloud layer information. The built environment requires field measurements of building materials, morphology, scale, and area. On the other hand, the green environment requires a field survey and a summary of information on the number, type, layout, and combination of vegetation. Finally, ground surface measurements are generally carried out on the humidity and temperature of the soil layers.

(2) Numerical modeling

The numerical model ENVI-met is used to create the 3D model by capturing the site measurements for

setting the geographical location, grid size, and general settings involving the simulated meteorological boundary mode (Simple Forcing / Full Forcing / Other BLC), the simulated time, and the CPU operation mode (Multi-Core / Single Core). This study focuses on the simple force mode, so the optional components in this mode are mainly related to the parameterization of buildings, vegetation, pollutants, and soils. The user database was created in ENVI-met, particularly for some new building wall structures, 3D models of trees, and vehicle emission settings on the road. After completing the above process, a three-dimensional space is created to reproduce the real site. The layouts and parameters of the receptors, emissions, buildings, and vegetation are prepared for setting. Subsequently, a SIMX simulation file is created in the sub-tool ENVI-guide, and the basic model is imported into the sub-tool of ENVI-core for the simulation procedure. The simulation procedure is divided into five main steps and is completed in the sub tools: ① Modeling in Spaces, ② Setting initial weather and boundary condition in ENVI-guide, ③ Simulation in ENVI-core, ④ Calculating the thermal index in Bio-met, ⑤ Heatmap visual analysis in Leonardo. The vegetation modeling process can be performed using the Albero sub-tool; the Japanese pagoda tree is modeled in ENVI-met V5 (Figure 3.6).

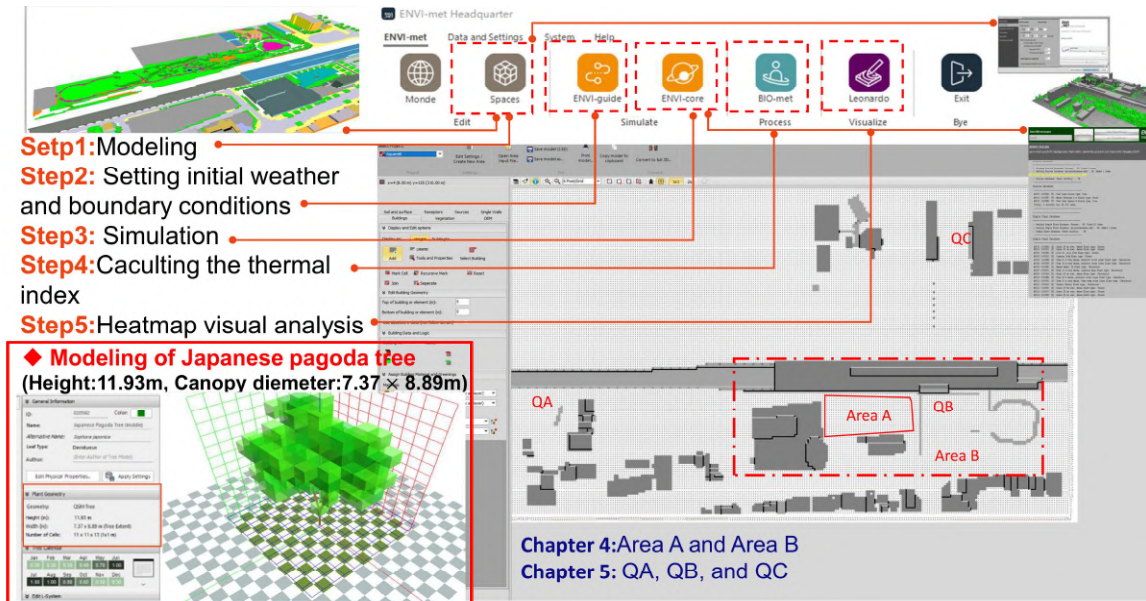


Figure 3.6 ENVI-met simulation in five specific steps.

(3) Model validation

Model validation requires fitting simulation results to field measurements as an appropriate evaluation procedure to ensure the reliability of the model outputs (Oreskes, 2003). The ENVI-met model grid sensitivity analysis is focused on getting a more accurate and efficient running of the base reference model for modeling the real study site. The relevant microclimate parameters become the object of validation results, especially for T_a . The most widely used statistics such as RMSE, non-systematic (RMSEu) values, mean deviation error (MBE), mean absolute error (MAE), the index of agreement d, and correlation metrics of R^2 .

(4) Environmental evaluation

The basis for creating numerical micro-scale models relies on the complex interaction between urban

structures (i.e., buildings and surfaces) and local weather parameters; in principle, solar radiation (including direct, diffuse, and reflected radiation and airflow) are considered in heat transfer from the urban surface to the atmosphere. One of the most widely used dynamic simulation tools for microclimate analysis is ENVI-met, which integrates the evaluation of microclimate conditions, the thermal environment, and air quality. ENVI-met simulation results can evaluate the cooling potential of various UHI mitigation strategies and the deposition and dispersion effects of atmospheric pollution gases ($PM_{2.5}/PM_{10}/NO$).

The thermal environment evaluation relies on the visualization of the thermal index in the Leonardo sub-tool of ENVI-met to result in a heatmap of the study area (microclimate parameter map/heat index map/pollution concentration map). The Bio-met sub-tool is applied to the thermal index calculation to provide timely sensitivity feedback on the surrounding environmental parameters via the thermal index response to the human body's perception scale of outdoor thermal comfort. Thus environmental evaluations determine the reasonable distribution and configuration of design plans. Bio-met sub-tool for body parameters, human body parameters, clothes parameters, person metabolism in a stable thermal environment, and detailed thermal index calculation involving personal human parameter settings are shown in Figure 3.7.

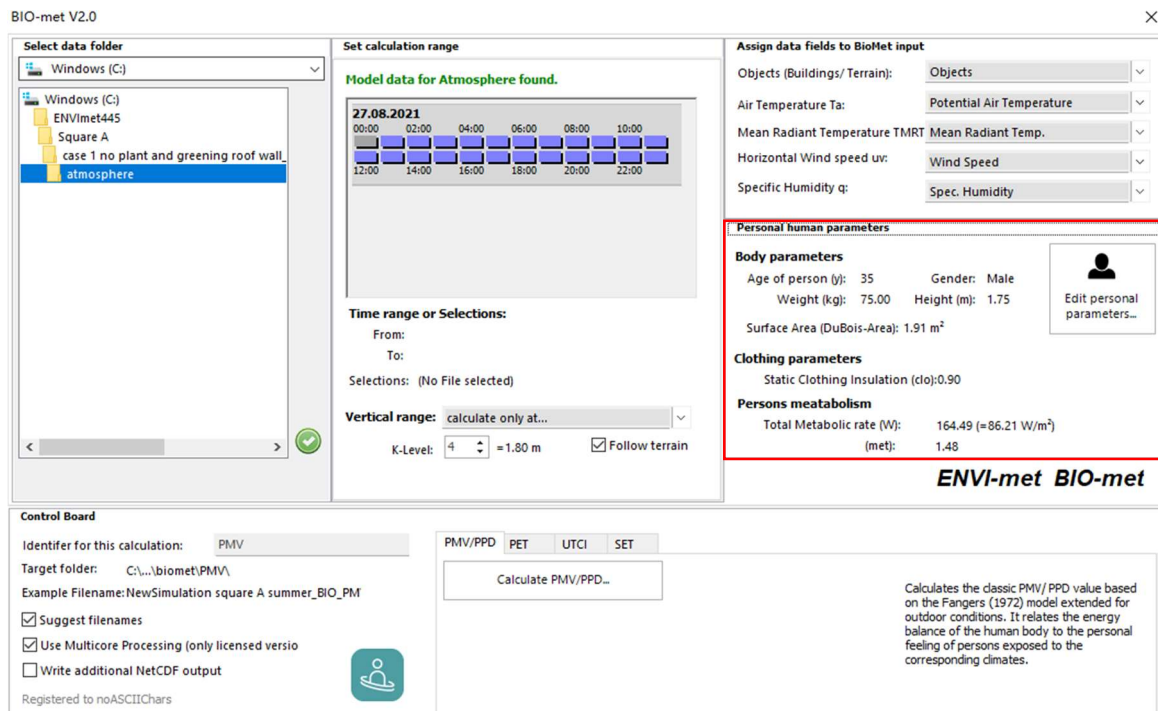


Figure 3.7 Thermal index calculation involves the setting of personal human parameters.

3.2 Quantitative and Qualitative Analysis Methods

3.2.1 Quantitative Methods in Urban Space

The urban ventilation potential, the cooling effect, and the deposition and dispersion effects of atmospheric pollution are crucial in determining the comfort and quality of the environment. These effects can be generated in isolation from exploring urban spatial characteristics (i.e., building morphology, degree of building opening

and closing, greening layout, vegetation combination, vegetation type, and tree species). Numerous studies have confirmed that urban morphological indicators are key factors in exploring the thermal environment and air quality (Krüger et al., 2011). Local design at the microscopic scale is relevant for the macroscopic thermal environment of the overall environment and follows urban design theory to control local space.

Quantitative indicators of the built environment include the aspect ratio of streets (H/W), SVF, and the building volume ratio (Jiaying Li et al., 2022). In 1988, Oke first identified urban morphological characteristics as closely related to microclimate and used H/W to combine airflow patterns in the wind field of street canyons (Ji et al., 2019).

There are more quantitative indicators of the green environment than of the built environment, which accordingly includes: Green space ratio, tree configuration ratio (Xiao & Yuizono, 2022), tree number ratio, grass and shrub cover ratio, ecological landscaping plot ratio, and green structure index et. c (Rui et al., 2018). Furthermore, some studies have focused on studying LAI and LAD in landscape spaces (Morakinyo & Lam, 2016; Rui et al., 2019). The quantification of these indicators facilitates cooling the thermal environment by green space and the deposition of atmospheric pollutants by green design.

This study applies new greening indicators by the deciduous to evergreen tree configuration ratio and the ratio of number of deciduous to evergreen trees in the NS_s and USRs strategies. In contrast, the NS_s strategy quantifies the thermal mitigation of extreme weather conditions in greening indicators (green space ratio, configuration ratio, number of trees). In the USRs, the greening (number ratio of deciduous to evergreen trees, LAD) and the building space (H/W) are quantified simultaneously, and the optimization of thermal comfort and air quality in summer by integrating tree species. Accordingly, both strategy scenarios are based on quantitative and qualitative analyses with similar numbers of trees.

3.2.2 Qualitative Methods for Thermal Comfort Evaluation

High-quality public space needs careful climate-sensitive design of urban spaces and the development of design guidelines responsive to the thermal environment to mitigate existing urban climate and pollution problems. These guidelines must verify that the characteristics of the urban space are compatible with human satisfaction and thus reduce discomfort levels from the environment (Lenzholzer et al., 2018). Since the 1920s, thermal comfort environments have been investigated in the human body's thermal perception of indoor and outdoor areas by thermal indices (Houghten, 1923). In 1970, Fanger proposed a thermal comfort model and an empirical heat balance equation for environmental engineering applications and analysis methods (Fanger, 1970). He also developed a physiological index to study thermal comfort based on a subjective perceived (dis)comfort scale obtained from a mass sample of individuals in 1972. PMV of thermal stress in comfort or discomfort levels could be derived. The PMV index was applied to indoor environments and gradually became widely used to evaluate outdoor environments. Outdoor evaluations are more complex and varied than indoor evaluations with climate variables. More thermal indexes have since been improved and revised by the International Organization for the Ergonomics of Thermal Environments (IOME) and the American Society of Heating, Refrigerating and Air-Conditioning Engineers (ASHRAE) standards. To address this problem, PET (Mayer et al., 1987) and UTCI (Höppe, 2002) were developed to evaluate outdoor conditions better. The

evaluation criteria for these thermal indexes involve measuring meteorological parameters of the thermal and microclimatic environment with sensitivity analyses to get different levels of thermal sensitivities and thermal index thresholds (Figure 3.8). The applicability of qualitative methods is related to the state, time, and spatial scales of the dynamics (Lenzholzer et al., 2018).

Thermal perception	Indices range			
	PMV	PET	UTCI	
Very cold ¹ (extreme cold stress ^{1,2})	−3	< 4	< −40	
(Very strong cold stress ²)			−40 to −27	
Cold ¹ (strong cold stress ^{1,2})	−2.5	4–8	−27 to −13	
Cool ¹ (moderate cold stress ^{1,2})	−1.5	8–13	−13 to 0	
Slightly cool ¹ (slight cold stress ^{1,2})	−0.5	13–18	0 to +9	
Comfortable ¹ (no thermal stress ^{1,2})	0	18–23	+9 to +26	
Slightly warm ¹ (slight heat stress ¹)	0.5	23–29		
Warm ¹ (moderate heat stress ^{1,2})	1.5	29–35	+26 to +32	
Hot ¹ (strong heat stress ^{1,2})	2.5	35–41	+32 to +38	
(Very strong heat stress ²)			+38 to +46	
Very hot ¹ (extreme heat stress ^{1,2})	3	>41	>+46	
¹ PET and PMV				
² UTCI				

Figure 3.8 Universal outdoor thermal comfort evaluation of thermal index referencing standards (Asghari et al., 2019).

For engineers and designers, the thermal index assessment criteria determine how hot or cold the thermal environment is and gives feedback on the level of pedestrian discomfort.

The visualization of the thermal map from the simulation results determines the hottest and coldest areas and the visualization of the space's ventilation, thermal radiation, and pollution levels. Visualizing the microclimate simulation results also facilitates the preliminary analysis of the site's strengths and weaknesses and determines the rationality of the planting structure, landscape layout, material, and building morphology.

Chapter 4 A New Synergistic Strategy (NSs) in Landscape Design

4.1 Landscape Design Theories

The implementation of high-quality landscape design enhances the well-being of people and visitors. Landscape design is an independent profession, a design and art tradition practiced by landscape designers to combine nature and culture. Landscape design bridges the space between landscape architecture and garden design (Bowles Wyer, 2012). Landscape design is a broad discipline consisting of natural and artificial landscape elements, which intersects with knowledge from many disciplines, including ecology, botany, geography, and urban planning. Practicality, aesthetics, horticulture, and environmental sustainability are integral to landscape design. An appreciative system and the management, planning, and design of regeneration processes require approaching the landscape as a system. Since landscape design must integrate diverse systems, it benefits from knowledge to active participation. Landscape can be considered a complex and dynamic system including many subsystems (e.g., atmospheric environment, natural environment, artificial environment).

The landscape design process comprises a comprehensive planning document, site features, user needs, design alternatives, final design, and implementation plan. Site characterization is primarily concerned with the use of land, topography, views, climate, pedestrian and vehicular circulation, and utility systems (Air Mobility Command, 1999).

The landscape has six main components: landform, ground, building, vegetation, water, and climate (Starke & Simonds, 2013). The climate has a bearing on people's physical health and mental state, which places specific demands on planning. Human behavior and perceptions of the environment vary between climatic conditions. In landscape design, microclimatic design guidelines should be responsive to the following principles:

1. To mitigate extremes of heat, cold, humidity, turbulence, and solar radiation can be provided by place design and planning to create a spatial environment appropriate to the local climate.
2. To adjust land and building layout following the solar radiation track.
3. To reduce energy consumption using natural energy sources (i.e., solar, wind, etc.).
4. Evaporations obtain a cooling effect from the water body and transpiration from the leaves.
5. To preserve existing vegetation and introduced vegetation.

These principles reduce heat loss, cooling requirements, and natural thermodynamics in outdoor spaces.

4.2 Greening Parameters and Indicators

Based on a review of the literature on urban greening to mitigate urban heat stress and enhance outdoor thermal comfort by the microclimate model ENVI-met, it can be understood that the key parameters of the simulation analysis are: trees, green roofs, vertical greening (Liu et al., 2021). The main aspects of tree analysis include the physical properties of individual trees (grown density, tree height, trunk height, crown

diameter, type) and tree planting designs (coverage ratio, planting location, planting arrangement, tree distribution). Green roofs are mostly from the distribution level of the cooling effect, physical properties, and planting design. Vertical greening, also known as façade greening or wall greening, is mainly from the spatiotemporal distribution of cooling effect and planting design. The trees of planting designs mainly involve selecting tree species, the number configuration of the tree, planting direction, vegetation structure, planting layout, planting interval, and other contents. The thermal benefits of trees vary by these specific designs. The tree effect is influenced by wind speed, wind orientation, and shade pattern. A good performance of tree planting design reveals the double advantages of ventilation and shadow. This study focuses on tree designs and green space configuration to mitigate extreme climates or weather conditions on typical summer days.

The greening indicators quantify the vegetation cover conditions (e.g., the green cover ratio, green space ratio), the planting pattern and structure, or configuration. The related planting pattern indicators include landscaping deviation, landscaping isolation indicator, and land shape indicator. This study of the NSs quantified two indicators: green space ratio and tree configuration ratio. The study of USRs adopted three indicators: green space ratio, the ratio of number of evergreen and deciduous trees, and LAD.

4.3 Case Study of NSs at the Komatsu Station Square

4.3.1 Motivation

In contrast to the previous studies mentioned above, there were some limitations in the existing studies. First, limited landscape designs consider station squares' seasonal and regional climatic characteristics compared to other public spaces. Second, few studies have examined the thermal environment of square landscape design at different scales (Stocco et al., 2021; Thorsson et al., 2007). Third, few mitigation approaches have investigated the role of landscape layout patterns, evergreen to deciduous tree configuration ratios, and vegetation structure in co-regulating thermal environments. To address this gap, this study evaluates the impact of new landscape design scenarios for a station square on winter and summer thermal comfort in different scale environments by applying the PMV thermal index in the ENVI-met V4 microclimatic model. The evaluation of the PMV thermal index provides positive urban design and planning guidance for improving the thermal environment (d'Ambrosio Alfano et al., 2011). The objectives of this study are as follows:

- i) To examine the thermal comfort and microclimate of station squares for the climatic characteristics of the Hokuriku region in Japan.
- ii) To quantify and qualify which landscape design elements and indicators influence thermal comfort and microclimate in winter and summer.
- iii) To investigate the deciduous tree and evergreen tree configuration ratios on a small and large scale to determine their effect on the thermal comfort level of the station square.

4.3.2 Study Area

This study was conducted at the Komatsu Station square, Ishikawa, Japan (36.40°N, 136.45°E). It is located in the Hokuriku region near the Sea of Japan's coastline. The study area is approximately 2,563 m² for the

small-scale in the red solid line zoon (area A in Figure 4.1), which requires consideration of the large-scale surrounding environment of approximately $280\text{ m} \times 115\text{ m}$ (area B in Figure 4.1). This space type represents the typical Japanese spatial layout of station squares with orthogonal connections to major parallel street relationships, accounting for 45% of station squares in the central and suburban areas of Japan (Gehan et al., 2000). We planned to explore the Komatsu Station square as a template to improve the thermal comfort and microclimate of the station square. The interior courtyard square is enclosed by the station platform, theater, hotel, and station canopy (Figure 4.1 (1-3)). It is close to the viaduct platform and the average daily flow of people is 7,823.

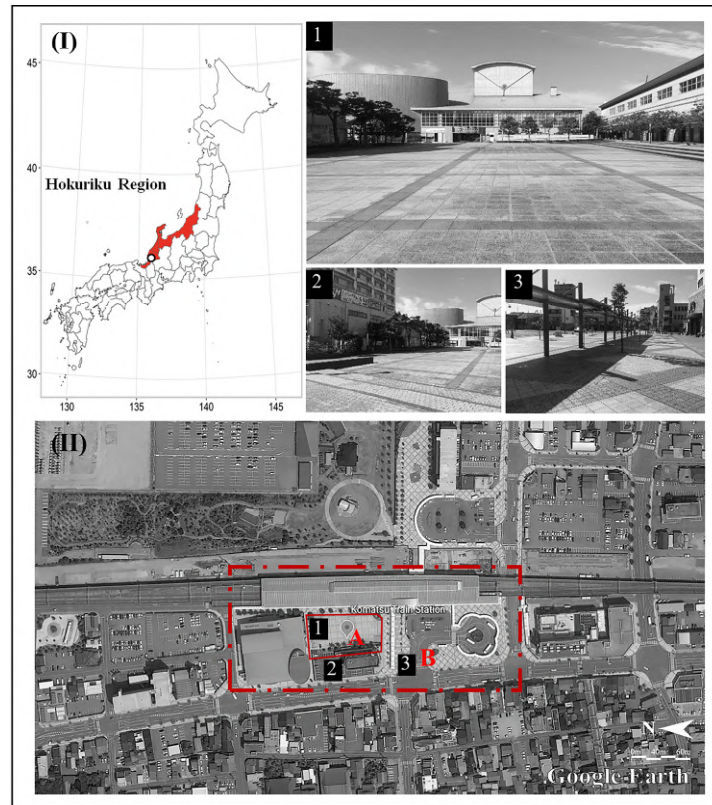


Figure 4.1 (I) Komatsu Station square location; (II) Google Earth map of study area divided to area A and area B scale, and the spaces include a square courtyard (1), a hotel (2), and the station canopy (3).

4.3.3 Climatic Contexts

The local climate is classified as humid subtropical, based on Köppen's climate classification system (Kottek et al., 2006). The winter and summer seasons were studied; summers are generally hot and humid, while winters are cold and dry. The coldest winter months are December to March, with mean temperatures as low as $0\text{ }^{\circ}\text{C}$ and frequent windy days. The prevailing wind in the city of Komatsu is typically from the north and west in winter. Summer's peak heat is in August, with mean temperatures of up to $31\text{ }^{\circ}\text{C}$ and frequent rainy days. The Japan Meteorological Agency (JMA) records real-time weather data from the Komatsu City Imaecho Observation Station.

Figure 4.2 shows the details of daily weather conditions, as well as monthly maximum and minimum

temperatures from 2018 to 2020. The data indicated that for three consecutive years, the maximum temperature reached around 38 °C in August each summer, and the minimum temperature was within -10 °C between December and March each winter. Within these periods, people provided timely feedback on discomfort perception under extreme weather conditions, and these measured meteorological data provided validity for modeling a better-quality environment. Therefore, based on climate data, for 2021, we selected February 27th and August 4th as representative extremely cold and hot days to examine the holistic mitigation strategy of landscape design for extreme climates.

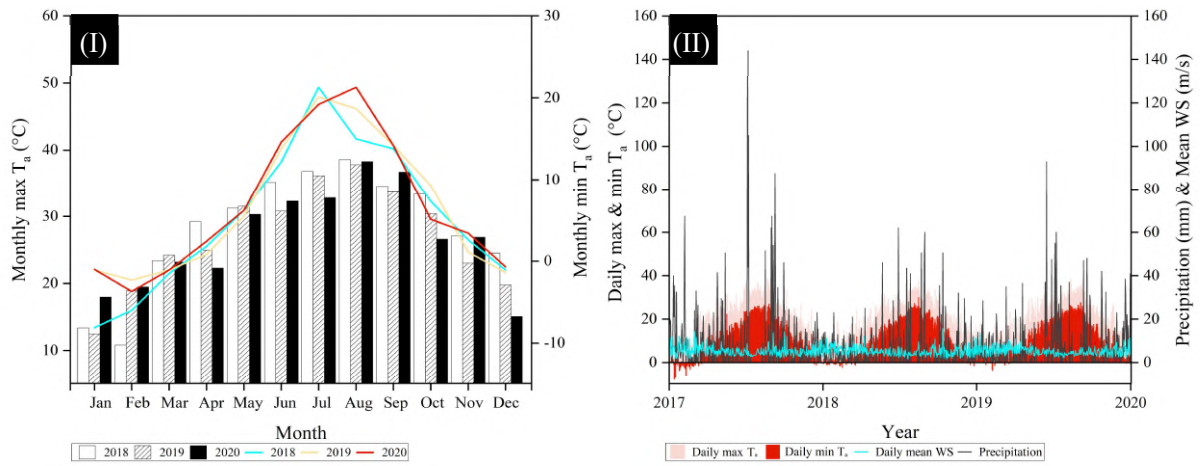


Figure 4.2 (I) The monthly maximum and minimum temperature (T_a); and (II) the daily maximum and minimum temperature (T_a), precipitation, and wind speed (WS) for Komatsu city from 2018 through 2021 recorded by JMA's weather station.

4.4 Methodologies for NSs

We followed four main steps: 1) Select the original case at a station square in the Hokuriku region; 2) Take an on-site measurement; 3) Construct a microclimate simulation model in ENVI-met; and 4) Develop the new landscape scenario simulation for a comparative study, which is described in detail in Section 4.5. The on-site measurement results were compared with the simulation results to validate the accuracy of the model and evaluate the optimal scenarios. The original scenario simulation model produced on-site conditions that were designed for new landscape design scenarios in different proposed configuration conditions with ENVI-met to predict the optimal effects on the thermal environment. The research methods and workflow used in this study are presented in Figure 4.3.

of trees, shrubs, and lawns on the perimeter of the station square. The vegetation configuration around the measurement area is dominated by deciduous trees (DT). There were fewer evergreen trees (GT) and coniferous trees (FT), the vegetation details are presented in Table 4.2.

Table 4.1 T_a , RH, WS, and T_g measured at Komatsu Station square on February 27 and August 4, 2021.

Time	Winter (on February 27)				Summer (on August 4)			
	T_a (°C)	RH (%)	WS (m/s)	T_g (°C)	T_a (°C)	RH (%)	WS (m/s)	T_g (°C)
00:00	3.5	56.9	3.3	2.6	27.0	74.3	0.0	28.2
01:00	3.0	58.0	0.7	2.3	25.9	71.3	0.0	27.2
02:00	2.8	56.1	1.0	2.0	25.5	73.6	0.0	26.9
03:00	2.6	52.1	0.8	1.5	26.3	76.2	0.0	26.7
04:00	2.0	50.8	0.4	0.8	33.6	80.1	0.0	25.6
05:00	1.9	49.0	1.7	1.0	33.0	80.4	0.0	25.2
06:00	1.6	49.3	0.7	0.4	31.0	75.8	0.8	26.5
07:00	1.3	50.4	0.7	0.8	33.8	50.8	0.0	39.9
08:00	2.4	46.4	3.5	3.8	32.7	61.8	0.6	43.9
09:00	4.6	38.1	0.5	14.6	33.1	66.8	1.3	45.5
10:00	5.2	35.8	0.8	18.6	33.8	54.0	0.5	47.6
11:00	7.5	33.5	1.8	19.5	33.7	57.9	2.9	45.8
12:00	6.9	38.8	1.5	18.3	31.9	56.6	1.1	47.1
13:00	6.2	41.2	2.3	11.4	31.9	55.8	0.7	45.5
14:00	7.5	36.3	1.0	16.8	32.0	54.7	1.6	45.0
15:00	5.9	38.7	3.6	7.0	30.4	61.6	0.9	34.4
16:00	5.5	41.5	1.4	5.8	30.2	62.1	0.5	33.7
17:00	4.6	44.7	1.7	4.6	30.1	59.6	0.0	33.6
18:00	3.7	50.1	0.7	2.8	29.5	66.0	1.2	31.7
19:00	3.1	54.9	1.4	2.1	28.1	69.0	0.0	29.8
20:00	2.4	57.7	0.5	1.6	27.6	68.7	0.0	29.7
21:00	2.2	59.8	0.0	0.8	27.7	72.0	0.0	29.1
22:00	0.3	68.2	0.8	-1.1	27.0	77.9	0.0	27.9
23:00	-0.2	73.7	0.6	-1.4	25.9	79.9	1.0	27.3

The main outdoor space of Komatsu Station is mainly the square space except for the traffic space, which forms the rectangular courtyard space. The on-site investigation found that within the Komatsu station area (50m × 50m, 80m × 80m), the hard paving of the station square reached 63%-83%, while the distribution of the green area only reached 6% (Figure 4.4). Moreover, the area of Komatsu Station is dominated by the dwarf deciduous tree of *Corrus Florida*, which has a limiting effect on the mitigation of urban heat stress, traffic noise, and dust reduction (Figure 4.5).

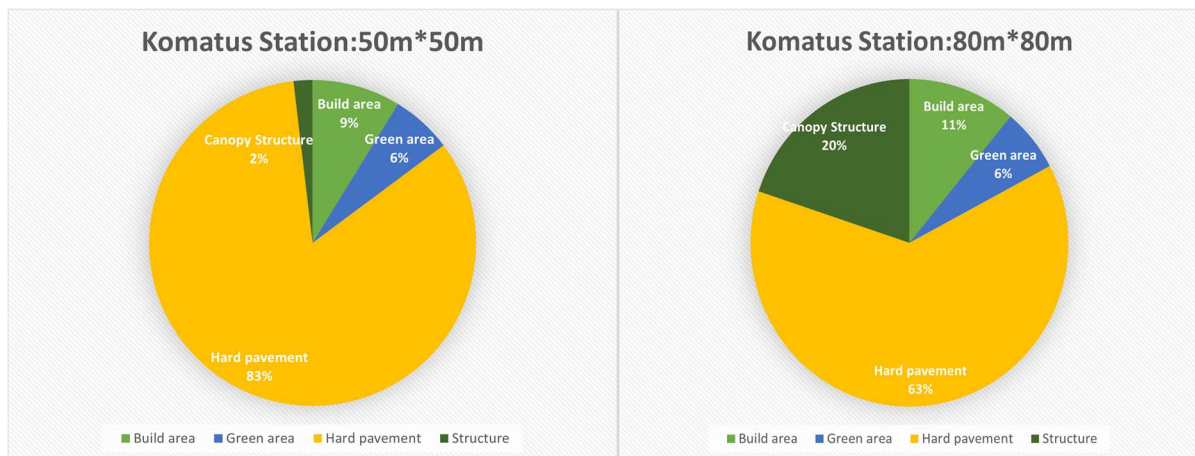


Figure 4.4 Komatsu Station Square (50m × 50m, 80m × 80m) configuration of building area, green area, hard pavement, and canopy structure.

In winter, there are no trees inside the square that can resist the wind, a maximum wind speed of up to 3.6m/s during the afternoon, and the lack of sunlight in the peripheral area has a low utilization rate in Komatsu Square. In summer, around 14:00 is the hottest period, and there are not enough outdoor resting places inside the square to provide shade (Figure 4.5). Providing wind resistance in winter and more shade in summer to regulate the climate effect has become a key landscape design challenge for the local square.



Figure 4.5 Distribution of urban trees and utilization condition of Komatsu Station Square on winter and summer days.

Concerning site surveys and related urban square thermal comfort studies, the contribution and impact of urban trees on the thermal environment of the site are much stronger than other vegetation (turf and shrubs)

(Zheng et al., 2016). Furthermore, in the horizontal structure of the landscape, the landscape design layout facilitates thermal mitigation and promotes the activity behavior and well-being of local pedestrians following the characteristics of the urban climate. In the vertical direction, the vegetation structure is related to wind speed, shade, humidity, and the absorption of thermal radiation (Zölch et al., 2019). Overall, it was found that increasing the thermal comfort of station squares requires the regulatory control of landscape design elements from horizontal and vertical structures.

Table 4.2 Vegetation configuration around the measurement area.

Type	Small-scale (area A)				Large-scale (area B)			
	Vegetation species	Height (m)	Canopy diameter (m)	Tree (n.) /Area (m ²)	Vegetation species	Height (m)	Canopy diameter (m)	Tree (n.) /Area (m ²)
DT	Prunus Lannesiana	5 m	3 m	6	Prunus Lannesiana	5 m	3 m	11
	Cornus Florida	5 m	3 m	3	Corrus Florida	5 m	3 m	25
	Magnolia Denudata	4 m	3 m	4	Magnolia Denudata	4 m	3 m	8
	Zelkova serrata	9 m	9 m	6	Sorbus pohuashanensis	5 m	3 m	3
GT	Cyclobalano-psis glauca	5 m	5 m	2	Machilus	3 m	3 m	2
	Camphor wood	9 m	9 m	5	Myrica rubra	5 m	3 m	1
	Ilex	3 m	3 m	4				
FT	Pinaceae	5 m	3 m	1				
Shrub	Buxus sinica	0.5 m		12.8 m ²	Buxus sinica	0.5 m		124.8 m ²
	Photinia	2 m		9 m ²	Photinia	2 m		64 m ²
Lawn				306 m ²				

4.4.2 Simulation Model with ENVI-met

The numerical simulations of landscape scenarios were implemented by ENVI-met 4.4.5, which typically models the impact of urban planning on environmental variables and microclimate (Salata et al., 2016).

In this study, the simulation area was 32,172 m². It was built within 53 × 30 × 30 grids in the X, Y, and Z directions, where the grid resolution was set to 5 × 5 × 2 m. The model inputs the study area of geographic location and zone time to establish the 3D model and optimize the vegetation, ground, and layout according to the new landscape design scenarios. DT and GT were created using the Alberio tool for tree 3D modeling. The DT type creates a GT by setting the tree calendar parameters. The total simulation time was consistent with the measured time at 24 h. To ensure the accuracy of the model and to reproduce the thermal stresses in the field under extreme climatic conditions, the simulation date was chosen to match the measurement date to facilitate validation and a comparative study. The fundamental parameter settings of the ENVI-met model are

presented in Table 4.3. The initial meteorological parameters of the simulation were derived from on-site measurements (Table 4.1). The analysis of the simulation results was performed at 14:00. The Biomet tool sets the height of the calculated output PMV map at a pedestrian level of 1.8 m.

Table 4.3 Fundamental parameter settings for the ENVI-met model simulation.

Simulation settings	Seasons	Winter	Summer
Meteorological parameters	Total simulation time (h)	24 h	24 h
	Output time interval (min)	60 min	60 min
	Number of nested grids	4	4
	Start of simulation	02/27/2021 at 00:00	08/04/2021 at 00:00
	Min. and max. air temperature (°C)	-0.2 °C, 7.5 °C	25.5 °C, 33.8 °C
	Min. and max. relative humidity in 2 m (%)	33.5%, 73.7%	50.8%, 80.4%
	Wind speed measured at 10 m height (m/s)	3.68 m/s	1.35 m/s
	Wind direction (Deg)	60 Deg	192.18 Deg
	Roughness length at the measurement site	0.01	0.01
	Upper soil layer (0-20 cm) humidity and temperature	16%, 10 °C	32%, 29.6 °C
Soil parameters	Middle soil layer (20-50 cm) humidity and temperature	20%, 15.8 °C	31%, 28.1 °C
	Deep soil layer (50-200 cm) humidity and temperature	20%, 15.2 °C	31%, 28.6 °C
Cloud setting	Fraction of cloud (x/8)	3	1

4.4.3 Thermal Comfort Index-PMV

The PMV thermal index was used to evaluate thermal comfort, as calculated by the ENVI-met model of the Biomet tool. It was calculated by the American Society of Heating Refrigeration and Air Conditioning Engineers (ASHRAE) standard 55-2004 using Fanger's heat balance equation to determine the scale of thermal comfort in Eq. (2) (Rui et al., 2018). The ASHRAE provides guidelines for designers to improve the performance of the building and thermal comfort standards. PMV calculations are based on measurable ambient meteorological parameters (T_a , RH, WS, and T_{mrt}) and two predictive parameters (clothing and metabolic rate), which determine the level of human thermal sensation (Gilani et al., 2015).

$$PMV = [0.028 + 0.303 \cdot \exp(-0.036 \cdot M/A_{Du})] \times (H/A_{du} - E_d - E_{sw} - E_{re} - L - R - C) \quad (2)$$

where M/A_{Du} is the mechanical energy of the body, H/A_{du} is the internal remaining energy, E_d is the vapor diffusion through the skin, E_{sw} is the evaporation of sweat on the skin, E_{re} is latent heat lost through breathing, L is sensible heat exchange through breathing, R is the radiative energy balance of the body, and C is the energy exchange balance of the body.

T_{mrt} reflects the radiant temperature from solar radiation and other material surfaces. It is directly influenced by the spatial layout pattern of vegetation, building morphology, and materials. Referring to the ISO7726 standard, T_{mrt} is calculated using Eq. (3) (Cui et al., 2021).

$$T_{mrt} = [(T_g + 273)^4 + 1.1 \times 10^8 WS^{0.6} / \varepsilon D^{0.4} \times (T_g - T_a)]^{1/4} - 273 \quad (3)$$

where T_g is the globe temperature, T_a is the air temperature, WS is the wind speed, ε is the emissivity of the globe ($\varepsilon = 0.95$), and D is the globe diameter ($D = 0.025$ m).

PMV is based on the Fanger thermal comfort model and the empirical heat balance equation to relate the human energy balance to human thermal sensation. ASHRAE Thermal Sensation (ASH) is a seven-point scale (-3, 3), based on which the outdoor PMV range can be extended from very cold to very hot (-4, +4), with 0 representing a neutral state. However, as the PMV is a mathematical function of the local climate, it can be above or below the (-4, +4) range in most research applications; further, validation is beyond the scale of the Franger experimental data (Gilani et al., 2015; Gatto et al., 2020; Karakounos et al., 2018). In particular, the PMV equation is still applicable for calculating outdoor thermal comfort in extremely cold winter or hot summer conditions (Gatto et al., 2020). The use of PET and the UTCI index to evaluate thermal comfort may yield different results. Hence, a comprehensive analysis of PET and UTCI was not possible in this study; future researchers are recommended to use PET and UTCI to study the effect of landscape configuration conditions on thermal comfort, and to compare the results with PMV (Abdi et al., 2020a).

Chapter 4 concentrates on the mitigation effects of landscape design strategies in extremely poor climates, focusing on the gap between assessing the thermal environment by high and low air temperatures. PMV deviations are closely related to the prevailing mean outdoor air temperature, and the PMV thermal index is more visually clear and easy to observe for the thermal perception scale of very cold and very hot (-4,4).

4.4.4 Greening Indicators

The landscape design involved correlated greening indicators, such as green structure ratio, tree number ratio, and morphological indicators (Rui et al., 2018). This study quantified and used two indicators: green space ratio and tree configuration ratio.

-Green Space Ratio

$$G_A(G_B) = G_a/A_e(B_e) \times 100\% \quad (4)$$

-Tree Configuration Ratio (R_{DT}/R_{GT})

$$R_{DT} = D_i/Q_A(Q_B) \times 100\% \quad (5)$$

$$R_{GT} = G_i/Q_A(G_B) \times 100\% \quad (6)$$

In Eq. (4), G_A and G_B represent the green area ratio within the small-scale area A and large-scale area B, respectively. G_a represents the green area within the simulated area, A_e is the floor area within area A, and B_e

is the floor area within area B.

In Eq. (5) and (6), R_{DT} and R_{GT} represent the DT and GT configuration ratios. D_i and G_i represent the number of deciduous and evergreen trees within the quantification area, respectively. Q_A and Q_B represent the number of trees in areas A and B, respectively.

4.5 Landscape Design Scenarios on Microclimate and Thermal Comfort Regulation of Station Square

New landscape design scenarios were used to optimize the thermal comfort and microclimate at different scales. It was re-landscaped with an equal green space ratio and similar tree quantity at small and large scales, characterized by specific greening indicators in a homogeneous built environment and infrastructure. The layout pattern and vegetation structure were continuously improved to optimize the landscape design in different dimensions. Here, we analyze which layout pattern is better for winter and summer thermal comfort by adjusting the tree configuration ratios. In this respect, the original irregular planting pattern would be regulated to the most common rectangular and circular design pattern, in which the layout would be changed from the original perimeter layout (L1) to the array (L2) and scatter layouts (L3). The array layout and scatter layout by reconfiguring the internal landscape design elements of the square, especially for the combination of deciduous and evergreen tree layout features, can specifically optimize the effect of ventilation and shading in all directions within the rectangular square and has a positive effect on the rearrangement of pedestrian rest areas. These two layouts regulate the problems of cold wind resistance and vegetation growth under the shade of the western buildings in winter when north-westerly winds are prevalent, as well as the problem of shaded resting areas in summer, especially in the eastern area where the deciduous trees are exposed. Finally, 10 landscape design scenarios were created to compare the optimal approaches by adjusting the landscape configuration conditions for thermal comfort and microclimate in winter and summer. They were adjusted from the original L1-1 scenario to nine scenarios from small-scale (area A) to large-scale (area B), as shown in Table 4.4.

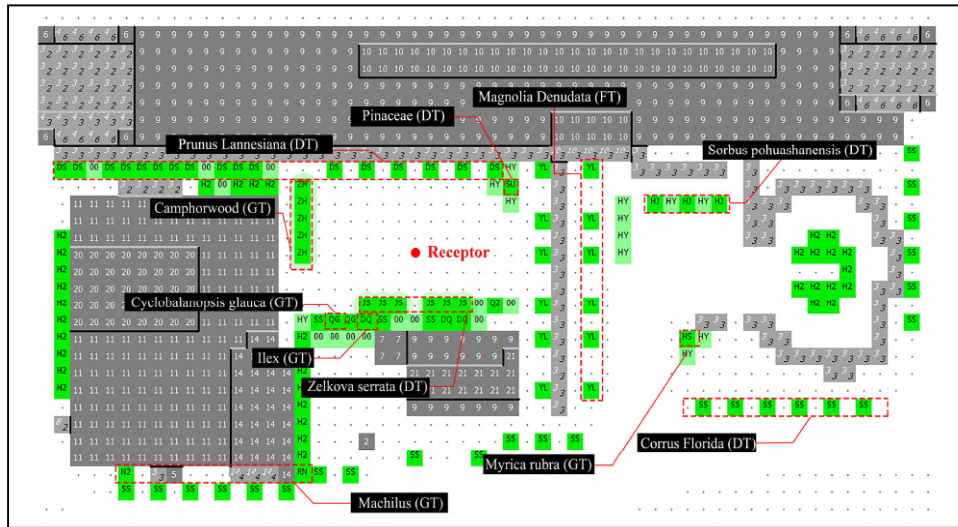
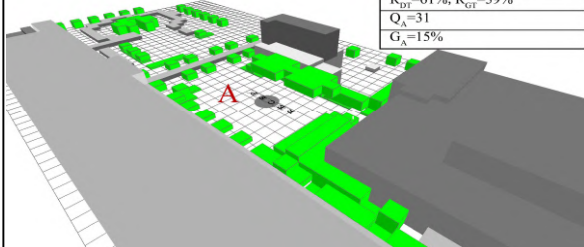
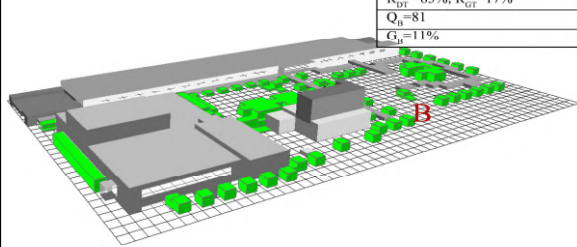
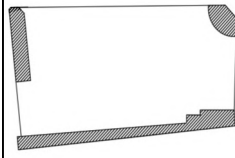
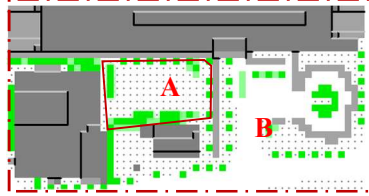


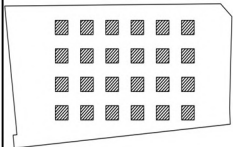

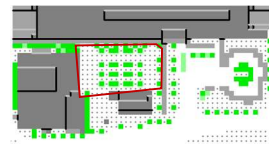

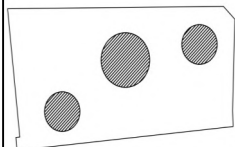
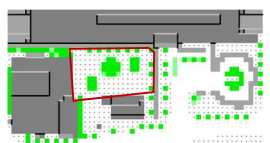

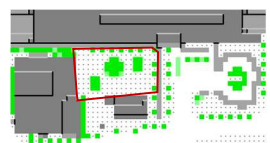
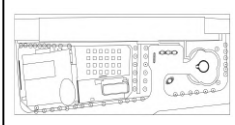


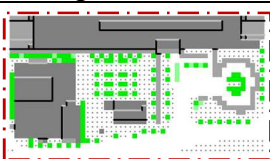


Figure 4.6 Distribution of tree configurations for the original scenario L1-1 in ENVI-met with the receptor.

The new landscape design scenarios further validate and comply with the regulation of the thermal comfort of the Komatsu Station square via landscape design elements and greening indicators. These scenarios were divided into four landscape configuration conditions for quantitative and qualitative comparison: a) layout pattern (L1-1 against L2-1 and L3-1); b) small-scale R_{DT}/R_{GT} (L1-1 against L2-1, L3-1, and L3-2); c) layout pattern, small-scale R_{DT}/R_{GT} , and vegetation structure (L1-1 against L2-2, L2-3, and L3-3); and d) large-scale R_{DT}/R_{GT} (L1-1 against L2-2, L2-2a, L2-2b, L2-2c, and L2-2d). Regarding the original L1-1 scenario, DT was the dominant type of tree distribution in ENVI-met with the receptor (Figure 4.6). The L2-2 and L2-2c scenarios used the same GT type of camphorwood ($LAD = 2$) to represent the remaining DT type in the simulated area.

Table 4.4 Basic conditions of the new landscape design scenarios.

Small-scale landscape design (area A)		Large-scale landscape design (area B)		
<div></div> <div>L1-1(Original scenario) $R_{DT}=61\%$, $R_{GT}=39\%$ $Q_A=31$ $G_A=15\%$</div>		<div></div> <div>L1-1(Original scenario) $R_{DT}=83\%$, $R_{GT}=17\%$ $Q_B=81$ $G_B=11\%$</div>		
Area A	Simulation scenarios with different vegetation configurations			
<div></div> <div>L1Peripheral layout</div>	<div></div> <div><div>Small-scale</div><div>Large-scale</div></div>			
Scenario L1-1				
<div></div> <div>L2Array layout</div>	<div></div> <div>Scenario L2-1</div> <div>$R_{DT}=60\%$, $R_{GT}=40\%$ $Q_A=34$ $G_A=15\%$</div>	<div></div> <div>Scenario L2-2</div> <div>$R_{DT}=0\%$, $R_{GT}=100\%$ $Q_A=34$ $G_A=15\%$</div>	<div></div> <div>Scenario L2-3</div> <div>$R_{DT}=100\%$, $R_{GT}=0\%$ $Q_A=34$ $G_A=15\%$</div>	
	<div></div> <div>L3Scatter layout</div>	<div></div> <div>Scenario L3-1</div> <div>$R_{DT}=60\%$, $R_{GT}=40\%$ $Q_A=34$ $G_A=15\%$</div>	<div></div> <div>Scenario L3-2</div> <div>$R_{DT}=50\%$, $R_{GT}=50\%$ $Q_A=34$ $G_A=15\%$</div>	<div></div> <div>Scenario L3-3</div> <div>$R_{DT}=0\%$, $R_{GT}=0\%$ Cover grass $G_A=15\%$</div>
		Area B	Simulation scenarios with different vegetation configurations	
<div></div> <div>Scenario L2-2</div> <div>$R_{DT}=70\%$, $R_{GT}=30\%$ $Q_B=84$ $G_B=11\%$</div>		<div></div> <div>Scenario L2-2a</div> <div>$R_{DT}=50\%$, $R_{GT}=50\%$ $Q_B=84$ $G_B=11\%$</div>	<div></div> <div>Scenario L2-2b</div> <div>$R_{DT}=20\%$, $R_{GT}=80\%$ $Q_B=84$ $G_B=11\%$</div>	<div></div> <div>Scenario L2-2c</div> <div>$R_{DT}=0\%$, $R_{GT}=100\%$ $Q_B=84$ $G_B=11\%$</div>

4.6 Results

4.6.1 Model validation

To calibrate and improve the accuracy of the ENVI-met model, focusing on validating the microclimate parameters of T_a combined with statistical indexes, we used R^2 and RMSE as the statistical indexes. Stocco et al. (2021) verified R^2 values to be from 0.9 to 1.0 and RMSE to be from 1.0 to 2.5 for T_a in urban square design scenarios. Furthermore, the closer R^2 is to 1, the closer the RMSE is to 0, indicating that the simulation results have minor errors (López-Cabeza et al., 2018). The simulated and measured T_a of February 27 was compared by linear regression to test the spatial grid size to determine the modeling performance, as shown in Figure 4.7. The performance was derived from a grid sensitivity analysis, where the results provided by models with different horizontal grid sizes ($2 \times 2 \text{ m}^2$, $5 \times 5 \text{ m}^2$, $10 \times 10 \text{ m}^2$, $10 \times 10 \text{ m}^2$, $15 \times 15 \text{ m}^2$) were compared with the on-site measurement values. The comparison results revealed that when a smaller grid was used in the model, the simulation time increased and the degree of fit of the simulation deviated. Table 4.5 and Figure 4.7 indicate that R^2 and RMSE were very close for all simulation runs. An R^2 of 0.976 and an RMSE of 0.242 in Running 2) were the best predictors of T_a . Then, Running 2) was used as a reliable model to evaluate thermal comfort and microclimate variations for the new landscape design scenarios.

Table 4.5 Validation accuracy performance of air temperature (T_a) in ENVI-met model simulations for running four times with statistical indexes of the coefficient of determination (R^2) and the root mean squared error (RMSE).

Settings	R^2	RMSE
Running 1) Grid size of $2 \times 2 \text{ m}^2$	0.959	0.279
Running 2) Grid size of $5 \times 5 \text{ m}^2$	0.976	0.242
Running 3) Grid size of $10 \times 10 \text{ m}^2$	0.955	0.306
Running 4) Grid size of $15 \times 15 \text{ m}^2$	0.951	0.337

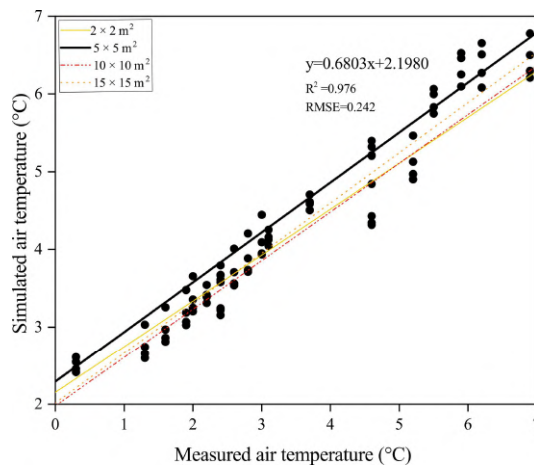


Figure 4.7 Validation results of coefficient of determination (R^2) and the root mean squared error (RMSE) by forcing simulated and measured air temperature (T_a) in a grid sensitivity analysis on February 27, 2021 (24 h).

4.6.2 Variations in Winter Microclimate Parameters

The original scenario L1-1 simulation was based on the most accurate model, as shown in Figure 4.8. The corresponding ENVI-met microclimate simulation scenarios were created using quantitative and qualitative analyses of landscape design elements and indicators. T_a , RH, WS, and T_{mrt} are the critical parameters for analyzing microclimate conditions (Liang Chen & Ng, 2012b; Huang & Peng, 2020a). Figure 4.8 and Table 4.6 present simulation variations in winter microclimate parameters compared to on-site measurements on February 27, 2021.

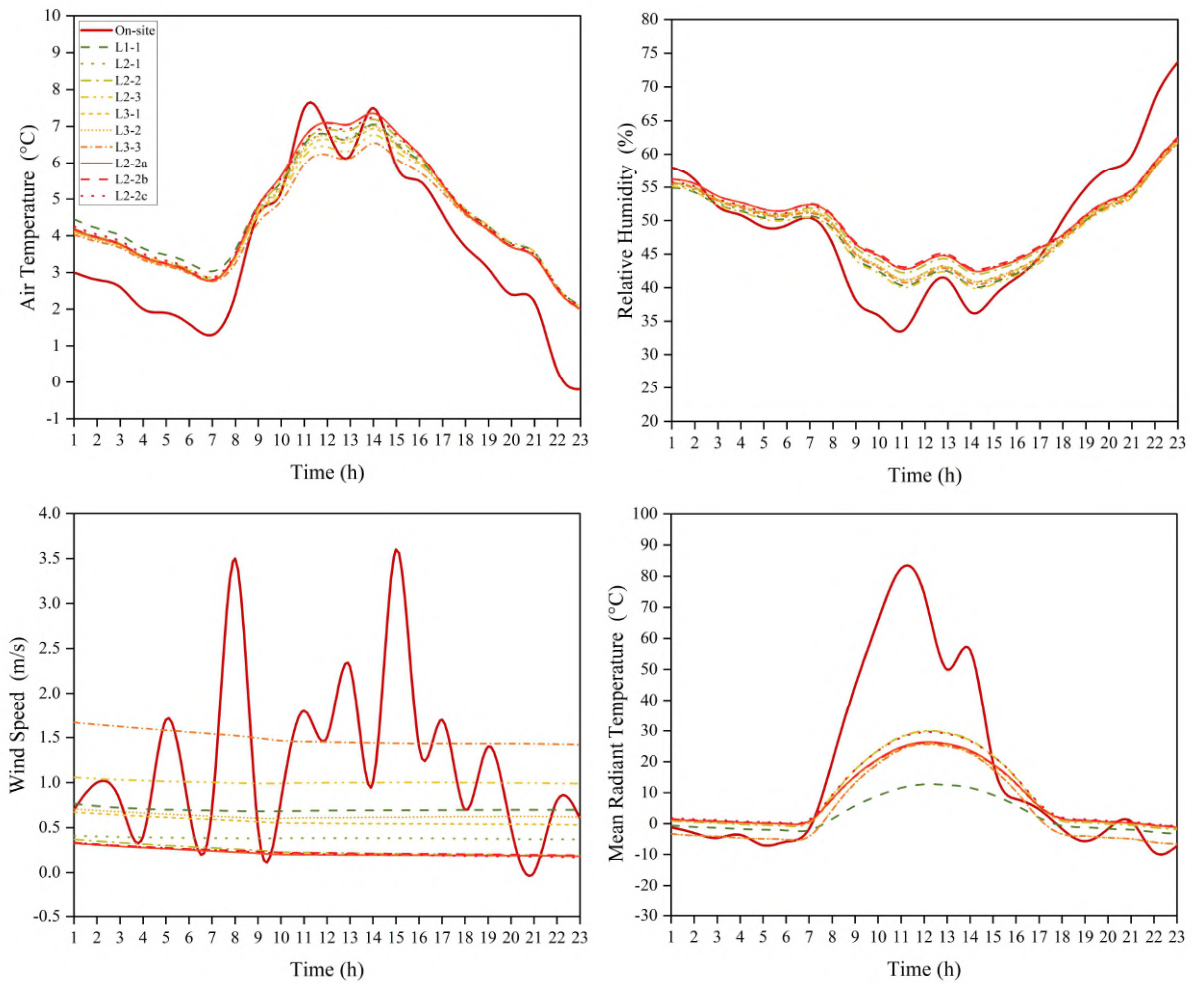


Figure 4.8 Variations of winter simulation microclimate parameters (T_a , WS, RH, and T_{mrt}) for 10 scenarios compared to on-site measurements.

The microclimate parameters varied mainly during daytime. T_a and RH were closer to the on-site measurements (Figure 4.8). WS and T_{mrt} were more variable than measured values. The primary reason is that the ENVI-met model is set in the simple force mode, where the WS simulations remain relatively stable and differ significantly (Zölch et al., 2019). The highest T_a was in the L2-2b, L2-2c, and L2-2a scenarios relative to the L1-1 scenario (Figure 4.8). The results showed that the effect of the array layout was relatively

significant in winter T_a , with the opposite effect of the scattered layout in the L3-3 scenario ($R_{DT}/R_{GT} = 0\%/0\%$).

In WS simulations, the prevailing northerly winds had the most significant impact on thermal comfort, with all scenarios remaining in a steady-state (0-2 m/s). The mean WS maximum value was 1.49 m/s in winter for the L3-3 scenario without trees. The mean WS minimum value of 0.22 m/s was simulated for both L2-2a ($R_{DT}/R_{GT} = 50\%/50\%$) and L2-2c scenarios ($R_{DT}/R_{GT} = 0\%/100\%$) (Table 4.6). A total of 80% of the simulated scenarios reduced the WS, and the maximum decrease was found in large-scale scenarios. These results indicated that planting trees in the L2 layout pattern is advantageous for wind resistance in winter.

In the RH simulations, the mean RH of the L1-1 scenario remained at a difference of 0.48% compared with on-site. The simulated results were consistent with the measured results (Table 4.6). A total of 90% of the simulated scenarios improved the RH through landscape configuration conditions. The simulated mean RH increased to a maximum of 1.21% for the L2-2b scenario ($R_{DT}/R_{GT} = 20\%/80\%$).

For T_{mrt} , increasing the thermal radiation in winter facilitates mobility for the surrounding pedestrians. The simulated T_{mrt} increased gradually in all scenarios according to the landscape configuration conditions. The maximum simulated T_{mrt} is 29.98 °C, while the minimum is -6.52 °C. The mean T_{mrt} increased by a maximum of 6.9 °C compared to the L1-1 scenario (Table 4.6). The simulations showed that the L2-3 scenario ($R_{DT}/R_{GT} = 100\%/0\%$) had the lowest T_{mrt} , and the L2-2c scenario had the highest T_{mrt} for all L2 series. The results verified that the GT configuration had a significant impact on T_{mrt} improvement in winter.

Microclimate meteorological parameters varied significantly between 10:00 and 16:00, while the opposite occurred during the night (Figure 4.8). The L2-2c scenario showed the best improvement in winter microclimate conditions for all simulated scenarios, followed by the L2-2b and L2-2a scenarios. This further indicates that the large-scale tree configuration ratio was positive for winter microclimate improvement.

4.6.3 Variations in Summer Microclimate Parameters

Figure 4.9 and Table 4.7 show the simulation variations in summer microclimate parameters for 10 scenarios compared to on-site measurements on August 4, 2021.

The simulated microclimate parameters varied mainly during the day. In the T_a simulation, the lowest T_a was in the L2-2c scenario relative to the L1-1 scenario (Figure 4.9). The maximum simulated T_a was 33.99 °C, while the minimum was 25.20 °C (Table 4.7). In addition, the scattered layout of the L3 series scenario reached a peak of T_a at 14:00, while T_a rose by 0.7 °C in the L3-2 scenario (Figure 4.9). In contrast, the mean T_a was reduced by a maximum of 1 °C with the large-scale tree-configuration ratio intervention. The L2-2c scenario simulated a maximum T_a reduction of 1.5 °C at 07:00, 0.9 °C at 14:00, and 1 °C at 23:00.

For all scenarios, the WS simulations have a discrepancy relative to the measured WS distribution. The results showed a steady state (0-1 m/s) (Table 4.7). The mean WS was lowered by the maximum of 0.55 m/s relative to the L1-1 scenario. In contrast, the L2-2 scenario had the worst summer ventilation, indicating that the array-planting layout impeded the wind flow in summer.

For RH, the distribution of the simulated RH results followed a trend consistent with the measured results (Figure 4.9). The maximum was 84.95%, and the minimum was 57.09% for the overall simulated RH (Table 4.7). The highest mean RH increased by 5.73% relative to the L1-1 scenario, with the best humidification

effect in the L2-2c scenario.

For T_{mrt} , the lowest T_{mrt} was the L2-2c scenario during the daytime and the lowest for the L2-1 scenario at night relative to the L1-1 scenario (Figure 4.9). The maximum simulated T_{mrt} was 67.67 °C, and the minimum was 21.02 °C (Table 4.7). Mean T_{mrt} had the highest reduction of 6.69 °C relative to the L1-1 scenario. The highest reduction was 18 °C observed at 14:00. The intervention under optimal regulation significantly reduced the mean T_{mrt} for all scenarios, and the reduction in radiant temperature improved thermal comfort. In addition, shading is an important factor in reducing T_{mrt} , which is why the L2-2c scenario with predominantly evergreen tree planting obtains a better cooling effect in summer during the daytime.

From Table 4.7, the most significant variations in microclimate conditions were observed in the L2-2c scenario, which was dominated by a decrease in T_a , WS, and T_{mrt} . The microclimate conditions were also optimized in the L2-2 scenario, followed by the L2-2b scenario. However, the reduction in wind speed affected airflow and ventilation. In comparison, the variations in winter and summer conditions were optimal for the L2-2c scenario. Thus, it is suitable for local seasonal changes and characteristics. Compared to the landscape layout pattern, L2 more effectively improved the microclimate environment of the station square. Regarding the adjustment of vegetation structure, the single structure of cover grass in the L3-3 scenario negatively affects microclimate conditions. Consequently, adjusting the tree configuration ratios at the large-scale, compared to the small scale, achieved the best optimal improvement for microclimate conditions.

Table 4.6 Maximum, minimum, and mean values of the winter simulation microclimate parameters (T_a , WS, RH, and T_{mrt}) relative to on-site measurements.

Scenario	T_a (°C)				WS (m/s)				RH (%)				T_{mrt} (°C)			
	Max	Min	Mean	Mean relative to on-site	Max	Min	Mean	Mean relative to on-site	Max	Min	Mean	Mean relative to on-site	Max	Min	Mean	Mean relative to on-site
L1-1	7.05	2.10	4.61	1.00	0.77	0.68	0.70	-0.52	61.67	40.22	48.43	-0.49	12.71	-3.30	2.59	-13.69
L2-1	7.07	2.03	4.52	0.91	0.41	0.37	0.38	-0.84	61.99	41.08	48.90	-0.02	29.79	-1.31	9.22	-7.06
L2-2	7.20	2.02	4.55	0.94	0.37	0.19	0.24	-0.98	62.10	42.20	49.53	0.61	29.81	-1.28	9.24	-7.05
L2-3	6.77	2.08	4.44	0.83	1.06	0.99	1.01	-0.21	61.57	40.04	48.24	-0.68	25.90	-6.52	4.62	-11.66
L3-1	6.94	1.98	4.43	0.82	0.67	0.53	0.57	-0.65	62.04	41.00	48.98	0.06	29.98	-1.87	8.91	-7.37
L3-2	7.01	1.99	4.45	0.84	0.71	0.60	0.63	-0.59	61.91	41.01	49.06	0.14	25.86	-1.41	7.88	-8.41
L3-3	6.54	2.00	4.29	0.68	1.67	1.42	1.49	0.27	61.59	40.66	48.75	-0.17	25.63	-6.52	4.54	-11.74
L2-2a	7.36	1.99	4.58	0.97	0.33	0.18	0.22	-1.00	62.42	42.58	49.99	1.07	26.32	-1.13	8.22	-8.07
L2-2b	7.36	2.01	4.60	0.99	0.33	0.19	0.23	-0.99	62.53	42.88	50.13	1.21	26.08	-0.97	8.24	-8.05
L2-2c	7.25	2.07	4.60	0.99	0.33	0.17	0.22	-1.00	62.19	42.72	49.82	0.90	29.55	-0.77	9.49	-6.79

Table 4.7 Maximum, minimum, and mean values of the summer simulation microclimate parameters (T_a , WS, RH, and T_{mrt}) relative to on-site measurements.

Scenario	T_a (°C)				WS (m/s)				RH (%)				T_{mrt} (°C)			
	Max	Min	Mean	Mean relative to on-site	Max	Min	Mean	Mean relative to on-site	Max	Min	Mean	Mean relative to on-site	Max	Min	Mean	Mean relative to on-site
L1-1	33.33	26.41	30.06	-0.23	0.81	0.73	0.76	0.19	79.98	57.09	68.33	1.69	67.67	16.71	38.53	-10.26
L2-1	33.60	26.01	30.05	-0.24	0.38	0.29	0.34	-0.23	81.84	57.12	69.09	2.45	61.90	10.51	33.12	-15.68
L2-2	33.19	25.75	29.60	-0.69	0.26	0.14	0.18	-0.39	83.24	62.93	72.83	6.19	54.94	21.17	34.56	-14.23
L2-3	33.26	26.28	29.94	-0.35	0.57	0.48	0.52	-0.05	80.48	57.19	68.72	2.08	65.16	14.13	34.41	-14.39
L3-1	33.76	25.87	29.86	-0.43	0.34	0.22	0.27	-0.30	82.61	60.00	71.17	4.54	56.20	21.02	34.54	-14.25
L3-2	33.99	25.94	29.96	-0.33	0.35	0.27	0.30	-0.27	82.25	58.38	70.44	3.81	48.96	20.84	31.84	-16.96
L3-3	33.79	25.86	29.87	-0.42	0.32	0.21	0.26	-0.31	82.68	60.40	71.33	4.69	55.24	20.70	34.03	-14.77
L2-2a	33.51	26.30	30.13	-0.16	0.45	0.36	0.40	-0.17	80.31	57.60	68.48	1.85	54.42	20.62	34.09	-14.71
L2-2b	32.86	26.00	29.68	-0.61	0.39	0.27	0.32	-0.25	81.77	61.39	70.96	4.32	54.32	21.12	33.75	-15.05
L2-2c	32.42	25.20	29.06	-1.24	0.26	0.17	0.21	-0.36	84.95	63.48	74.06	7.42	50.86	21.04	32.79	-16.01

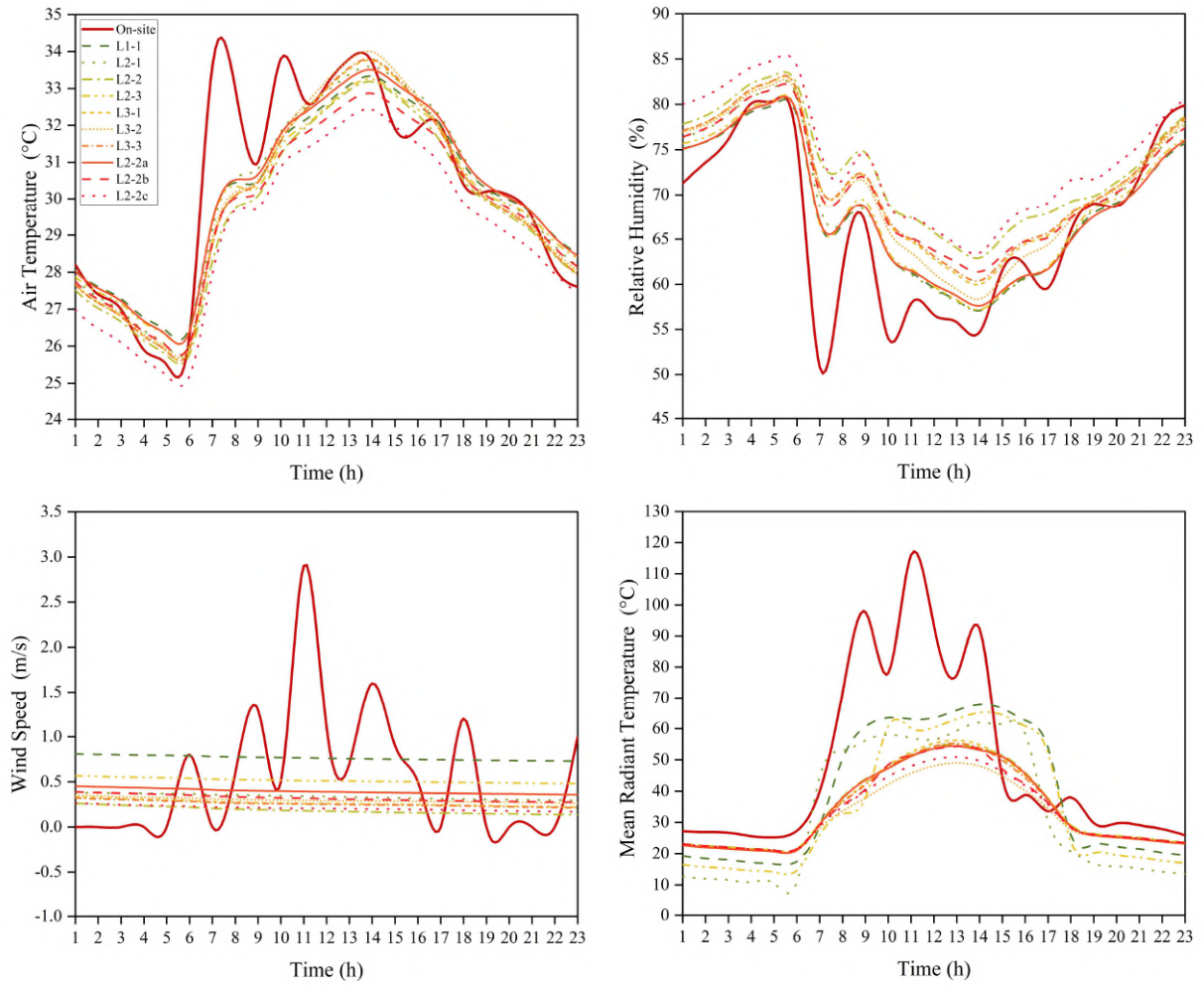


Figure 4.9 Variations of summer simulation microclimate parameters (T_a , WS, RH, and T_{mrt}) for 10 scenarios compared to on-site measurements.

4.6.4 Thermal Environment Mitigation by Landscape Designs

This study validated thermal comfort regulation in winter and summer using landscape design elements and indicators. The thermal comfort levels for the new landscape design scenarios were analyzed under configuration conditions (a, b, c, and d) described in detail in Section 4.5.

(1) Analysis of thermal comfort improvements in winter

The PMV varied significantly between 10:00 and 16:00 in all scenario simulations; the results indicated a more pronounced improvement in thermal comfort during the daytime in winter. The simulation of a very cold condition gradually results in the scenario being between cold and very cold during the day ($-4 < PMV < -3$) through the optimizing landscape configuration conditions. In the L1-1 against L2-1 and L3-1 scenarios, the PMV values remained almost identical in the latter two scenarios (Q_A , small-scale R_{DT}/R_{GT} , and G_A were similar). The thermal comfort varied very little when regulating the landscape layout patterns (Figure 4.10a). In the L1-1 against L2-1, L3-1, and L3-2 scenarios, the PMV values were significantly reduced when the R_{DT}/R_{GT} was changed from 60% / 40% to 50% / 50%. It directly affected thermal comfort during the day and

night (Figure 4.10b). In the L1-1 against the L2-2, L2-3, and L3-3 scenarios, the PMV varied significantly during the day for the L2-2 scenarios under the same G_A . The winter thermal comfort ranking compared to the L1-1 scenario, in order, varied as follows: $L2-2 > L2-3 > L3-3 > L1-1$ (Figure 4.10c). In the L1-1 scenario against the L2-2, L2-2a, L2-2b, and L2-2c scenarios, the all-day PMV varied with the R_{DT}/R_{GT} , resulting in a significant alteration in thermal comfort during both day and night. The L2-2 and L2-2c scenarios were more optimal than the others (Figure 4.10d).

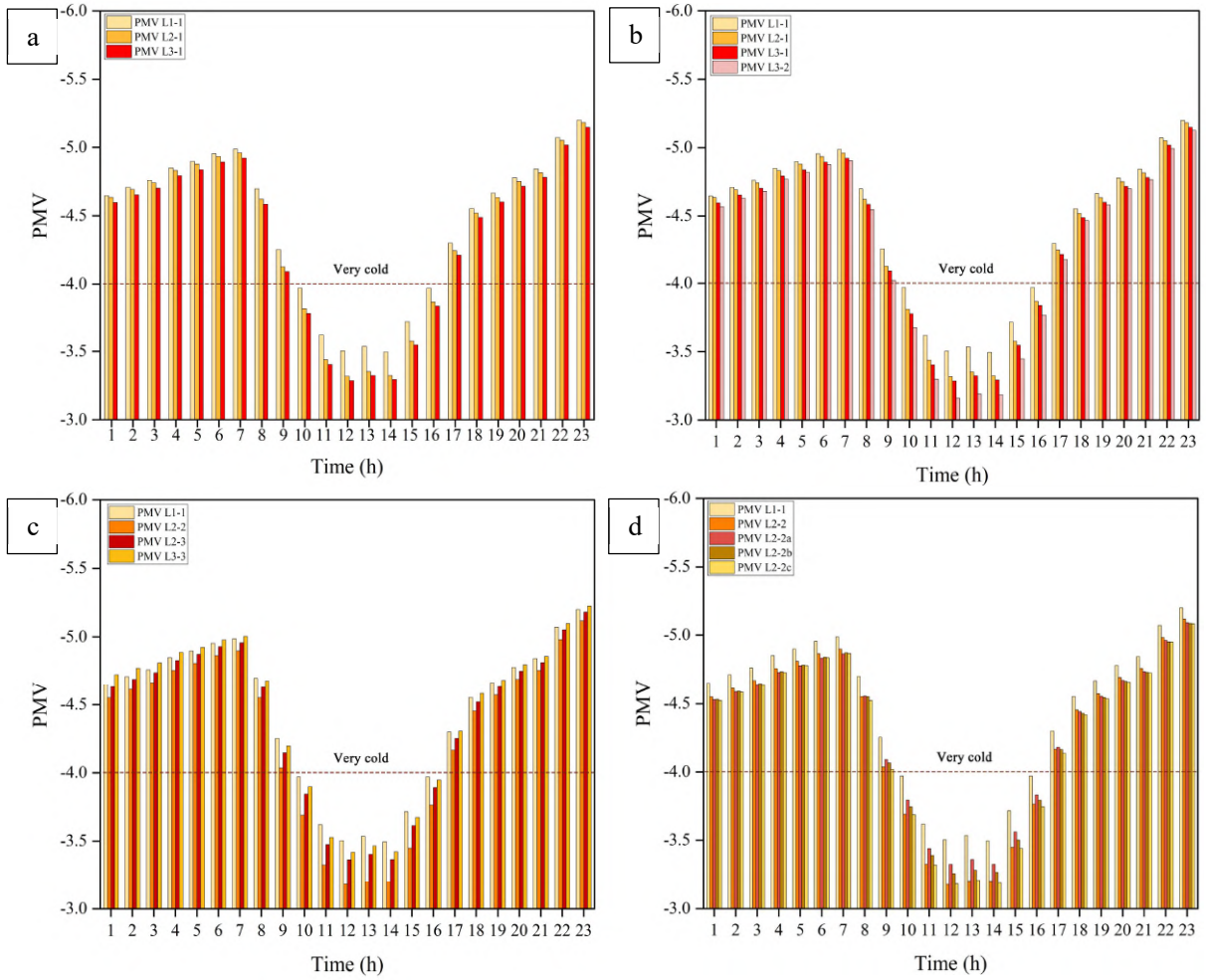


Figure 4.10 PMV distribution (at 1.8 m height) of winter simulated scenarios at configuration conditions (a, b, c, and d).

(2) Analysis of thermal comfort improvements in summer

As shown in Figure 4.11, we analyzed and simulated the thermal comfort variations of 10 scenarios in summer under the configuration conditions.

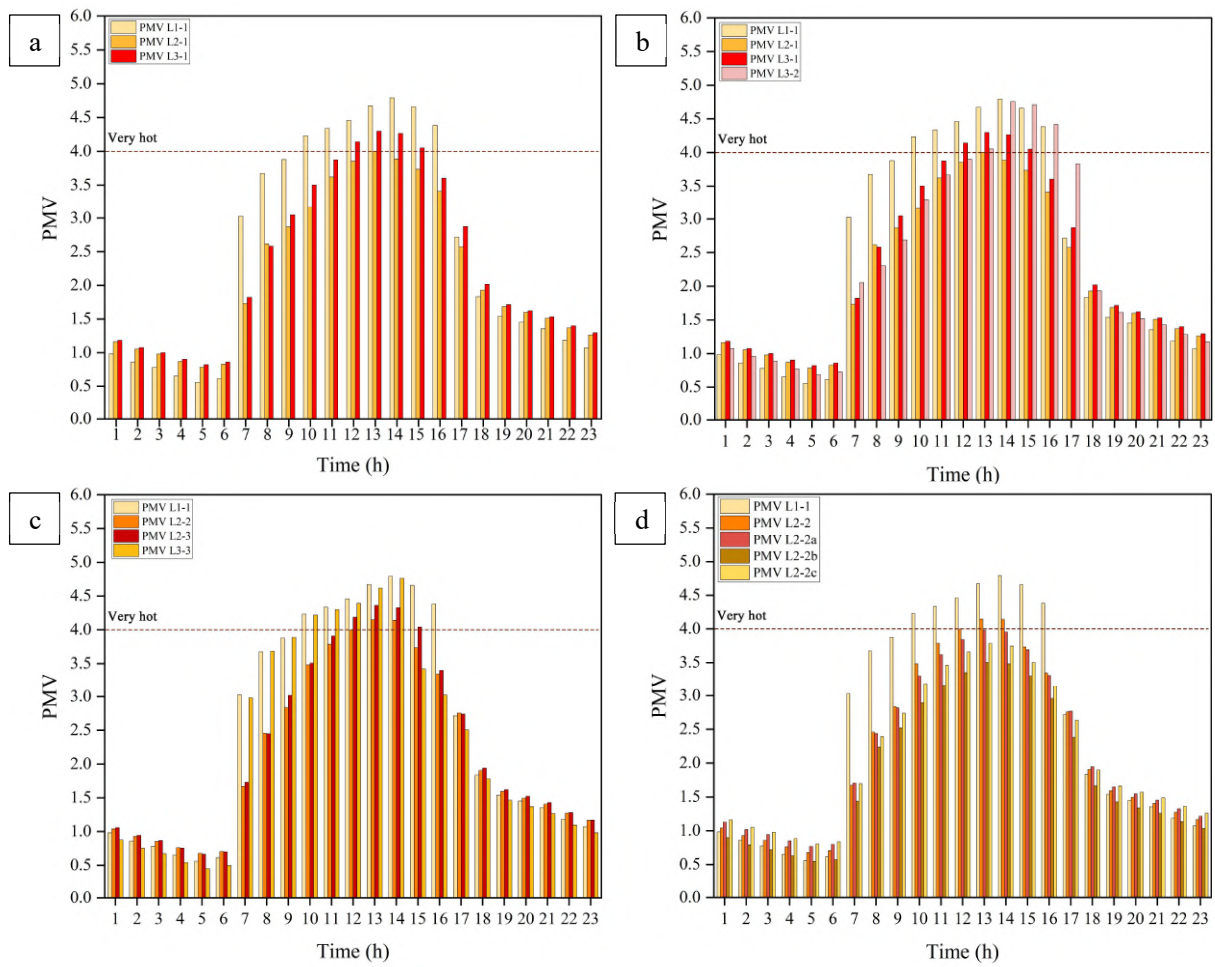


Figure 4.11 PMV distribution (at 1.8 m height) of summer simulated scenarios at configuration conditions (a, b, c, and d).

In the summer daytime simulation, the L1-1 scenario shows extreme thermal pressure ($PMV > 4$) from 10:00 to 16:00, with thermal comfort at night in warm and slightly warm conditions. The highest PMV of the day reached 4.79 in the L1-1 scenario. The PMV distribution was reduced by adjusting the configuration conditions during the extremely hot daytime. Under configuration conditions (a), the mean PMV varies over a range of 0.31 more optimally than the mean PMV variation in winter (Figure 4.11a). Under configuration conditions (b), the L2-1 scenario optimizes the performance of summer thermal comfort better, with improvements during the day (Figure 4.11b). Under configuration conditions (c), the L2-2 (Cover GT) scenario had the best optimized summer thermal comfort performance during the day, while the L3-3 (Cover grass) scenario had the best optimized thermal performance during the night. Optimal performance during the day was ranked in the order of $L2-2 > L2-3 > L3-3 > L1-1$ (Figure 4.11c). Under configuration conditions (d), the mean PMV of the L2-2b scenario was reduced by a maximum of 0.63 PMV relative to the L1-1 scenario, which improved thermal comfort during the day and night (Figure 4.11d). The thermal comfort changed from very hot to hot ($3 < PMV < 4$). The L2 series scenarios performed most optimally. In particular, the adjustment of the large-scale tree configuration ratios significantly reduced the thermal stress on a hot day.

4.6.5 The Optimized Scenarios and Thermal Conditions

The ENVI-met scenarios compared the standard error (SD), diurnal variation values, and mean PMV for 24 h. The PMV errors of the new scenarios against the L1-1 scenario during the co-optimum period are presented in Figure 4.12. The co-optimum period is up to 9 h from 08:00 to 16:00 in winter and up to 10 h from 07:00 to 16:00 in summer under landscape configuration conditions. In Figure 4.12, yellow indicates the winter simulation results, and green indicates the summer simulation results. The final ranking of the top four optimized scenarios for mean PMV in winter is L2-2c > L2-2 > L2-2b = L3-2, and in summer is L2-2b > L2-2c > L2-2a = L2-2. There was a maximum increase of 0.33 PMV at 13:00 in winter and a maximum decrease of 1.59 PMV at 07:00 in summer compared to the L1-1 scenario. The L2-2c and L2-2b scenarios achieved the best co-optimization in winter and summer.

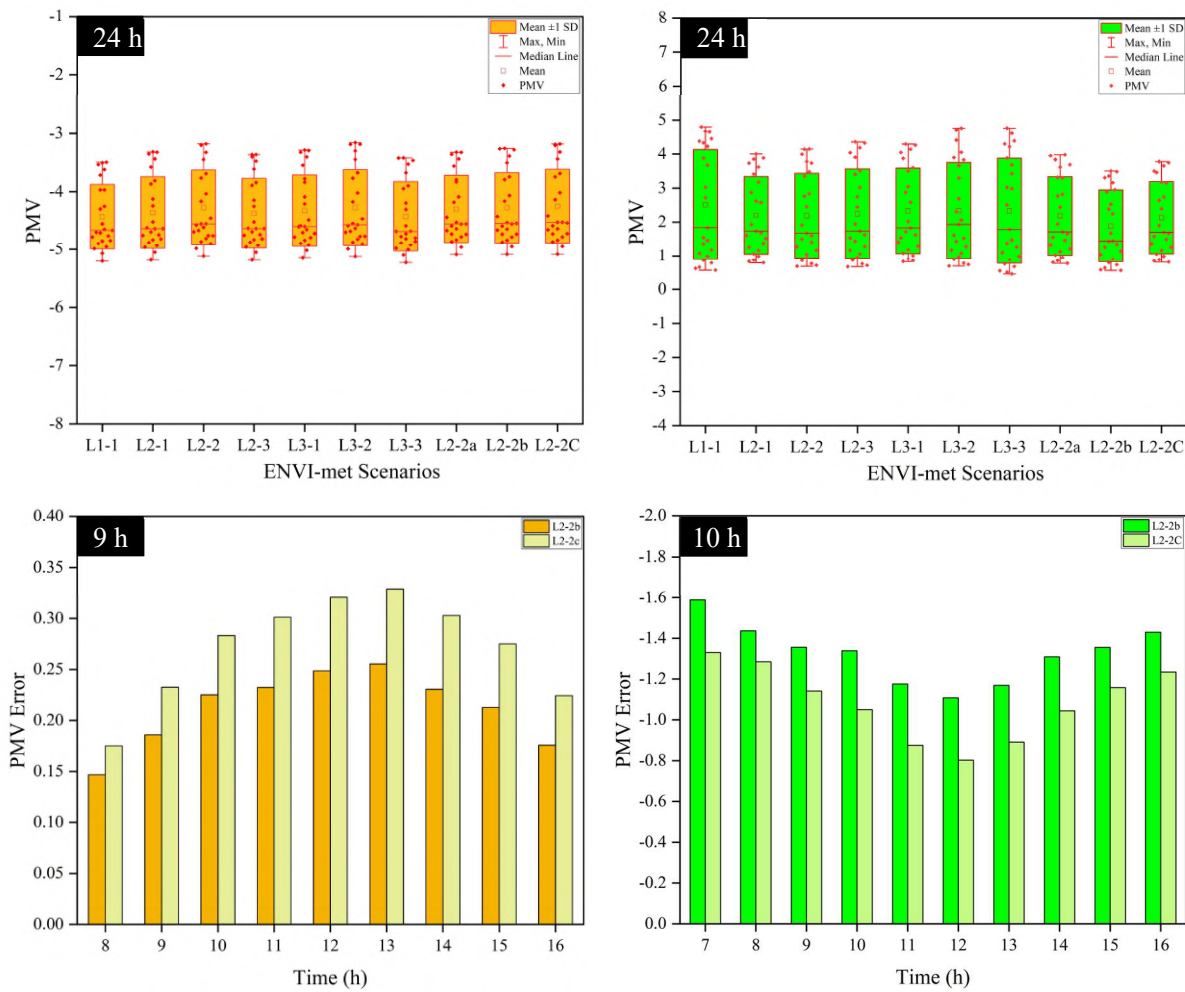


Figure 4.12 PMV results of 24 h, and distribution of PMV error results (L2-2b and L2-2c scenarios against L1-1 scenario) at the co-optimum period (at 1.8 m height) in winter and summer.

(1) Air temperature

Based on the microclimate and thermal comfort simulation results, T_a and T_{mrt} were considered the main parameters for thermal condition comparison. The simulated T_a in the co-optimized scenarios was compared

to the L1-1 scenario for analysis at 14:00 (Figure 4.13). The maximum mean T_a in winter increased by 0.31 °C for the L2-2b scenario. In contrast, the L2-2c scenario reduced the mean T_a by 1 °C than the L1-1 scenario in summer.

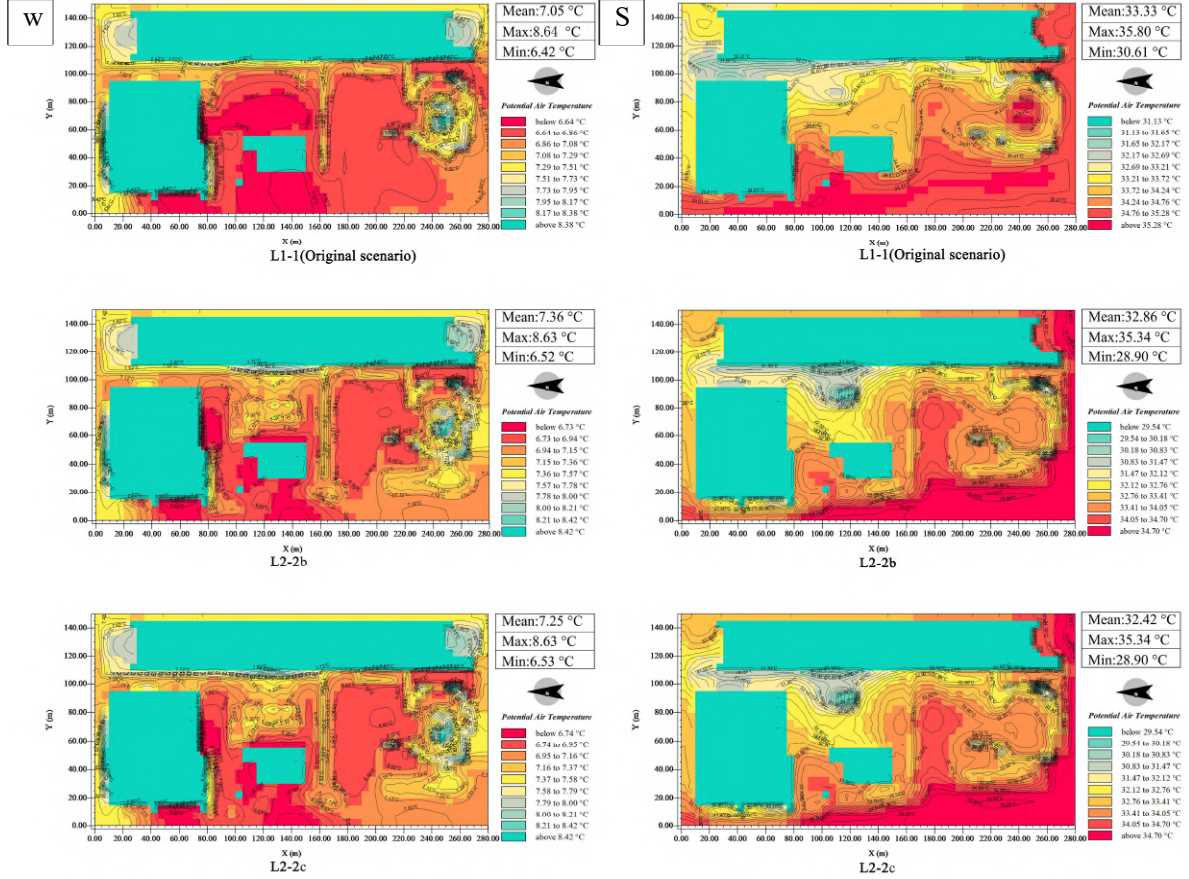


Figure 4.13 Simulated T_a maps of winter (W) and summer (S) in the original L1-1 scenario and co-optimized scenarios (L2-2b and L2-2c) at 14:00 (at 1.8 m height).

(2) Mean radiant temperature

T_{mrt} changed significantly with the large-scale tree configuration ratio in the L2-2c scenario. The mean T_{mrt} was 15.08 °C higher than that of the L1-1 scenario in winter, while it was 18.05 °C lower in summer. The results showed an increased radiant temperature during winter and cooling in summer. On the simulated T_{mrt} maps, the thermal environment of the outer streets improved in winter by 1.79 °C and reduced in summer by 15.82 °C (Figure 4.14).

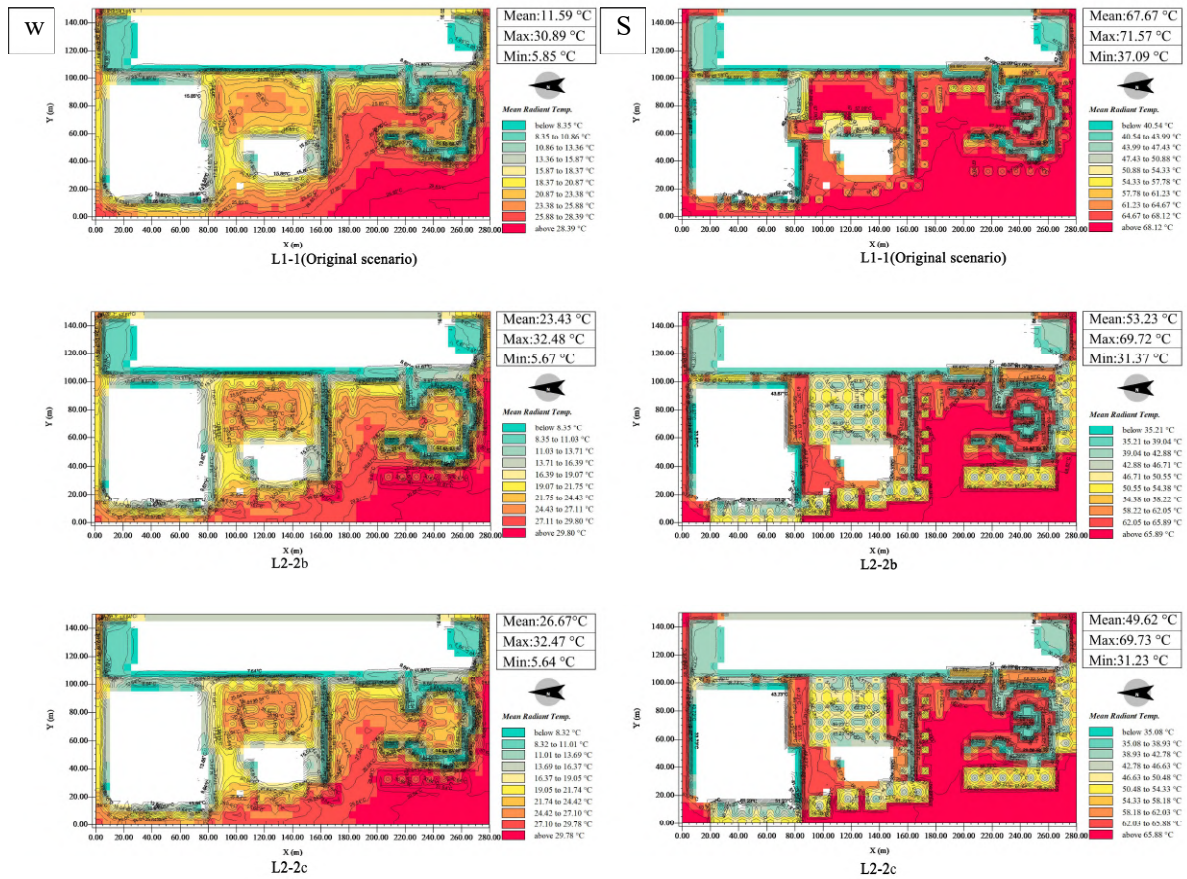


Figure 4.14 Simulated T_{mrt} maps of winter (W) and summer (S) in the original L1-1 scenario and co-optimized scenarios (L2-2b and L2-2c) at 14:00 (at 1.8 m height).

4.6.6 The PMV Thermal Index Map

According to the configuration conditions (a, b, c, and d), the PMV thermal index maps generated local variations at 14:00 at a height of 1.8 m. The configuration conditions yield new scenarios that do not fully satisfy both the winter and summer thermal comfort (Figure 4.15).

From the winter simulation, the PMV varied, with the landscape configuration conditions remaining stable. While the landscape layout patterns affected the local thermal index PMV distribution, the PMV maximum value was -3.2 at 14:00. The mean increased by 0.3 PMV for the L3-2 scenario compared with the L1-1 scenario. This indicated better thermal comfort in winter when different R_{DT}/R_{GT} and vegetation structures were adjusted. In comparison, the best winter thermal comfort effect with different structures was $GT > DT > Grass$. The mean PMV of the L2-2 scenario was 0.29 lower than that of the L1-1 scenario and differed from the L2-3 scenario by 0.16. The L2-2c scenario was based on the L2-2 scenario (the G_B , Q_B , and vegetation structure were the same), and the R_{DT}/R_{GT} was reconfigured. The mean PMV varied range from -3.19 to -3.49. The maximum improvement of the 0.3 PMV. These results indicate that the L2-2c scenario exhibits the best improvement in winter thermal comfort.

In the summer simulation, the first analysis was the configuration condition (a). The corresponding

scenarios with similar vegetation configurations had mean PMV values between 3.89 and 4.79. The mean PMV continued to vary around 0.9. For the L3-2 scenario, the mean PMV was similar to that of the L1-1 scenario. The L3-3 scenario reached peak PMV in summer. Moreover, the mean PMV was 3.48 in the L2-2b scenario, which reached optimum thermal comfort. At 14:00, Figure 4.15 shows a PMV 1.3 lower than the L1-1 scenario under the hot level. It altered the extremely hot conditions around the station square, especially from 07:00 to 16:00 (Figure 4.12).

This study evaluated winter and summer thermal comfort concerning spatial scales, landscape design elements, and green indicators. For the small-scale adjustment, the L2-2 scenario has the most optimal winter and summer thermal performance at 14:00, with improvements of 0.3 PMV in winter and reductions of 0.65 PMV in summer, respectively. By adjusting the landscape layout pattern, the study found a minor effect in improving the thermal environment, in contrast to adjusting the large-scale tree configuration ratio, which improved thermal comfort and microclimate conditions in winter and summer. At 14:00, the L2-2c scenario increased PMV by a maximum of 0.3 to improve extremely cold winter conditions, whereas L2-2b decreased PMV by 1.3, thereby improving extremely hot summer conditions. The thermal improvement was better in summer than in winter. The L2-2c and L2-2c scenarios achieved the best optimized thermal conditions in both winter and summer, but the large scale was superior to the small-scale at the same simulated receptor.

4.7 Discussion

Scale, duration, and seasonal variation are essential concerns for improving the microclimate and thermal comfort using ENVI-met simulations. This study showed that an enclosed station square is more suitable for an array landscape layout pattern. Variations in the tree configuration ratios at a large scale positively affect thermal comfort in winter and summer, especially during the day and night.

4.7.1 Landscape Layout Pattern Improvement Effect

The landscape layout pattern is an important greening horizontal indicator that contributes to thermal mitigation, which is strongly related to tree planting designs (Gaspari et al., 2018; Z. Liu et al., 2021; Yujun Yang et al., 2018). In addition, the PMV values vary by the planting patterns. For example, the PMV index is lower in rectangular vegetation layouts than in randomly arranged layouts, as observed in (El-Bardisy et al., 2016; Abdi et al., 2020a).

Here, L2 with an array layout with a rectangular pattern and landscape scenarios were more successful in optimizing thermal comfort performance under configuration conditions (c) and (d). The contribution was small through a variable only in the landscape layout patterns to the thermal comfort improvement effect, which is similar to the findings of (B. Hong & Lin, 2015) and (Gaspari et al., 2018). This result is evident due to variations in wind speed, direction, shade pattern, radial orientation, etc. The thermal performance of the surrounding areas with similar tree cover changes according to the landscape layout pattern. In microclimate improvement, landscape scenarios in L2 achieve an appropriate regulation of T_a and T_{mrt} during the winter and summer, with the L2 layout pattern having a significant resistance effect in winter when north winds are prevalent (Table 4.6 and 4.7).

4.7.2 Effect of the Landscape Design Elements and Indicators

This study found a co-regulated effect between landscape layout pattern, vegetation structure, and tree configuration ratio, which improved thermal comfort mainly during the day. These results are similar to those of other studies that adopted vegetation to mitigate thermal effects (Abdi et al., 2020; Srivanit & Hokao, 2013). However, this study validated that PMV was optimized both day and night only with large-scale adjustments in winter and summer. In the L2-2c and L2-2b scenarios, we found that the rational distribution of tree configuration ratios contributes more to the thermal conditions complying with seasonal changes and optimizing the duration (Figure 4.10 and 4.11).

Compared to other studies that have improved cooling potential by increasing the number of trees (Zhang et al., 2018; Zölch et al., 2019; Zhang et al., 2017), this study seeks a better thermal contribution under a quantified tree cover. It focuses on holistic landscape design elements and indicators to optimize thermal comfort in the horizontal and vertical dimensions. Previous studies on square designs (Zölch et al., 2019; Marçal et al., 2019; Stocco et al., 2021; Stocco et al., 2015) have not yet considered the configuration ratios of evergreen and deciduous trees as a key indicator of thermal comfort in winter and summer. Similarly, vegetation structures potentially impact the modification of outdoor thermal comfort (Zölch et al., 2019; Stocco et al., 2015), with tree-structured squares providing shade and cooling effects during the daytime, and grass-structured squares providing significant thermal improvements during the night. Our findings are consistent with this: we also found that the single grass-structured in the L3-3 scenario cannot realize summer thermal comfort regulation during the day. In addition, the GT-based L2-2 and DT-based L2-3 scenarios optimize winter thermal comfort but offer limited thermal regulation during the night in summer (Figure 4.10 and 4.11). Trees provide shade but block ventilation. In contrast, grass is suitable for nighttime cooling effects, but cannot provide daytime shade. The new design approach of planting trees on one side combined with grass achieves daytime and nighttime thermal reduction (Zölch et al., 2019). Still, this does not sufficiently account for the seasonal changes in thermal comfort. Thus, the sensible vegetation configuration choice depends on the wind direction, the combination of vegetation, tree types, planting intervals, climatic characteristics, etc., as suggested by (Abdi et al., 2020; Hong & Lin, 2015; Zhang et al., 2018; Gatto et al., 2020).

4.7.3 Effects of Seasonal Changes on Climate-adaptive Design

The vegetation growth and climate dynamics change with seasonality; outdoor thermal demand also changes, especially during extremely hot and cold days. The average duration of the co-optimized time was 10 h in summer, but only 9 h in winter. Because outdoor thermal radiation contributes more strongly to winter thermal comfort, thermal evaluation in winter with long-term cold temperatures tends to bias the vote toward cold (W. Liu et al., 2016). The combination of tree types affects the optimized duration, with evergreen and deciduous trees changing the thermal environment due to seasonal changes, affecting microclimatic conditions such as wind speed, direct sunlight, and humidity (Abdi et al., 2020). In this study, the L2-2 and L2-2c scenarios were dominated by evergreen tree cover, whereas the L2-3 scenario was based on deciduous trees. A comparison of winter and summer thermal comfort simulated at 14:00 generated thermal index maps (Figure 4.15), where the scenario based on evergreen trees resulted in reduced mean PMV values. The results show

that evergreen trees have stronger thermal optimization performance than deciduous trees in winter and summer, which is also consistent with the findings of El-Bardisy et al. (2016) and Abdi et al. (2020). The radiant temperature increased in winter and decreased in summer compared to the L2-2c and L2-2b scenarios for improving the thermal demand in winter and summer (Figure 4.14). In general, the co-optimized new landscape design scenarios for the station square are adapted to the climatic characteristics in a homogeneous building context simulation, thereby achieving duration and seasonal changes in thermal comfort requirements. However, the climate in the Hokuriku region of Japan, with its high temperatures and frequent rainfall in summer, makes grass paving inappropriate for local climate conditions. Instead, a rational configuration of tree ratios meets the climatic requirements of shading in summer and wind resistance in winter.

4.7.4 Regulation of Thermal Comfort at Different Scales

Station squares provide pedestrians with public spaces to wait and rest. Importantly, the balance of thermal comfort between internal and external square spaces can affect activities. Sufficient consideration of pedestrian thermal perception at different scales promotes the efficient use of infrastructure and energy saving. The wind environment and the shade location at different building scales affect the surrounding thermal conditions variation. Furthermore, the holistic spatial context considerations are more effective in mitigating thermal stress in an urban context. This study showed that the thermal performance of the L2-2 scenario at a small scale was lower than that of the L2-2c and L2-2b scenarios in large-scale simulations (Figure 4.15). This further validates that the simulation spatial scales positively affect thermal regulation at the same simulated receptor. Simulations use multiple receptors for different scale building context conditions, as indicated by (Zhang et al., 2017; Fabbri et al., 2020), which has a similar positive impact on regional thermal comfort.

4.7.5 Limitations for the ENVI-met Simulation

Landscape design consists of different elements (buildings, vegetation, water bodies, and ground) that generate the total radiation of the scenario (i.e., direct, reflected, diffuse solar radiation, and long-wave radiation), where reaching an energy balance is a complex combinatorial process. This study focused only on vegetation configuration conditions. One limitation of our study is that new landscape designs do not provide simulations for all possible scenarios in tree configuration ratios. Moreover, efforts should be undertaken to further improve the green infrastructure for heat mitigation, as suggested in some studies, e.g., the combination method, type of tree species, diversity of vegetation community structure, and vegetation crown (Rahman et al., 2018; Moser et al., 2016; Sodoudi et al., 2018). Water bodies and trees can be more effective in improving thermal comfort and natural ventilation. Thus, synergistic cooling methods, such as the combination of green and blue infrastructure, can be more effective (Robitu et al., 2006).

This study used the ENVI-met V4 model, a numerical simulation that uses hydrodynamics and thermodynamic rules to simulate meteorological variables in the diurnal cycle. However, there are some limitations to the simulation procedure. The simplification of the building and vegetation models failed to precisely match the actual site. The vegetation types failed to differentiate well between evergreen tree classifications. Most studies use lower LAD tree models utilizing representative species to act as plantings for

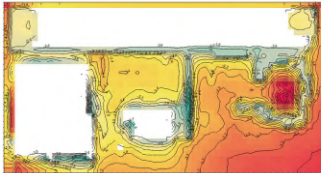

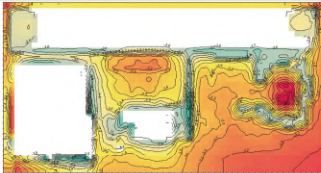

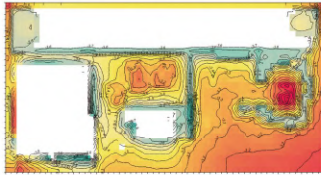
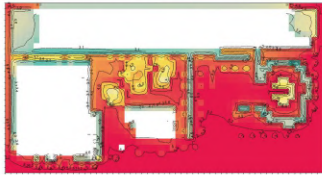
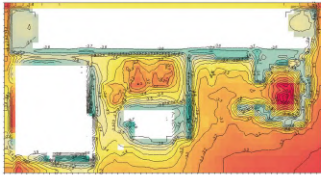
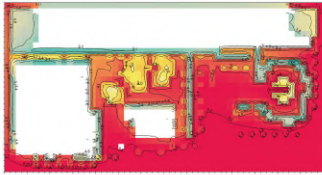
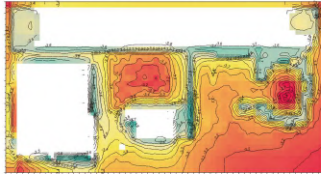
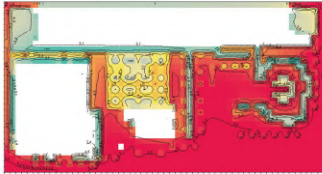
different LAD and tree shapes. There are limited empirical cases using coniferous trees instead of evergreen trees (Abdi et al., 2020). In this study, the deciduous tree altered the LAD calendar to represent the evergreen tree. The preceding approach is similar to that of the present study. In this regard, LAD measurement errors in foliage distribution have not been described in detail. The various vegetation layers of distribution LAD values, root setting, and leaf albedo need to be measured with more accurate equipment and standardized techniques. Future refinement of the ENVI-met vegetation-type database and more detailed vegetation with water body models are recommended research areas, as observed in (Liu et al., 2018; Simon et al., 2020). These studies bring more precise technical support and experience to microclimate and thermal comfort evaluation in different heterogeneous landscape environments.

4.8 Conclusions

This study predicted climate-adaptive landscape design scenarios integrating the evaluation of microclimate and outdoor thermal comfort in winter and summer using a case study from the Hokuriku region, Japan. The thermal index PMV was applied to analyze the thermal conditions. Moreover, the microclimate parameters and thermal results from the ENVI-met scenario simulation under extremely cold and hot days were used to compare the different landscape configuration effects. Finally, we holistically processed station square landscape design strategies in terms of the design optimal mechanism.

By integrating thermal comfort demand of the scale, duration, and seasonal variation in a station square, a complex comparative study was created here to consider the effective mitigation strategies within the landscape layout patterns, the tree configuration ratio, and the vegetation structures in each landscape configuration condition. This landscape configuration strategy is beneficial for the regulation of extreme climate conditions at the station square: it improves the cooling effect on a high-temperature day and reduces the discomfort time by 40%, especially in winter, where 90% of new scenarios co-optimize the daytime and nighttime. Furthermore, the large-scale regulation has a positive effect on the activity area; thus, the large-scale tree configuration ratio is an important indicator for co-regulating thermal comfort on both winter and summer days. The tree planting structure in an array layout pattern can be more effective for improving the microclimate conditions. This is because the use of suitable deciduous and evergreen configuration ratios has a significant thermal benefit for regulating the seasonal changes in radiation flux and wind flow.

These findings have a particular relevance for increasing urban resilience via Japan's TOD urban development plans and station square design in the Hokuriku region. In particular, the fixed station squares with the parallel street orthogonal connection relationship types, with the internal and external of the special building canopy configuration, are more influential on ventilation and shade. Research on thermal comfort mitigation strategies is vital considering the high health risks to outdoor-exposed populations from climate change and extreme weather events. Future researchers should consider other varied landscape layout patterns with combinations of blue infrastructure. Evaluations of the cooling potential of different tree shapes and canopy density distributions will be especially important for future studies. In addition, we suggest synergetic investigations of different combinations of landscape configuration modes from the leeward and windward zones.

PMV thermal index map		PMV thermal index map	
In winter		In summer	
At 14:00		At 14:00	
at 1.8 m height		at 1.8 m height	
	Mean:-3.49 Max:-2.95 Min:-3.94 Q _A =34 G _A =15%		Mean:4.79 Max: 5.37 Min:2.64 Q _A =34 G _A =15%
Senario L1-1 (R _{DT} /R _{GT} =61%/39%)		Senario L1-1 (R _{DT} /R _{GT} =61%/39%)	
a Layout pattern (L1-1 against L2-1 and L3-1)			
	Mean:-3.32 Max:-2.94 Min:-3.90 Q _A =34 G _A =15%		Mean:3.89 Max: 5.37 Min:2.63 Q _A =34 G _A =15%
Senario L2-1 (R _{DT} /R _{GT} =60%/40%)		Senario L2-1 (R _{DT} /R _{GT} =60%/40%)	
	Mean:-3.29 Max:-2.95 Min:-3.87 Q _A =34 G _A =15%		Mean:4.27 Max: 5.37 Min:2.64 Q _A =34 G _A =15%
Senario L3-1 (R _{DT} /R _{GT} =60%/40%)		Senario L3-1 (R _{DT} /R _{GT} =60%/40%)	
b Small-scale R _{DT} /R _{GT} (L1-1 against L2-1, L3-1, and L3-2)			
	Mean:-3.19 Max:-2.95 Min:-3.86 Q _A =34 G _A =15%		Mean:4.76 Max: 5.37 Min:2.64 Q _A =34 G _A =15%
Senario L3-2 (R _{DT} /R _{GT} =50%/50%)		Senario L3-2 (R _{DT} /R _{GT} =50%/50%)	
c Layout pattern, small-scale R _{DT} /R _{GT} , and vegetation structure (L1-1 against L2-2, L2-3, and L3-3)			
	Mean:-3.20 Max:-2.98 Min:-3.86 Q _A =34 G _A =15%		Mean:4.14 Max: 5.35 Min:2.58 Q _A =34 G _A =15%
Senario L2-2 (R _{DT} /R _{GT} =0%/100%)		Senario L2-2 (R _{DT} /R _{GT} =0%/100%)	

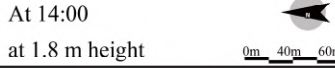

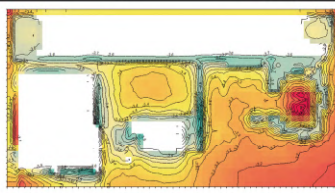
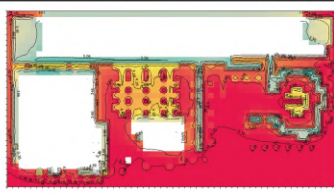
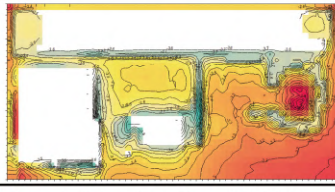
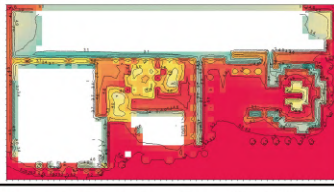
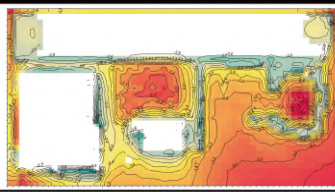

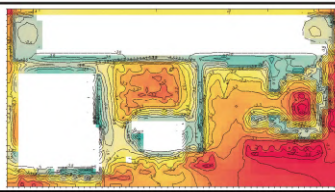
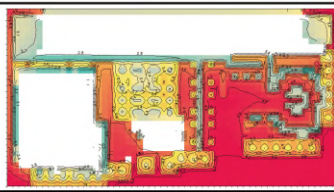
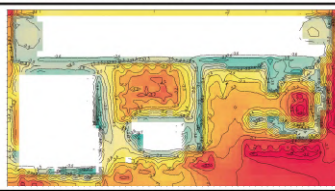
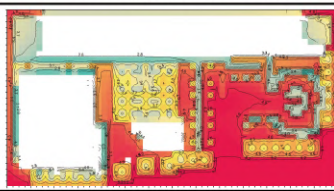
PMV thermal index map In winter At 14:00 at 1.8 m height		PMV thermal index map In summer At 14:00 at 1.8 m height	
			
	Mean:-3.36 Max:-2.93 Min:-3.90 Q _A =34 G _A =15%		Mean:4.33 Max: 5.36 Min:2.63 Q _A =34 G _A =15%
Senario L2-3 (R _{DT} /R _{GT} =100%/0%)	SD=0.06	Senario L2-3 (R _{DT} /R _{GT} =100%/0%)	SD=0.23
	Mean:-3.42 Max:-2.94 Min:-3.99 Q _A =34 G _A =15%		Mean:4.76 Max: 5.36 Min:2.63 Q _A =34 G _A =15%
Senario L3-3 (R _{DT} /R _{GT} =0%/0%)	SD=0.04	Senario L3-3 (R _{DT} /R _{GT} =0%/0%)	SD=0.02
d Large-scale R _{DT} /R _{GT} (L1-1 against L2-2, L2-2a, L2-2b, and L2-2c)			
	Mean:-3.33 Max:-2.99 Min:-3.86 Q _B =81 G _B =11%		Mean:3.95 Max: 5.34 Min:2.57 Q _B =81 G _B =11%
Senario L2-2a (R _{DT} /R _{GT} =50%/50%)	SD=0.08	Senario L2-2a (R _{DT} /R _{GT} =50%/50%)	SD=0.42
	Mean:-3.26 Max:-2.95 Min:-3.80 Q _B =81 G _B =11%		Mean:3.48 Max: 5.29 Min:2.16 Q _B =81 G _B =11%
Senario L2-2b (R _{DT} /R _{GT} =20%/80%)	SD=0.12	Senario L2-2b (R _{DT} /R _{GT} =20%/80%)	SD=0.65
	Mean:-3.19 Max:-2.95 Min:-3.80 Q _B =81 G _B =11%		Mean:3.75 Max: 5.29 Min:2.16 Q _B =81 G _B =11%
Senario L2-2c (R _{DT} /R _{GT} =0%/100%)	SD=0.15	Senario L2-2c (R _{DT} /R _{GT} =0%/100%)	SD=0.52

Figure 4.15. Winter and summer PMV thermal index maps at 14:00 (at 1.8 m height) for landscape configuration conditions (a, b, c, and d).

Chapter 5 Urban Space Regulation Strategy (USRs)

5.1 Urban Morphology Theories

Urban morphology aims to study the urban form in the urban, town, and rural regions, which is the formation and transformation along with the time and space changes. Suitable urban interventions have updated these regions' spacial and physical features on different scales to promote sustainable development. The study of concepts and methods in urban morphology is multidisciplinary. The related disciplines include human geography, urban planning, urban design, building, sociology, and culture study. Urban morphology is conducive to urban management, design planning, urban reservation with reconstruction, and universal urban policy decision-making to promote the social economy and environmental resilience. The earliest influential study of urban morphology is probably the Noli Map by Giambattista Noli in 1748, which divides the spatial fabric of the city into two parts: public space (in void/white) and private space (in solid/black).

The urban design experience is from urban morphologies. Morphology means knowledge of form. Rowe (1978) characterized the urban with a Picture-Ground analysis and defined two extremely different urban figures: one dominated by mass and one with a void as an entry point. The urban morphologist interprets and visualizes the patterns and elements of the city. Typo-morphology is an approach in urban morphology that systematically classifies urban elements based on their morphological properties. Typo-morphology also is an unusual approach to urban form: 1) It considers all scales of the built landscape from the small scale or park to the large urbanized area; 2) It characterizes urban form as a dynamic and continuously changing entity immersed in a close relationship with it produces and inhabitants (Anne VernezMoudon, 1994). The building morphology has classified the public space for describing detail in typo-morphology. It divides the different spaces according to scale, function, building density, geometry, and other properties in urban form. Based on their functional properties, outdoor public spaces are classified as schools, parks, squares, blocks, courtyards, etc. The building height also can be classified as low rise (2-4 floors), mid-rise (3-5 and 5-8 floors), and high rise (>7 floors) (Stojanovski & Axelsson, 2019). The geometry and structural morphology of urban buildings tend to form "urban canyons," which divide into symmetrical and asymmetrical canyons. Typo-morphology divides the specific building, street, or block, capturing morphology features in urban space. Typo-morphologists intuitively identify and simplify urban elements and morphology in physical shape. A typo-morphological approach to defining building type differs from other approaches in three ways: 1) Type in typo-morphology combines the volumetric characteristics of built structures with their related open spaces to define a built landscape type; 2) The inclusion of land and its subdivisions as a constituent element of type makes land the link between the building and city scale; 3) The built landscape type is a morphogenetic (Anne VernezMoudon, 1994). In principle, understanding the perception and cognition of the urban environment formed by the urban morphology is an obvious way for designers to follow pedestrians' actual needs and optimize the design scheme. The urban environment into "physical, operational, perceptual and behavioral environments," as shown in Figure 5.1. The perception and behavior of the spatial environment occur mainly at the meso-microscale, especially between buildings or between buildings and streets (Stojanovski & Axelsson, 2019).

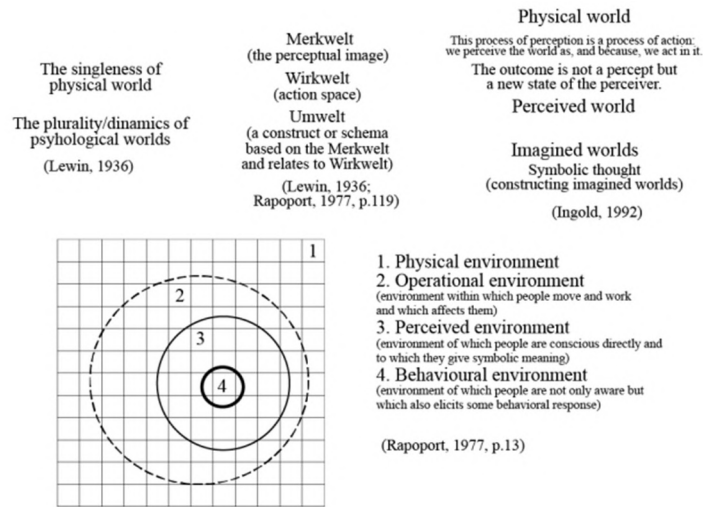


Figure 5.1 Conceptual model of perceived environment.

We have redefined and fragmented the urban form into five aspects, as shown in Figure 5.2: (A1) human activities, which are related to the spatial distribution and behavior of the population; (A2) building morphology, where high-density buildings are important artificial materials and component of the urban form; (A3) transport system, which consists of the road network at different levels; (A4) public infrastructure which refers to institutions that provide public services, including hospitals, government organizations, schools, banks, etc.; (A5) ecological infrastructure, which refers to public spaces covered by greenery and water bodies (Zhang et al., 2019).

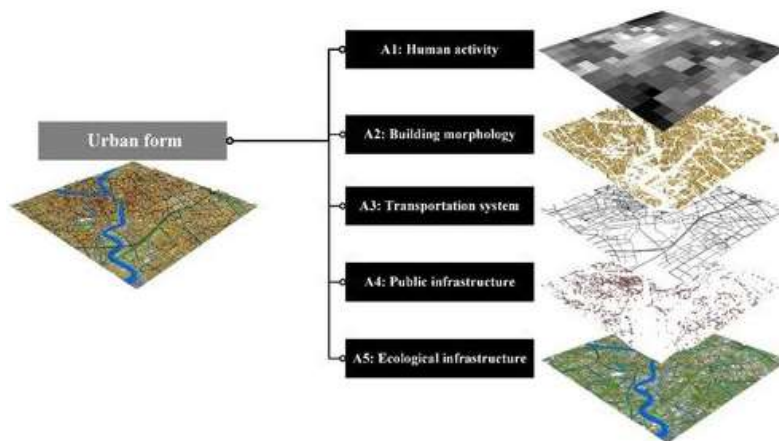


Figure 5.2 Urban form combination system (Zhang et al., 2019).

The building type, tissue, and urban fabric together form the structure and scale of urban form. Building type, typology, and urban form are in a relationship of compatibility (Anne VernezMoudon, 1994) (Figure 5.3). Urban form can also change the climate in cities, creating an urban climate to distinguish it from the surrounding rural areas. The space created by urban buildings up to the roof is called the ‘urban canopy.’ The energy demand and human thermal comfort conditions of buildings are mainly influenced by the prevailing microclimate conditions (Gaitani et al., 2007). The present study focuses on the microclimate, thermal comfort, and atmospheric pollutants regulation by changes in building morphology at small and medium scales in the

city.



Figure 5.3 The relationship between building types, typomorphology, and urban form.

5.2 Space Parameters and Indicators

Outdoor thermal comfort in urban environments is a complex problem with many dimensions. Environmental incentives (i.e., local microclimate conditions) are the most important factors influencing people's thermal perception and comfort evaluation. Physical parameters include building morphology, green cover, microclimate, traffic and vehicles, roads, and water bodies (Chen & Ng, 2012b; Jianwei Li & Liu, 2020). Spatial parameters are mainly related to building space and green space.

5.2.1 Influencing Parameters and Indicators of Building Space

The arrangement and location of building spaces impact outdoor shading and ventilation. Related studies have shown that building style, orientation, height, density, floor area ratio (FAR), H/W, and building materials are important building space parameters influencing heat exchange in the thermal environment. Thus, changes in microclimatic parameters around the human body lead to different levels of human thermal perception feedback presenting comfortable, uncomfortable, or neutral (Jianwei Li & Liu, 2020). The concentration of urban buildings creates different forms and geometries, thus changing the urban canopy in different areas, influencing urban climate change and the UHI. The corresponding building indicators are SVF, H/W, FAR, and building coverage ratio (Figure 5.4).

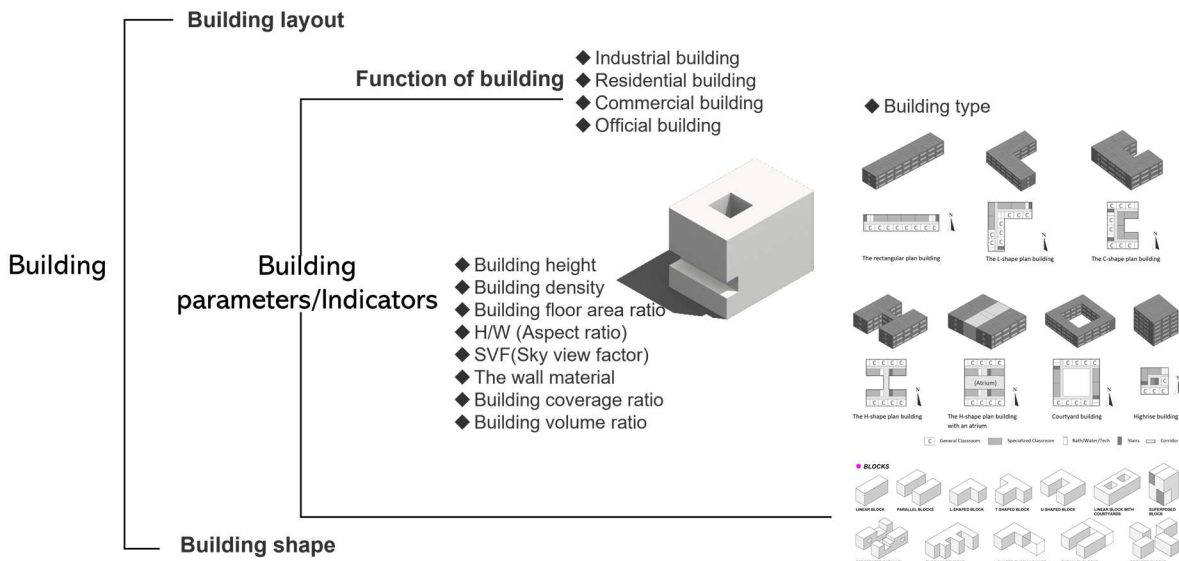


Figure 5.4 Major building parameters and indicators are influencing the outdoor thermal environment.

5.2.1 Influencing Parameters and Indicators of Green space

The green space primarily has different vegetation planting designs resulting in different combinations of vegetation structures and landscape layouts (Figure 5.5). Among the terms related to greening optimization strategies are vegetation pattern, landscape design, green space, plant configuration, tree configuration, greening configuration, vegetation structure, canopy shape, etc. The main vegetation species are grass, shrubs, trees, and vines. Tree types can be classified as evergreen, deciduous, and coniferous. The combination of tree patterns can be divided into arrays, concentrated and scattered. The tree canopy is divided into cylindrical, conical, spherical, inverted conical, etc. Numerous numerical simulations on the ENVI-met computer have concluded that trees improve outdoor environmental comfort more than other vegetation species, followed by shrubs. It has also been shown that green design is an important approach to improving the thermal comfort of urban squares. The relevant greening indicators are the green area ratio, tree configuration ratios, etc. In Chapter 4, the evergreen to deciduous tree configuration ratios is specified for an optimal design approach for extreme climatic conditions in the NSs. The main greening indicators are the LAD and the ratio of number of evergreen to deciduous trees applied in the USRs.

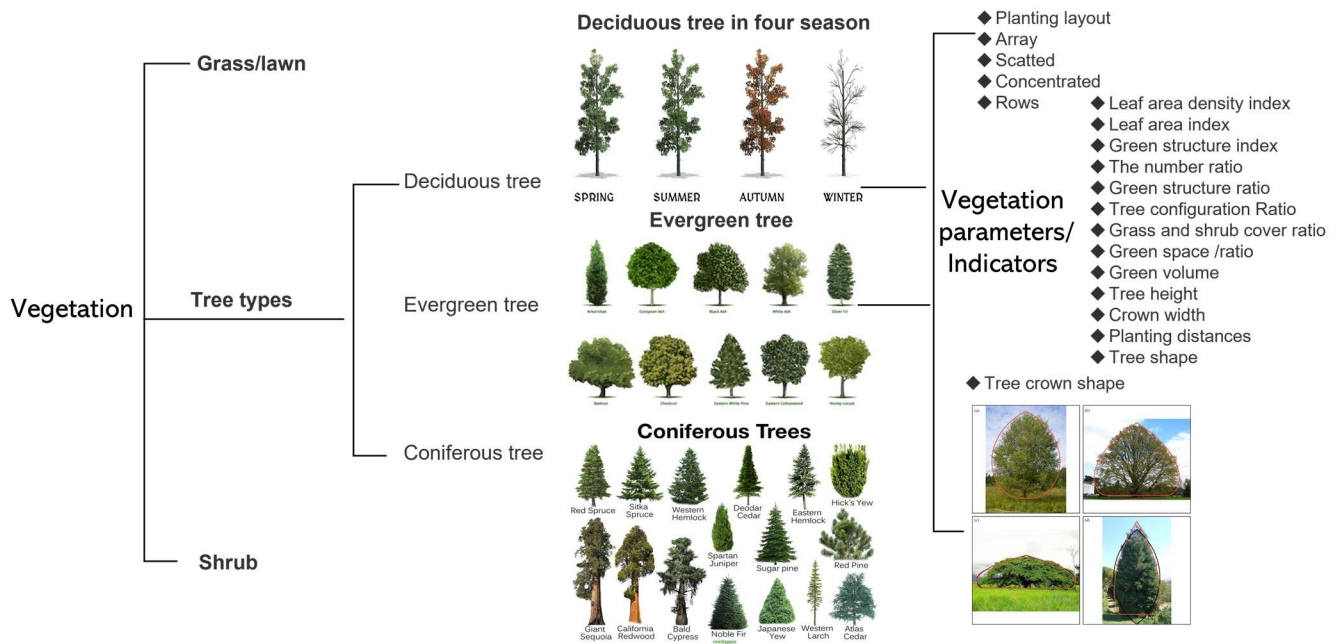


Figure 5.5 Major greening parameters and indicators influencing the outdoor thermal environment.

5.3 Case Study of USRs in Station Square Area

5.4 Motivation

In contrast to previous studies mentioned above, there remain certain gaps in the current knowledge. First, the environmental benefits of station squares as an urban center construction area that integrates various aspects of microclimate, thermal comfort, and air pollution have rarely been studied. Second, systematic design strategies to optimize the environment in synergy with the overall green spatial configuration characteristics (vegetation structure, quantity, species, type, combination, etc.) in a homogeneous urban space have not been clearly validated, particularly in crowded station areas. Third, small-scale typologies of building morphology affect the HUI of the integral urban canopy. The combined effects of building and green spaces in analogous squares on thermal stress and air quality are relatively understudied.

To address these gaps, we conducted quantitative and qualitative studies of building morphology and green space configuration to predicate the optimal design in microclimate, thermal environment, and air quality. We explored how the combination of evergreen and deciduous trees in a station square can integrate the synergistic effects of building morphology on $PM_{2.5}$ abatement and summer cooling.

To this end, the objectives of the present study were 1) to analyze the microclimatic environmental effects in station squares from a green building aspect by quantifying the cooling impacts of different building space typologies (A: block, B: courtyard, and C: canyon) and green space configurations (vegetation structure, tree species, and combinations) on the surrounding environment; 2) to develop strategies for optimizing space configuration by synergizing microclimatic conditions, thermal environment, and air quality; and 3) to predict a universal green space configuration for station squares based particularly on the effects of novels green

patterns on the thermal environment and air quality under different meteorological conditions on hot summer days.

5.5 Study Area

5.5.1 Overview of Komatsu City

The Komatsu Station Square ($36^{\circ}24'8''\text{N}$, $136^{\circ}27'10''\text{E}$) is located in the Komatsu City, Ishikawa Prefecture, Japan, and is a railway station of the urban core on the Hokuriku Main Line of JR West. The area borders the plains to the west, the Sea of Japan to the south, and the surrounding mountains to the east. The station square area is adjacent to the Hokuriku Shinkansen viaduct (Figure 5.6). Three sampling sites were set at the station square area. The Doihara Machi Square (QA) is a small historical transport square located on the west side to enjoy and visit for pedestrians. The Komatsu Station West Square (QB) sees an average daily pedestrian flow of 7,823 people, with a usable space of $7,500\text{ m}^2$. The Komatsu Station East Square (QC) harbors the Komatsu Station Hotel as part of the redevelopment of the area and has a large bus station scheduled to be completed by 2022. The observatory for macro-meteorological weather stations is located in Imaimachi of Komatsu City and Komatsu airport, which is located as a distance of approximately 2.8 km from the station square (Asanobu, 2004; Magic, 2015).

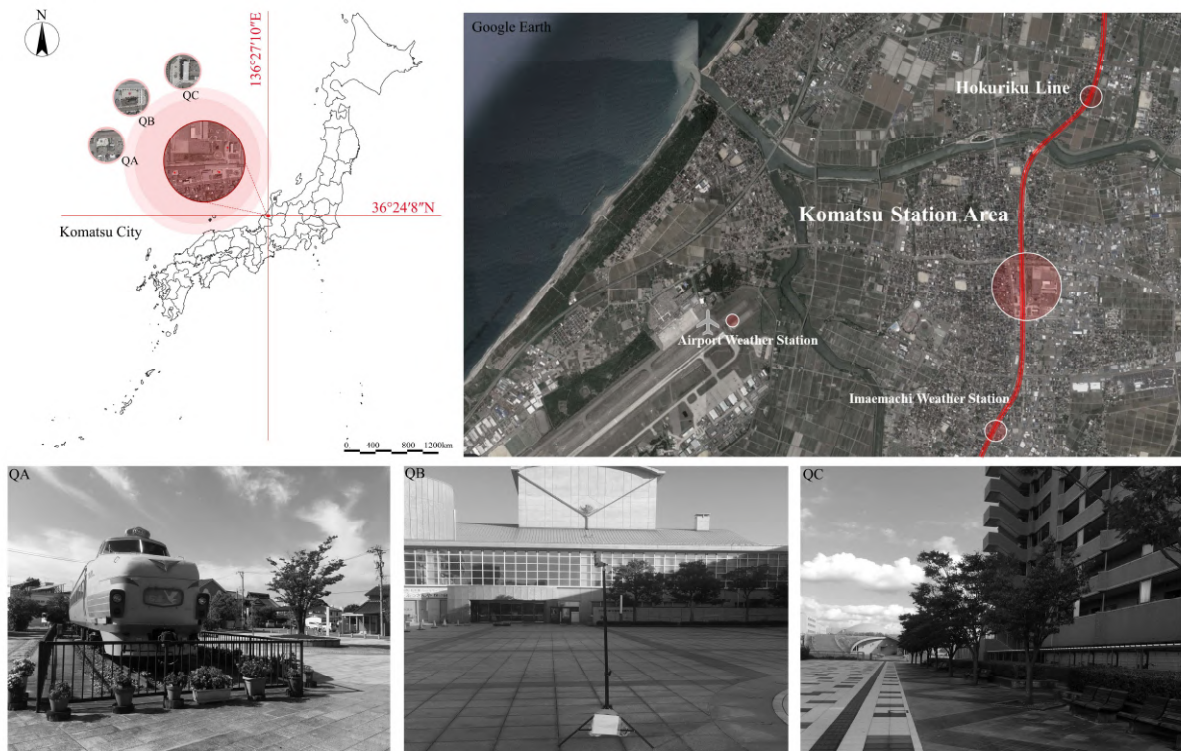


Figure 5.6 Locations of the major station square areas in Komatsu (QA: Doihara Bonnet Space; QB: Komatsu Station West Square, QC: Komatsu Station East Square).

Komatsu city belongs to the humid subtropical climate (Cfa) with hot and humid summers (Kottek et al.,

2006). The hottest month is August, when the mean air temperature is 30 °C. The hottest period is between 12:00 and 16:00 hours. The average yearly rainfall is 182 mm, which is one of the wettest regions in Japan (Magic, 2015). The annual mean PM_{2.5} in Komatsu City is approximately 15µg/m³ with moderate levels of air pollution. The mean yearly PM_{2.5} has a mean value of 25.6µg/m³ in Komatsu city for 2020 (PM_{2.5} Annual Report, n.d.). However, this concentration is significantly higher than the annual average air quality standard (AQG=10µg/m³) (Figure 5.7).

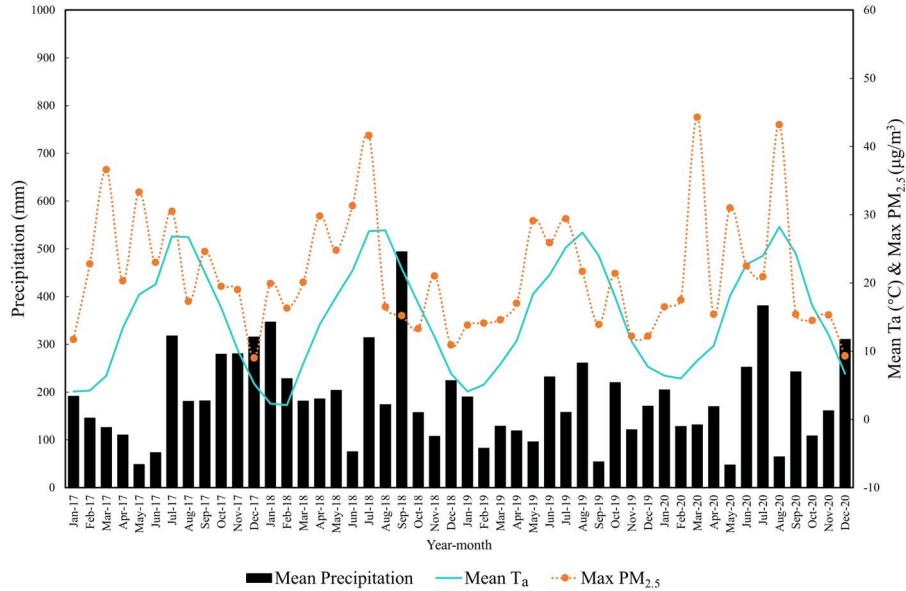


Figure 5.7 Mean monthly precipitation and air temperature (T_a) and mean monthly maximum PM_{2.5} in Komatsu city in 2017 to 2020.

5.5.2 Space Configuration

The station square area is divided into three types of small-scale squares. The area is approximately 14,820 m² for QB, approximately 32,200 m² for QC, and approximately 4,788 m² for QA. According to the layout of the different building typologies, A is a block type, B is a courtyard type, and C is a canyon type. Thus, QA, QB, and QC areas correspond to the three building morphologies in the present study. The QA sub-district is surrounded by concrete roads on all sides and is approximately 9 m from the Hokuriku Shinkansen viaduct and approximately 136 m from the QB area. The surrounding buildings range from the minimum height of 4 m to the maximum height of 12 m, and the ground material is mainly square tiles. The primary building materials include ceramic and resin wall panels, with the middle hollow walls insulated with wooden frames. The QB sub-district is part of the central station square, with ancillary buildings, such as a hotel, restaurant, and music theatre. The tallest building is 21 m. The station canopy surrounds half of the square, creating a shaded area linking the station's indoor and outdoor spaces. The rest of the square is paved with tiles to create a “courtyard” layout. The primary ground material is permeable square tiles, and the station building material is aluminum metal with concrete walls. The QC sub-district is an ancillary space to the QB area, with access to places including the hotel, park, science museum, and bus station. The primary measurement area is the square space between the residential apartment building and the station hotel, forming an east-west canyon

space with a maximum building height of 31 m. The ground material is mainly grey and white permeable square tiles, and the primary building material is ceramic wall panels and tiles.

Regarding green spaces in the station square, QA has a rich vegetation community with a combination of trees and shrubs; QB has a mixed vegetation structure with trees, shrubs, and grass; and QC has a similar vegetation structure to QB, albeit with a single configuration of vegetation types. The primary vegetation in each square includes deciduous trees (TD), with a few evergreen (TE) and coniferous (TC) trees. Configurations of the three small-scale squares are shown in Table 5.1.

Table 5.1 Vegetation configuration modes of different types of squares in station square area.

Vegetation type	Species	Canopy diameter (m)	Height (m)	Number (n)
Deciduous trees	<i>Prunus lannesiana</i>	3	5	17
	<i>Cornus florida</i>	3	5	106
	<i>Magnolia denudata</i>	3	4	12
	<i>Zelkova serrata</i>	9	9	14
	<i>Acer palmatum</i>	3	5	3
	<i>Sapium sebiferum</i>	3	5	3
	<i>Liquidambar styraciflua</i>	4	8	5
	<i>Sorbus aucuparia</i>	3	5	3
	Pinaceae	3	5	2
	<i>Podocarpus macrophyllus</i>	5	3	8
Evergreen/coniferous trees	<i>Juniperus chinensis</i>	3	5	1
	<i>Quercus glauca</i>	5	5	14
	<i>Ilex sp.</i>	3	3	13
	Camphorwood	9	9	15
	<i>Machilus sp.</i>	3	3	2
	<i>Acer palmatum</i>	2	2	-
Deciduous shrubs	<i>Lagerstroemia indica</i>	3	3	-
	<i>Hibiscus syriacus</i>	3	2	-
	<i>Photinia</i>	2	2	-
Evergreen shrubs	<i>Camellia japonica</i>	1	2	-
	<i>Buxus sinica</i>	0.5	0.5	-
Herbs	Grass	-	-	-

5.6 Methodologies for USRs

The methods used in the present study include the following: 1) on-site measurements and 2) simulations using the CFD model in ENVI-met. The methodology is schematically presented in Figure 5.8. On-site measurements were obtained to monitor the meteorological and air quality parameters of the station square area. The measured meteorological parameters were used to validate the accuracy of the simulation results. ENVI-met was applied to simulate and reproduce the actual conditions for predicting the mitigation effects of five green space configurations in the three building morphologies.

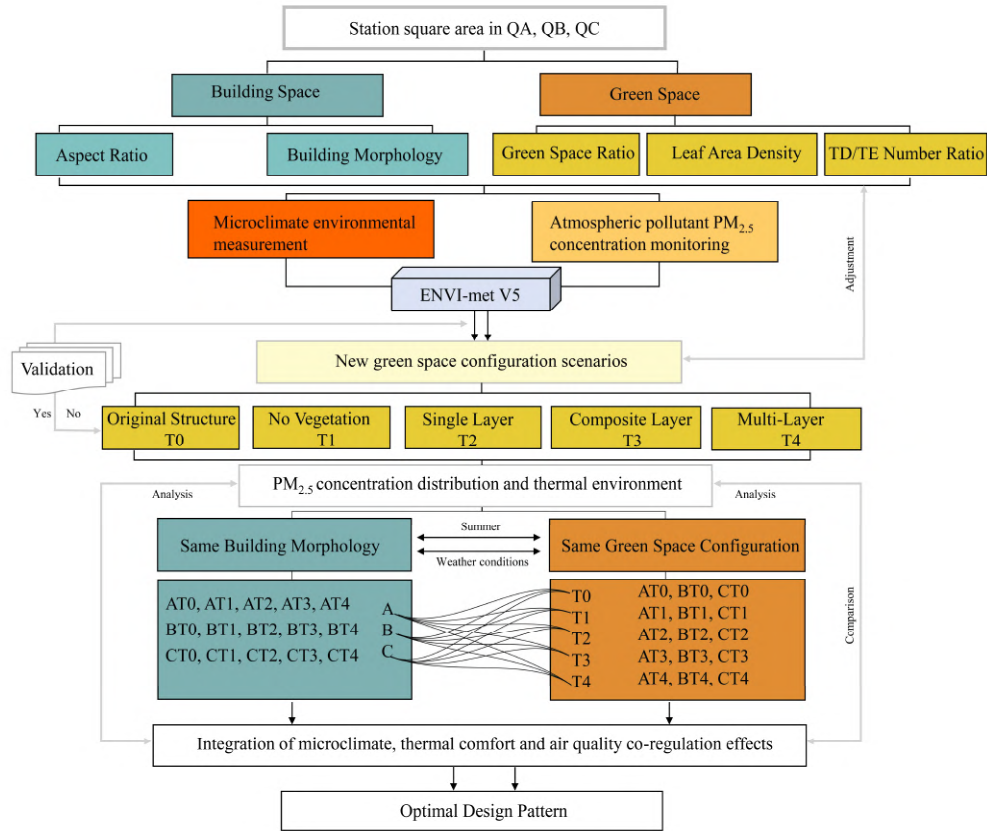


Figure 5.8 Station square area with green space reconfiguration following the optimal design for microclimate, thermal comfort, and PM_{2.5} mitigating effect.

5.6.1 On-site Measurement

On-site measurements were obtained using a handheld air quality tester (Temtop, M2000 2nd, CNA) to determine atmospheric PM_{2.5} concentration and distribution. Meteorological parameters were measured using a handheld thermal tracker (NK, Kestrel 5400, USA) to monitor T_a , relative humidity (RH), wind speed (WS), and global temperature (T_g). On-site microclimatic and air quality measurements are essential as a real-time reference for accurate modeling results. We considered three hot days during the summer of August 2021. Thus, the measurements for QA, QB, and QC were obtained on typical summer days under different weather conditions: August 27, 29, and 31, 2021, respectively. Measurement points at each site were set in M1, M2, and M3. The air quality monitor was switched on for a day at each of the three measurement points to collected PM_{2.5} concentration data (Figure 5.9). Moreover, the handheld thermal trackers were installed at each sampling site to obtained meteorological data for the three dates. The measurement devices were placed on a tripod at a height of 2 m from the ground. Macro-meteorological data were derived from Komatsu City's local meteorological agency (Japan Meteorological Agency (JMA), 2007) and Komatsu City Airport (Magic, 2015). Measurement data were used to evaluate the performance of the numerical model, and macro-meteorological data were set as the initial meteorological parameters for modeling.

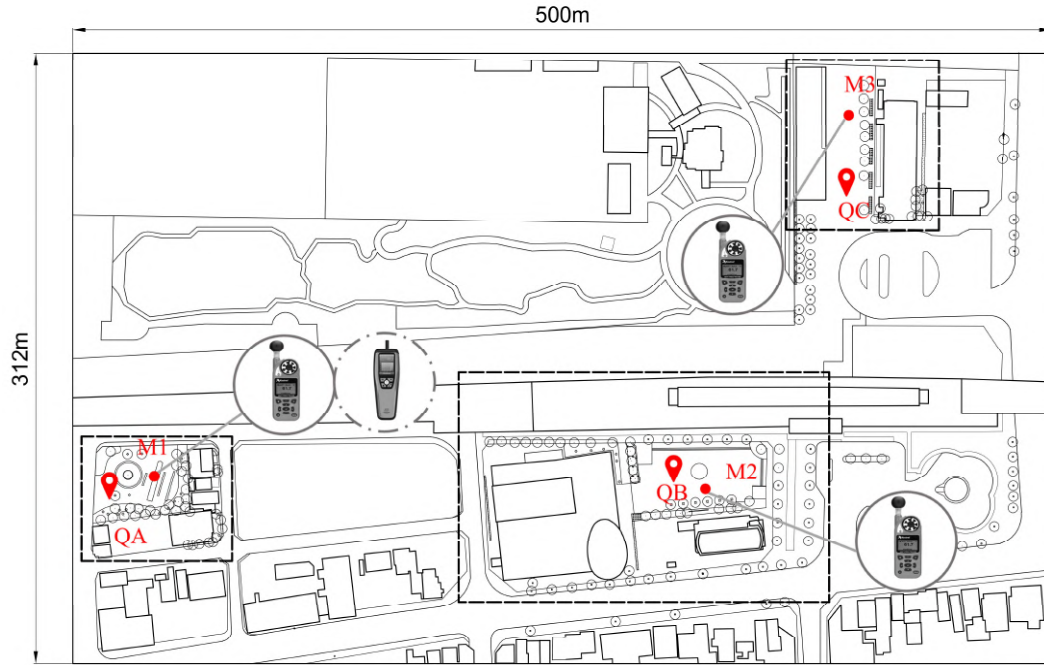


Figure 5.9 Meteorological and air pollution monitoring points distributed as M1, M2, and M3 in QA, QB, and QC squares, respectively.

5.6.2 CFD Simulation Modeling-ENVI-met V5

For simulations, we applied ENVI-met V5 (Bruse, 2021)—a standard software based on CFD and thermodynamics for microclimate simulation to output primary raw data of the atmosphere, buildings, inflow, pollutants, thermal radiation, and receptors. ENVI-met has been used to assess the impact of urban planning on environmental variables and microclimate contributing to the reduction of urban thermal stress and energy consumption on HUI, energy conservation, and air pollution (Salata et al., 2016). Three micro-scale sites in the Komatsu station square area were set as the three-dimensional simulation areas. Three receptors (M1, M2, and M3) for the simulation results at 2.5 m high were selected inside QA, QB, and QC (Figure 5.9). For each scenario, ENVI-met was run for a hot period of 8 h (11:00 am to 19:00 pm). Simulations were consistent with the measurement dates on typical summer days. The initial and boundary conditions in the ENVI-met models are presented in Table 5.2 and 5.3.

A large-scale model was created as a three-dimensional model with a grid size of 5 m in the x, y, and z-axes in the directions of $100 \times 63 \times 24$ using a vertical grid creation method with a scaling factor of 10% and a starting height of 20 m. The nested grid was set to 4 to prevent boundary space exceedance problems. In ENVI-met, the linear pollutant emissions depend on the settings of traffic volume, number of roads, and emission factors ($PM_{2.5}$ or PM_{10}) of different vehicle types. The traffic volume measurements during the COVID-19 pandemic significantly contrasted the usual number of vehicle trips. Thus, the traffic volume and emission factors were set as per the normal organizational standards. In the present study, following the Japan Road Association (JRA) quantification of road traffic volumes (DTV) by road classification, the two main roads near the Komatsu Station are linked to the local automatic vehicle lanes and belong to the third road-type of the second class ($DTV > 4000$ veh/24 h). The traffic volume of the city, town, and village roads is

approximately 500–1500 or 1500–4000 veh/24 h. Next, the vehicle emission factors (PM_{2.5}) were set following the new emission regulations of the Ministry of Land, Infrastructure, Transport and Tourism (MLIT) in Japan for different categories of autonomous vehicles. The model settings of meteorological parameters were derived from the macro-meteorological data of the Japan Meteorological Agency (JMA) and Komatsu Airport weather stations as well as on-site measurements of soil temperature and humidity. ENVI-met V5.0.1 allows for the optimized selection of meteorological boundary conditions using the ENVI-guide sub-tool. The simple force mode was adopted in the present study.

Table 5.2 Basic model initial settings in ENVI-met V5.

Parameter	Detailed information	
Location	Komatsu Station, Japan	
	Latitude (deg, +N, -S), Longitude (deg, -W, +E)	36.41, 136.45
	Total simulation time (h)	8
Time setting	Output time interval (min)	60
	Start of simulation date and time	On August 27, 29, and 31, 2021, at 11:00 a.m.
Create model	Model dimensions (X × Y × Z) (m)	100 × 63 × 24
	Grid size (m)	5 × 5 × 5
	Telescoping factor (%)	10
	Start telescoping after height (m)	20
	Number of nested grids	4
Pollution source	Species	PM _{2.5}
	Source geometry	Linear source at 0.4 m height
	Daily traffic value (veh/24 h)	9,000
	Number of lanes in the segment	2
	Passenger cars (%)	90.04

Table 5.3 Meteorological, soil, and cloud conditions settings in the simulation dates.

Parameter	Detailed information	27 August	29 August	31 August
Meteorological parameters	Minimum–maximum air temperature (°C)	23.3–29.4	21.7–30.1	23.1–28.6
	Minimum–maximum relative humidity in 2 m (%)	70–94	70–100	70–100
	Wind speed measured at 10 m height (m/s)	1.5	1.36	1.13
	Wind direction (°)	174	207	162.2
	Roughness length at the measurement site	0.01	0.01	0.01
	Soil layer (0–200 cm) humidity and temperature	16%, 10 °C 20%, 15.8 °C 20%, 15.2 °C	16%, 10 °C 20%, 15.8 °C 20%, 15.2 °C	16%, 10 °C 20%, 15.8 °C 20%, 15.2 °C
Cloud setting	Fraction of cloud (x/8)	4	2	5

5.6.3 Space Indicators

Building morphology is a critical factor affecting the microclimate environment and air quality. Moreover, H/W is an important indicator for urban planning and quantitative analysis of urban structure morphologies (Francisco Gómez et al., 2004). These green space indicators regulate the thermal environment and air quality. In the present study, the green space ratio (C_g), TD/TE number ratio (R_g), and LAD (Eqs. 7-9) were used to quantitatively analyze the thermal environment (Rui et al., 2019; Xiao & Yuizono, 2022).

Green space ratio (C_g)

$$C_g = \frac{Q_i}{G} \times 100\% \quad (7)$$

Where Q_i is the area of green space around the station square within the large-scale simulation area, and G is the total floor area.

TD/TE number ratio (R_g):

$$R_g = \frac{D_i}{E_i} \quad (8)$$

where D_i is the number of TDs and E_i is the number of TEs in the simulated square area. In the present study, we focused only on the ratio of number of TDs and TEs, and the number of TCs was not considered because of the small planting area.

The LAD of vegetation is defined by LAI, as follows:

$$LAI = \int_0^h LAD \cdot \Delta z$$

$$LAD = \partial_m \left(\frac{h-z_m}{h-z} \right)^n \exp \left[n \left(1 - \frac{h-z_m}{h-z} \right) \right] \quad (9)$$

where h is the average canopy height, ∂_m is the maximum value of ∂ at the vertical height Z_m when $0 \leq Z \leq Z_m$, $n=6$ or when $Z_m \leq Z \leq Z_m$, $n=0.5$ (Lalic & Mihailovic, 2004; Qin et al., 2019).

5.6.4 Thermal Index-PET

PET has been applied to investigate the effects of building green spaces on thermal comfort. PET characterizes the influence of meteorological and thermophysiological parameters, and it is significant index to assess the health effects of climate change (Matzarakis & Amelung, 2008). PET is derived from a model of human energy balance and is widely applied in outdoor thermal comfort assessments (Höppe 1993; Taffé 1997). Simultaneously, it can be applied in the human biometeorological assessments of different climates (Matzarakis et al., 1999). The PET value is primarily affected by microclimatic parameters (e.g., T_a , RH, WS,

and T_{mrt}), human metabolism, and clothing barrier coefficients (Höppe, 1999). PET is divided into nine classes, and a PET in the range of 18–23 °C is generally considered “comfortable” in the European region. Based on previous studies (Lin and Matzarakis, 2008; Zhang et al., 2017; Cui et al., 2021) in which the tested areas belonged to the same subtropical humid climate background as the area in the present study, a PET in the range of 26–30 °C, which is considered “comfortable” in Taiwan and Tokyo, was adopted as suitable. Thus, PET was divided into nine levels from 14 °C to 42 °C, representing the gradients of thermal sensation from very cold to very hot: very cold (<14 °C), cold (14–18 °C), cool (18–22 °C), slightly cool (22–26 °C), comfortable (26–30 °C), slightly warm (30–34 °C), warm (34–38 °C), hot (38–42 °C), and very hot (>42.0 °C). In addition, PET was calculated using the sub-tool Biomet in ENVI-met.

Chapter 5 discusses the mitigation effects of building space and green space configuration patterns on thermal comfort, microclimate, and air quality under the heat island effect in summer. Emphasis is on considering the effects of wind and thermal radiation environments. PET has proven to be very suitable for human biometeorological assessment of the thermal components of different climates. Its units (°C) make it easily understandable as an indicator of thermal stress (Matzarakis et al., 1999). Correspondingly, the advantage of the PET index is that it is based on a thermophysiological heat balance model and can predict the cooling effect of the wind (Roshan et al., 2020). The diffuse, reflected solar radiation and the surface temperature influence increasing the PET thermal index within the city, while the wind velocity and building height are the essential variables reducing the PET thermal index (Qaid et al., 2016).

5.7 New Space Configurations in ENVI-met Scenarios

Based on the original scenario at the station square area, new scenarios were reconfigured as four updated scenarios developed to compare the cooling potential and $\text{PM}_{2.5}$ mitigation in the different building spaces with simulation models. The simulations involved updated green strategies by implementing integrated building morphologies proposed to improve the thermal environment and air quality. Specifically, the interventions for green space reconfiguration included the original structure (T0), a no vegetation structure (T1), a single-layer structure (T2), a composite layer structure (T3), and a multi-layer structure (T4). Among these, the combination of TEs, TDs, and TCs in T0 was replaced by TE (camphorwood LAD=1) in the single-layer structure. In the composite layer structure, TDs were combined with grass (LAD=0.3) and the TEs and TCs in T0 were replaced by the native Japanese pagoda trees (LAD=1). In the multi-layer structure, a layer of camphorwood or *Machilus sp.* was added (LAD=1) as street trees based on T0 to form a double-layer tree layout in the station square area. These street trees served as the replacement for the combination of TDs and TEs. The basic building morphologies were integrated with five green space configurations at the same quantitative space indicators, as shown in Figure 5.10.

The five scenarios (T0, T1, T2, T3, and T4) were realized using the SPACE sub-tool in ENVI-met, in which each scenario yielded results with three receptors, namely a block receptor area (AT0, AT1, AT2, AT3, and AT4), a courtyard receptor area (BT0, BT1, BT2, BT3, and BT4), and a canyon receptor area (CT0, CT1, CT2, CT3, and CT4). The building morphologies in the receptors were designed with the same green space configurations, classified as the original structure (AT0, BT0, and CT0), no vegetation structure (AT1, BT1,

and CT1), a single-layer structure (AT2, BT2, and CT2), a composite layer structure (AT3, BT3, and CT3), and a multi-layer structure (AT4, BT4, and CT4).

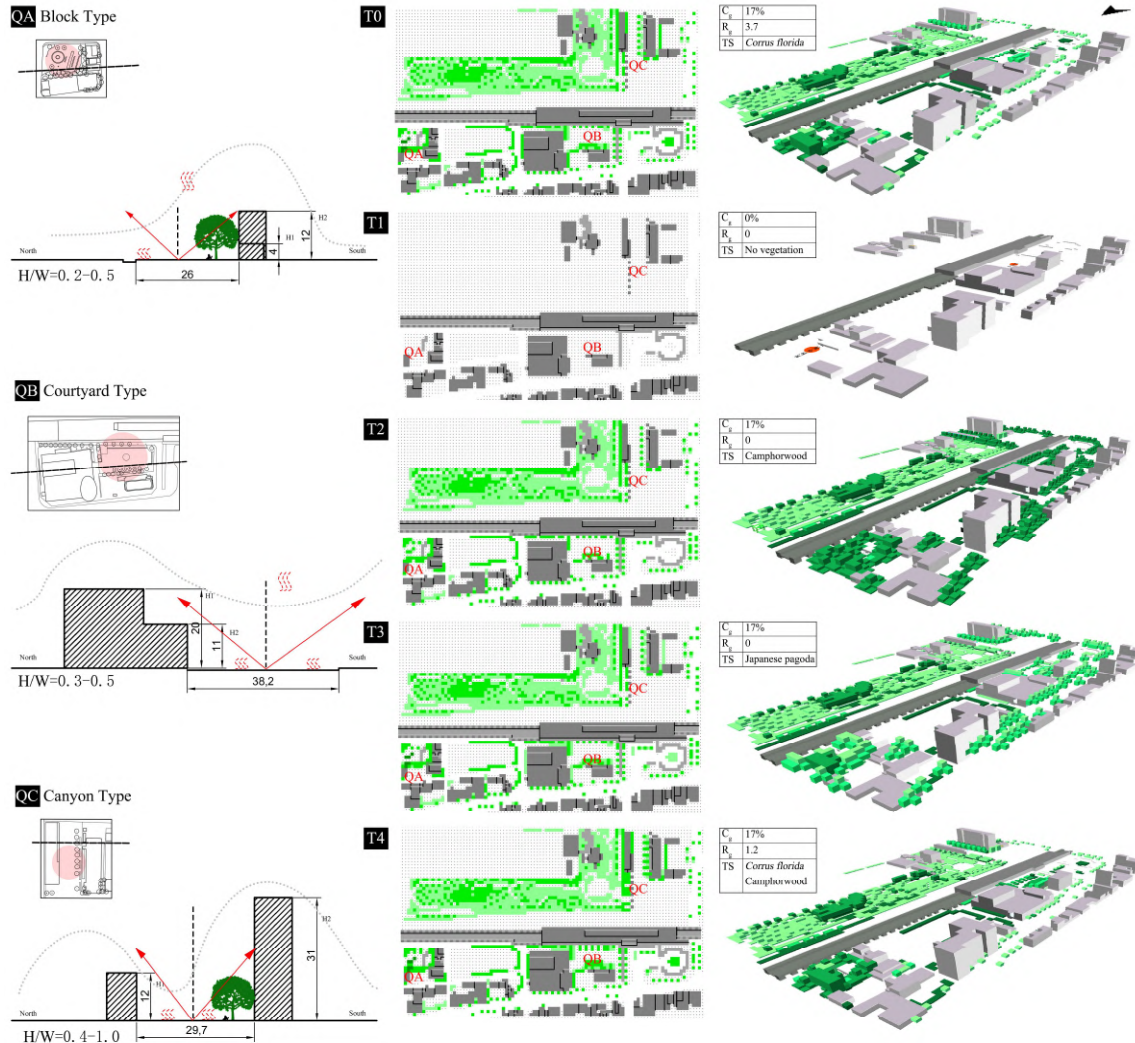


Figure 5.10 Updated ENVI-met models of typical tree species (TS) compositions and new green space configurations.

5.8 Results and Discussion

5.8.1 ENVI-met Validation of the Base Model

In previous studies, the ENVI-met models were validated by comparing the measured and simulated results of metrological parameters to ensure the accuracy of the model output. The relevant widely applied statistical indices for model validation include the root mean square error (RMSE), medium bias error (MBE), mean absolute error (MAE), and coefficient of determination (R^2) (Willmott, 1982). In the present study, RMSE, R^2 , and MAE were used to validate the model accuracy for T_a . In previous validation studies, the simulation accuracy of ENVI-met models for T_a was found to be satisfactory, with an R^2 of 0.9–1.0, RMSE of 1.0–2.5, and MAE of around 0.5 (Stocco et al., 2021). For ENVI-met of simulated T_a , the acceptable ranges of 0.66–

0.92 for R^2 , 0.52–1.51 for RMSE, and 0.27–1.34 for MAE have been reported (Tsoka et al., 2018). Specifically, an accurate model must yield an R^2 approaching 1 and an RMSE near 0 (Zölch et al., 2019).

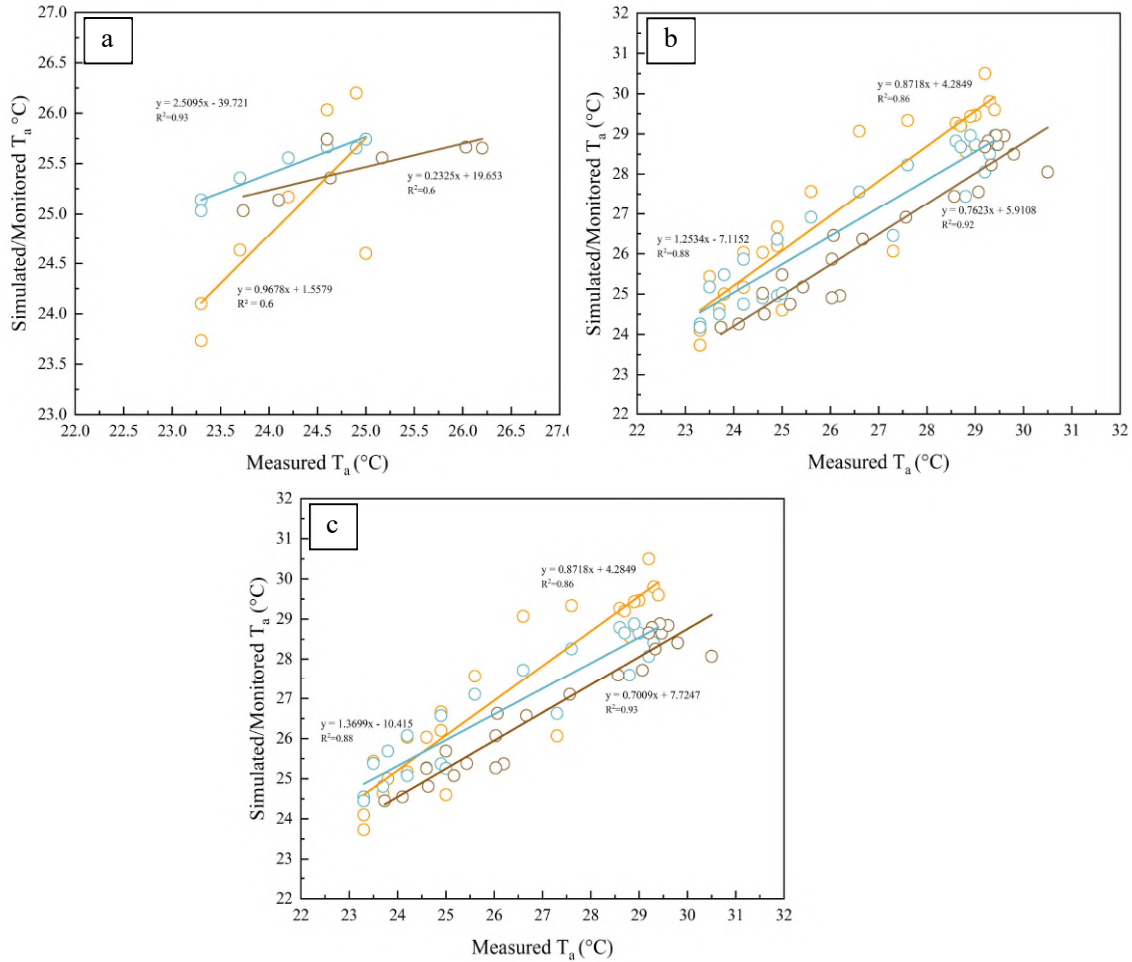


Figure 5.11 Fitting regressions between macro-monitored and on-site measured air temperatures against simulated air temperatures of ENVI-met at different sensitivity grids: $2 \times 2 \text{ m}^2$ (a), $4 \times 4 \text{ m}^2$ (b), and $5 \times 5 \text{ m}^2$ (c).

Here, the performance of the ENVI-met model was assessed using sensitivity grid analysis. Measurements from the weather station and on-site measurements of T_a were linearly fitted to simulated T_a on August 27, and the model performance was evaluated using grid sensitivity analysis ($2 \times 2 \text{ m}^2$, $4 \times 4 \text{ m}^2$, and $5 \times 5 \text{ m}^2$) using three runs of simulation and comparison of model output between the simulated and actual scenarios. As shown in Figure 5.11 and

Table 5.4, run (3) yielded an R^2 of 0.93 (close to 1) for the measured and simulated values, an RMSE of 0.45 (close to 0), and a relatively small MAE of 0.69. Thus, the simulation performance of run (3) was the best within the given simulation duration and error range. An ENVI-met model with a $5 \times 5 \text{ m}^2$ grid was used as the base model in the present study.

Table 5.4 Sensitivity grid analysis of the base model.

Settings	Force time	Simulation duration	R ²	RMSE	MAE
Running 1) 2×2m ²	8 h	84 h	0.93	0.08	1.31
Running 2) 4×4m ²	24 h	72 h	0.92	0.51	1.08
Running 3) 5×5m ²	24 h	24 h	0.93	0.45	0.69

5.8.2 Microclimate Condition in Original Scenario

T0 represents the original building and green space scenario, in which the local microclimatic conditions varied due to the impact of spatial configuration in the station square area. The distribution of microclimatic parameters (T_a , RH, WS, and T_{mrt}) in T0 scenario at 14:00 pm on August 27 is illustrated in Figure 5.12. The maximum values were 29.53 °C for T_a , 73.49% for RH, 1.34 m/s for WS, and 68.52 °C for T_{mrt} . Notably, the distribution of T_a did not significantly vary among the three morphologies. However, WS, RH, and T_{mrt} varied significantly depending on space configuration. Specifically, RH increased from the north to south within QB and QC. T_{mrt} decreased from east to west within QB and QC areas, and this reduction was more significant than that in QA. WS distribution in QA and QB remained stable (0.3–0.6 m/s) at 14:00, but it peaked to 0.9 m/s in QB. Simulation results showed that the microclimatic conditions of QB and QC were more advantageous than those of QA. The vegetation pattern of the total environment within the site at 14:00 affected humidity and solar radiation absorption. As such, in unshaded areas lacking vegetation, thermal radiation and T_a reached the maximum values, producing significant HUI, as evidenced in the south and west directions of the main automobile road. North-south and east-west orientated high-rise buildings experienced lower heat fluxes and greater shade, consistent with the effects observed previously (Schaefer et al., 2021).

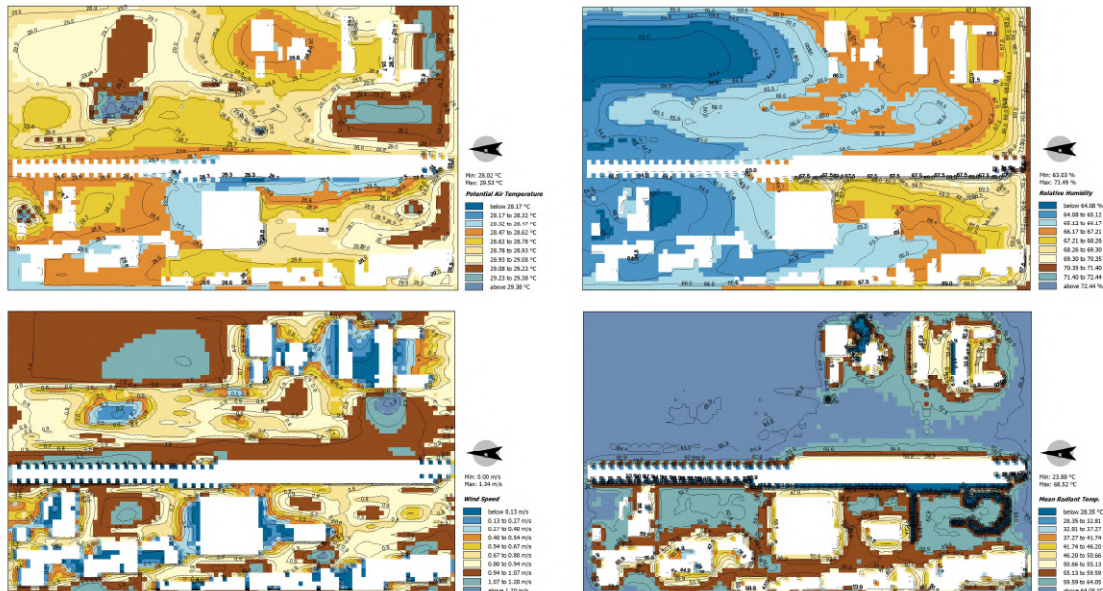


Figure 5.12 Distribution of microclimatic parameters (T_a , RH, WS, and T_{mrt}) in three small squares under the T0 scenario at 2.5 m height on August 27, 2021, 14:00 pm.

Analysis of different weather conditions revealed that the simulated mean T_{mrt} was higher on August 27 than on August 29 and 31, consistent with the trend of the actual measured values. Moreover, between on-site measurements and T0, mean T_a error ranged from -0.4 °C to -1.2 °C, mean RH error from 6.1% to 11.7%, mean WS error from -1 to 0.1 m/s, and mean T_{mrt} error from -4.4 °C to 5.2 °C (Table 5.5). The base model only allowed for dynamic changes in T_a and RH under the simple force mode of ENVI-met. Meanwhile, T_{mrt} could be adjusted by a built-in factor (0.5–1.5), whereas WS could not be forced for hourly changes to maintain a steady-state. Overall, vegetation patterns and thermodynamic conditions affect the local microclimate.

Table 5.5 Simulation results of microclimate parameters under different green space configurations on August 27 (a), 29 (b), and 31 (c), 2021.

(a) On August 27								
Scenario	Mean T_a	T_a error relative to T0	Mean RH	RH error relative to T0	Mean WS	WS error relative to T0	Mean T_{mrt}	T_{mrt} error relative to T0
On-site	27.2 °C	-1.2 °C	75.6%	8.8%	0.7 m/s	0.0 m/s	45.9 °C	-4.4 °C
T0	28.4 °C	-	66.8%	-	0.7 m/s	-	50.3 °C	-
T1	28.2 °C	-0.2 °C	65.8%	-1.0%	1.1 m/s	0.4 m/s	52.0 °C	1.7 °C
T2	27.8 °C	-0.6 °C	70.5%	3.7%	0.9 m/s	0.2 m/s	46.1 °C	-4.2 °C
T3	27.9 °C	-0.5 °C	68.9%	2.1%	0.8 m/s	0.1 m/s	45.1 °C	-5.2 °C
T4	27.8 °C	-0.6 °C	70.2%	3.4%	1.0 m/s	0.3 m/s	46.4 °C	-3.9 °C

(b) On August 29								
Scenario	Mean T_a	T_a error relative to T0	Mean RH	RH error relative to T0	Mean WS	WS error relative to T0	Mean T_{mrt}	T_{mrt} error relative to T0
On-site	27.2 °C	-1.1 °C	72.5%	6.1%	0.5 m/s	-0.1 m/s	42.1 °C	1.9 °C
T0	28.3 °C	-	66.4%	-	0.6 m/s	-	40.2 °C	-
T1	28.2 °C	-0.1 °C	66.2%	-0.2%	1.1 m/s	0.5 m/s	39.3 °C	-0.9 °C
T2	28.0 °C	-0.3 °C	67.8%	1.4%	0.6 m/s	0.0 m/s	39.8 °C	-0.4 °C
T3	28.2 °C	-0.1 °C	66.4%	0.0%	0.9 m/s	0.3 m/s	39.6 °C	-0.6 °C
T4	28.1 °C	-0.2 °C	67.5%	1.1%	0.8 m/s	0.2 m/s	39.7 °C	-0.5 °C

(c) On August 31								
Scenario	Mean T_a	T_a error relative to T0	Mean RH	RH error relative to T0	Mean WS	WS error relative to T0	Mean T_{mrt}	T_{mrt} error relative to T0
On-site	26.2 °C	-0.4 °C	79.5%	11.7%	0.7 m/s	0.1 m/s	41.6 °C	5.2 °C
T0	26.6 °C	-	67.8%	-	0.6 m/s	-	36.4 °C	-
T1	26.5 °C	-0.1 °C	67.6%	-0.2%	1.0 m/s	0.4 m/s	36.0 °C	-0.4 °C
T2	26.4 °C	-0.2 °C	69.3%	1.5%	0.8 m/s	0.2 m/s	36.6 °C	0.2 °C
T3	26.6 °C	0.0 °C	67.9%	0.1%	0.9 m/s	0.3 m/s	36.3 °C	-0.1 °C
T4	26.4 °C	-0.2 °C	68.7%	0.9%	0.7 m/s	0.1 m/s	36.3 °C	-0.1 °C

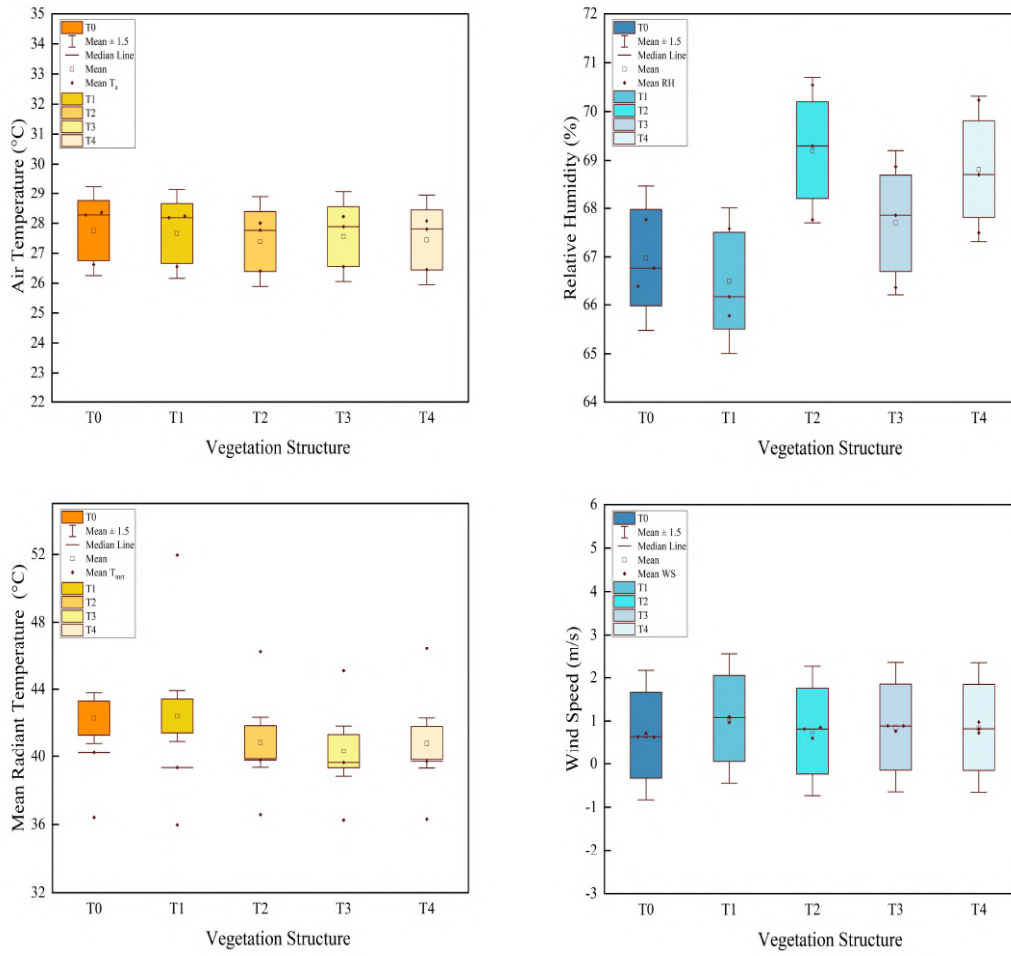


Figure 5.13 Microclimate condition variation under different green space configurations on August 27, 29, and 31, 2021.

5.8.3 The Effect of Green Configuration

Adjusting the green space configurations (T0, T1, T2, T3, T4) creates different microclimate conditions for homogeneous building morphology, as shown in Table 5.5 and Figure 5.13. In the simulation dates, T2 and T4 configuration patterns were particularly remarkable in cooling effect, with the highest mean T_a reduction of 0.6 °C compared to the T0 pattern. The T3 pattern adjustment significantly reduces the thermal radiation for the full scale, reducing the mean T_{mrt} by a maximum of 5.2 °C compared to the mean T_{mrt} in the T0 pattern. For all green configuration patterns, the WS remains stable in the simulation dates and enhances the ventilation of the space in the new green configurations, with the maximum WS increasing up to 0.5m/s in the T1 pattern. The results validated better ventilation in the T1 pattern without vegetation blocking the airflow (Xiao & Yuizono, 2022). Green configuration patterns have significant cooling and humidifying effect in the single-layer evergreen tree planting pattern (T2) and the multi-layer mixed evergreen and deciduous tree planting pattern (T4). This effect can also be evidenced by these finds (Abdi et al., 2020; Xiao & Yuizono, 2022). However, the composite pattern of deciduous trees and grass planting (T3) can effectively mitigate the heat radiation flux and relieve thermal stress. The T3 pattern is modeled with the Japanese Pagoda (LAD=1.0) as

the primary street tree species. The parametric modeling of this tree is 11.93m in height and the canopy width reaches 7.37×8.89 m. It is a typical urban tree more effective in reducing the T_{mrt} of pedestrian height with a large canopy, short trunk, and high-density shape, which is consistent with the study by Kong et al. (2017) that confirmed that these features of the urban tree could result in a T_{mrt} reduction of 5.1 °C in outdoor spaces. The different composition of tree species creates some disparity in the degree of latent heat loss from transpiration and affects the summer thermal comfort in square area (Moser et al., 2017; Rahman et al., 2018). Deciduous trees (Japanese Pagoda) and grasses contribute to transpiration cooling on summer days.

5.8.4 Effect of Building Morphology

As shown in Table 5.6, the impacts of buildings and green spaces on microclimate were qualitatively analyzed based on receptors in QA, QB, and QC, which exhibited various patterns of green configurations under heterogeneous spatial conditions, namely AT0, AT1, AT2, AT3, and AT4 in QA; BT0, BT1, BT2, BT3, and BT4 in QB; and CT0, CT1, CT2, CT3, and CT4 in QC. Simulations of the same green configuration in different blocks revealed that QB ($H/W=0.3-0.5$) showed the lowest T_a and the highest RH in 93% and the highest WS in 90% of the receptor scenarios. Meanwhile, QC ($H/W=0.4-1.0$) showed the lowest T_{mrt} in all receptor scenarios. These results indicate that building morphology significantly affects the microclimate (Kariminia et al., 2015; Galal et al., 2020). QA ($H/W=0.2-0.5$) showed poorer microclimatic conditions in all receptor scenarios, T_{mrt} and T_a were higher in QA than in QB and QC. Thus, a higher building aspect ratio positively regulate microclimatic conditions, and canyons with a high aspect ratios increase shade to improve thermal comfort (Muniz-Gaal et al., 2020).

Table 5.6 Variations in microclimatic conditions in updated scenarios under different receptors area on August 27, 29, and 31, 2021.

Scenario / Date	Mean T_a (°C)			Mean RH (%)			Mean WS (m/s)			Mean T_{mrt} (°C)		
	08.27	08.29	08.31	08.27	08.29	08.31	08.27	08.29	08.31	08.27	08.29	08.31
AT0	28.2	28.2	26.8	65.2	65.6	66.0	0.4	0.6	0.5	48.4	42.2	36.3
AT1	28.0	28.2	26.8	68.2	64.9	65.1	0.7	0.8	0.7	49.3	41.4	37.9
AT2	27.9	28.0	26.6	67.4	67.0	67.1	0.3	0.4	0.3	46.8	41.4	38.0
AT3	28.1	28.3	26.8	65.7	65.5	65.7	0.6	0.7	0.5	47.5	41.7	38.9
AT4	28.0	28.0	26.7	66.8	66.0	66.2	0.6	0.6	0.4	47.5	42.2	38.6
BT0	28.1	28.1	26.6	67.9	67.2	67.8	0.9	0.2	0.9	45.8	38.6	35.5
BT1	27.9	28.2	26.6	68.0	66.1	67.6	1.0	1.0	1.0	46.2	38.6	35.3
BT2	27.8	28.0	26.4	70.8	68.0	69.7	1.0	0.8	0.8	45.4	38.8	35.8
BT3	27.9	28.3	26.6	69.1	66.4	67.9	1.2	0.9	0.9	45.1	38.5	35.4
BT4	27.9	28.1	26.5	71.0	66.0	69.6	0.6	0.7	0.5	44.3	39.6	36.4
CT0	28.3	28.3	27.0	67.1	65.6	67.2	0.2	0.4	0.4	40.3	35.5	32.6
CT1	28.2	28.3	27.0	67.1	65.2	67.0	0.2	0.4	0.4	41.5	34.8	31.8
CT2	28.0	28.2	26.8	68.4	66.0	67.7	0.2	0.4	0.3	41.0	34.9	32.0
CT3	28.2	28.3	27.0	67.9	65.4	67.4	0.3	0.4	0.4	39.1	35.2	32.2
CT4	27.7	28.3	27.0	68.3	65.9	67.7	0.2	0.4	0.4	42.3	35.5	32.6

Similarly, in the context of small-scale homogeneous building morphologies with different planting patterns, 88% of the scenarios in T2 showed the lowest simulated T_a and all updated scenarios produced a humidifying effect, consistent with the results of full-scale simulation. Therefore, evergreen trees produce a greater cooling effect. Accordingly, the T1 and T3 configurations showed lower thermal radiation, while 30% receptor scenarios in T1 showed the maximum WS due to the lack of vegetation. The simulation results of receptors in various building morphologies indicated that courtyards are well ventilated with cooling and humidification, and canyons with high H/W reduce thermal stress due to building shadows blocking the transmission of heat radiation. On the contrary, blocks have the poorest microclimate due to the dense vegetation surrounding the concrete-covered road, resulting in poor ventilation and heat dissipation. Hence, this pattern is unsuitable for to meet the cooling demands of crowded areas during hot hours. Overall, BT2, CT3, and CT4 are the better optimized receptor scenarios in terms of the microclimate under different weather conditions and spatial configurations.

5.8.5 Improvement of Thermal Comfort in Updated Scenarios

The next part describes simulation results of PET on August 27, 29, and 31, 2021, from 12:00 to 19:00, particularly during the hottest hours (12:00 to 14:00 pm). Percentage-stacked PET distribution classes and visualized thermal maps were evaluated and compared with the thermal comfort levels (Figure 5.14 and 5.15).

The updated scenarios with simulated microclimatic conditions resulted in different PET distribution levels on summer days, as shown in Figure 5.14. On August 27, approximately 18% of the simulated PET results were in the very hot level ($PET > 42\text{ }^{\circ}\text{C}$) under all green space configurations from 12:00 am to 19:00 pm. Moreover, nearly 50% of simulated PET results were in the hot level ($38\text{--}42\text{ }^{\circ}\text{C}$) in Figure 5.14a. The highest mean PET reached $44.5\text{ }^{\circ}\text{C}$ at 14:00 in T0, and the PET thermal map showed the maximum value of $50\text{ }^{\circ}\text{C}$ within the small-scale square areas (Figure 5.15). On August 29, the thermal level gradually stabilized from warm to slightly cool compared with that on August 27, when the thermal stress was relatively moderate. As shown in Figure 5.15, on August 29, the maximum PET in T0 was $40\text{ }^{\circ}\text{C}$ in QA, but the value in QB and QC was $2\text{ }^{\circ}\text{C}$ lower. On August 31, thermal conditions in all configurations were between warm and cool, which was more comfortable than the thermal environment on the two previous days. The maximum PET was $38\text{ }^{\circ}\text{C}$ in QA at 14:00, which was $3\text{ }^{\circ}\text{C}$ higher than the value in QB and QC.

During the hottest hours, the PET level is generally in a very hot state. Most notably, the thermal conditions were worse thermal condition at 12:00 pm and 13:00 pm. As shown in Table 5.7 and Figure 5.14b-5.15, the T3 pattern achieves the optimal comfort level under different weather conditions, and the mean PET was reduced by $3\text{ }^{\circ}\text{C}$ on August 27. At the focused time of 14:00 pm, the mitigation of thermal stress lowed mean PET values by $4.2\text{ }^{\circ}\text{C}$ to alleviate very hot to hot levels (Figure 5.15). Thermal conditions were relatively moderate on August 29 and more comfortable on August 31; corresponding mitigation of thermal comfort was significantly weaker than on August 27, with a mean PET highest reduction of only $0.5\text{--}0.6\text{ }^{\circ}\text{C}$ (Table 5.7). These results indicate a more positive effect of extremely hot weather on the thermal comfort mitigation level, which is similar to mitigation strategies that have improved the urban thermal environment to a greater extent in hotter and drier climates (Lai et al., 2019). For $R_g=0$, the simulated mean PET errors varied by $0.7\text{ }^{\circ}\text{C}$,

0.3 °C, and 0.2 °C for these green patterns (T1, T2, and T3) (Table 5.7). The mitigation effect on thermal comfort levels was not strong and further illustrated that the same TD to TE number ratio had a weak effect on thermal comfort levels. In contrast, the T3 pattern ($R_g=0$) compared to the T0 pattern ($R_g=3.7$) on thermal mitigation was significantly effective in reducing the mean PET (Table 5.7 and Figure 5.15). Following this line of thought, solar radiation and airflow are important climatic components influencing the thermal performance in urban areas, which is the primary reason for the lower mean PET levels in the T1 pattern compared to the T0 pattern, where airflow in the presence of no vegetation is an essential factor influencing the thermal environment (Jamei et al., 2016). Thus, the green space configuration via the vegetation structure and the combination of tree species has a wide range of applicability to regulating the thermal environment compared to the existing T0 pattern.

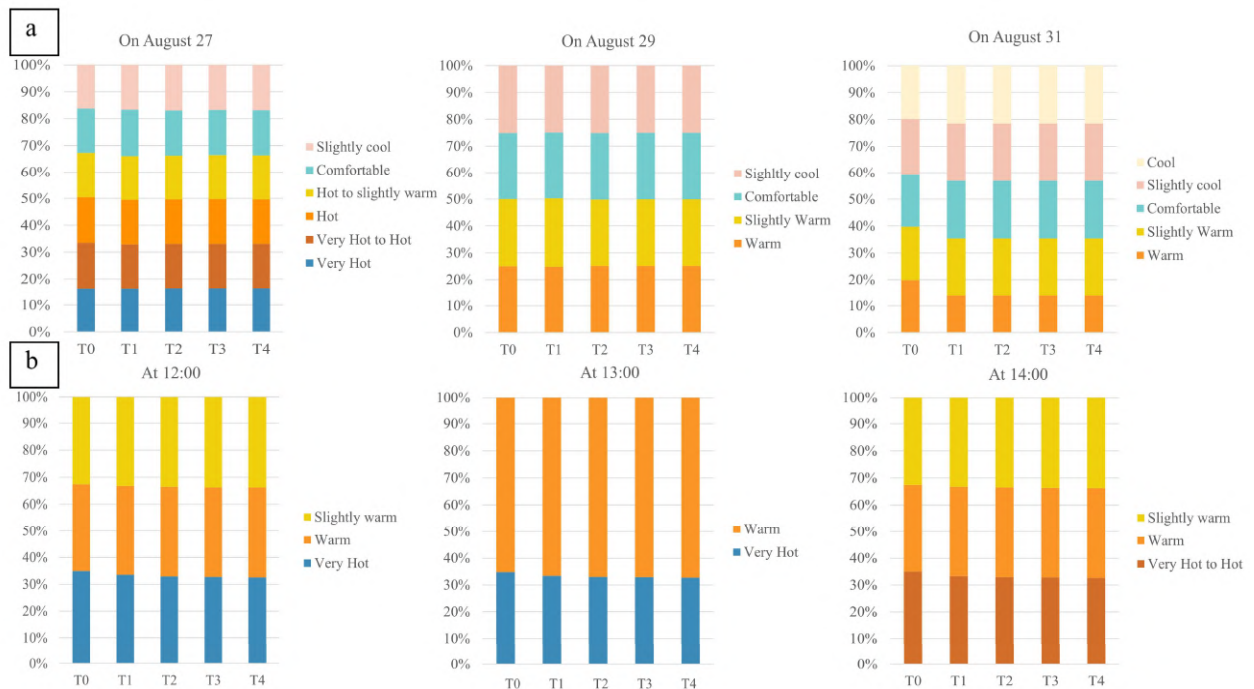


Figure 5.14 PET distribution at 2.5 m height from 12:00 pm to 19:00 pm on August 27, 29, and 31, 2021, under updated building morphology integrated with green space configurations (a). PET distribution during the prime hottest hours (12:00 pm to 14:00 pm) (b).

Table 5.7 Mean PET distribution at 2.5 m height from 12:00 pm to 19:00 pm on August 27, 29, and 31, 2021, under different green space configurations.

Pattern / Date	Mean PET (°C)		
	08.27	08.29	08.31
T0	36.9	31.8	29.3
T1	34.6	31.6	28.7
T2	34.4	31.6	28.9
T3	33.9	31.3	28.8
T4	34.3	31.9	29.2

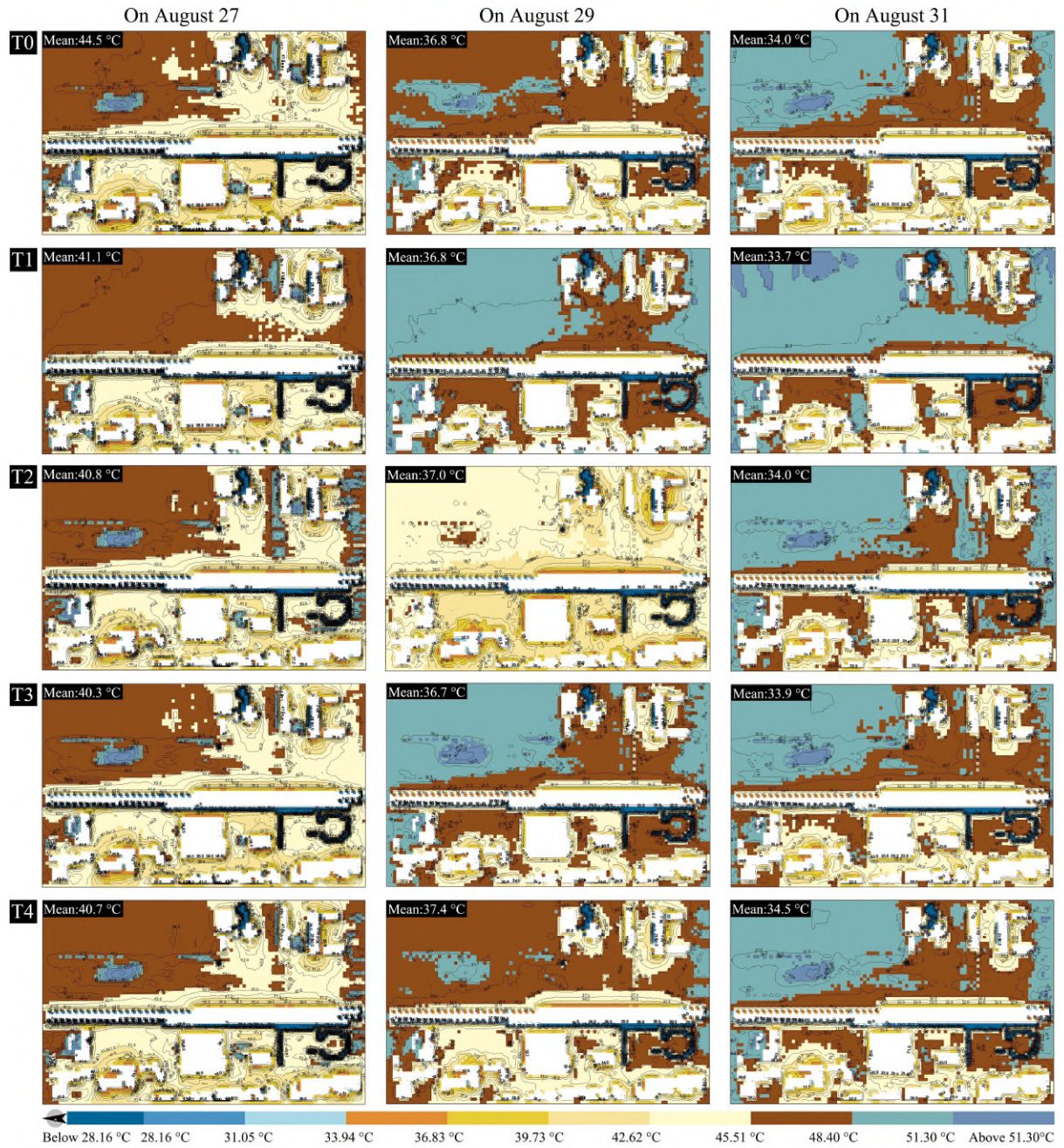
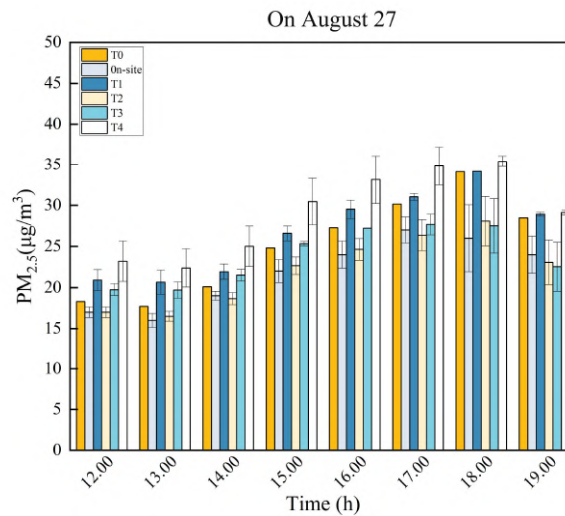


Figure 5.15 PET distribution at 2.5 m height at 14:00 pm on August 27, 29, and 31, 2021, under updated integrated building morphology and green space configuration.

5.8.6 Mitigation in PM_{2.5} Deposition

The configuration characteristics of buildings and green spaces affect the distribution of pollutants, particularly PM_{2.5} emissions, playing an important role in improving the ambient air quality (Schaefer et al., 2021). Trees show a more positive aerodynamic effect on pollutant deposition and form a green barrier to deal with air pollution at the local scale, ultimately affecting airflow patterns and pollutant levels (Taleghani et al., 2020; Buccolieri et al., 2018). As shown in Figure 5.16, the overall standard deviation (SD) of PM_{2.5} concentration between T0 and on-site measurements remained stable, with mean PM_{2.5} retention deviation ranging from 1.3 to 1.8 and showing variable deviations compared with the output concentration. Different configurations altered the distribution of PM_{2.5} concentrations in the homogeneous building context under different thermodynamic conditions. In contrast, PM_{2.5} concentrations on simulated dates were higher in the evening than at midday. On August 27, the lowest concentration distribution was noted in T2 and T3, particularly from 16:00 to 17:00 pm, with an SD of 2–3 compared with the value in T0. The corresponding maximum PM_{2.5} concentration attenuation was 6.6 $\mu\text{g}/\text{m}^3$ in T3 (16:00 pm). On August 29, the reduction in PM_{2.5} concentrations was more pronounced in T3 and T4; the maximum reduction in PM_{2.5} concentration was 4.2 $\mu\text{g}/\text{m}^3$ (16:00 pm) in T4, with an SD of 2.1. Consistently, on August 31, T3 and T4 produced the most optimized effects on PM_{2.5} concentrations, with the maximum reduction of 13 $\mu\text{g}/\text{m}^3$ in T4 (16:00 pm). Overall, the green configuration in T3 simultaneously optimized the weather conditions with different thermodynamic levels on all three days. The composite layer structure integrating deciduous Japanese pagoda trees in combination with grass achieved optimal climate regulation and air quality mitigation (Table 5.7 and Figure 5.16). Simultaneously, simulation results (12:00 to 19:00 pm) confirmed that 16:00 pm is the key hour for abating PM_{2.5} concentration. The reduction in PM_{2.5} concentration on August 31 was significant compared with that on August 27 and 29 (Figure 5.16 and Table 5.8). As illustrated in Table 5.6, the variation in T_a and T_{mrt} on the simulation dates was very large, indicating that temperature variations alter air viscosity and density and thus affect the deposition of atmospheric particles, indirectly influencing the ability of plants to retain atmospheric particles, that is, increasing the capture and uptake of PM_{2.5} by leaves due to condensation or humid conditions (Xie et al., 2022).



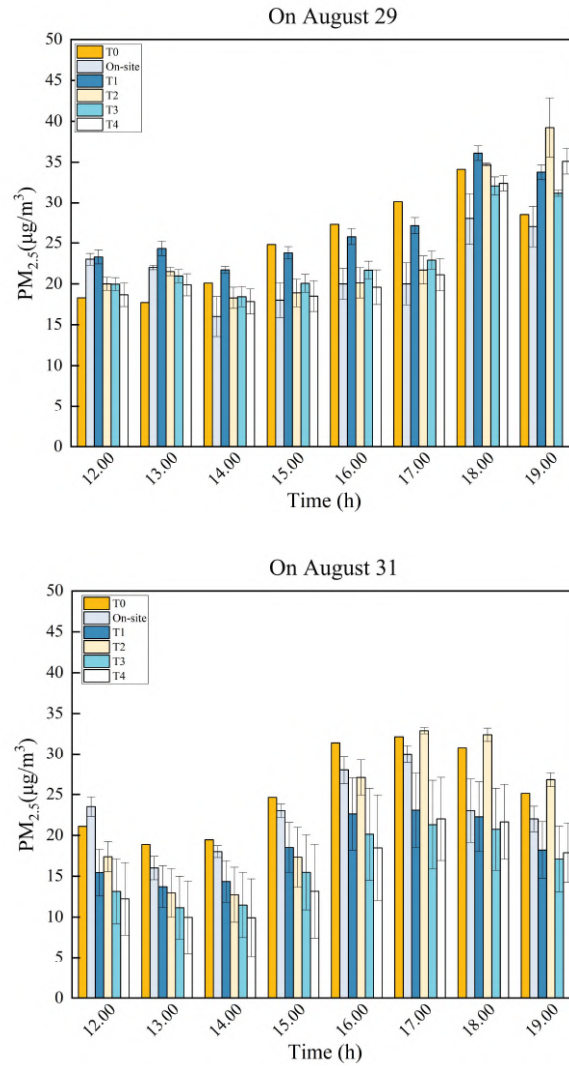


Figure 5.16 PM_{2.5} distribution with green space configurations compared with on-site measurements in a homogeneous building context on August 27, 29, and 31, 2021.

Further, the mitigation of PM_{2.5} concentrations was observed between squares with different building morphologies within the overall environmental context, as shown in

Figure 5.17. PM_{2.5} concentrations varied with microclimatic conditions and green space configurations within QA. QA is arranged in a block layout surrounded by traffic roads, and atmospheric PM_{2.5} concentration reached the maximum of 30 µg/m³ under the same green configuration. QB is central to the station traffic, with the highest PM_{2.5} concentration reaching 75 µg/m³ in T2. In contrast, the canyon building layout of QC resulted in a low PM_{2.5} concentration, with the minimum value of 5 µg/m³ in T4. In T0 pattern, *Cornus florida* (LAD=1) is predominantly planted as street trees, and these scenarios (AT0, BT0, and CT0) showed the highest PM_{2.5} concentration. Therefore, modifying the composition of tree species and their combinations on external streets significantly changed the PM_{2.5} removal effect. Our modeling results confirm the impact of tree design on air quality depending on their proximity to the sources of intensive traffic emissions in street canyons

(Abhijith et al., 2017).

In addition to tree design, H/W, wind direction (WD), WS, weather conditions, distance from pollutant sources, and tree density with height uniquely affect pollutant exposure in street canyons in a square area (Buccolieri et al., 2018; Abhijith et al., 2017). The aspect ratio shares a complex relationship with building morphology and green space configuration. Specifically, the aspect ratio determines the degree of pollutant dispersion by influencing airflow (Zhong et al., 2016). Street canyons in the square area of the present study are of the regular type ($0.5 < H/W < 2$) and shallow ($H/W \leq 0.5$). The main pollutant removal mechanism is determined by the primary vortex and distance from the emission source of intensive traffic. Additionally, meteorological parameters (RH, T_a , WS, and WD) are an important factor affecting the air quality of surrounding neighborhoods and open roads. In particular, humidity plays a crucial role in the analysis of exposure to ambient gas pollution. With the adjustment of vegetation patterns, T2, T3, and T4 produced a more significant effect on $PM_{2.5}$ abatement than T0 and T1. The major reason for this phenomenon is the lower mean RH distribution in T0 and T1 (Figure 5.13), and the positive effect of increased RH on $PM_{2.5}$ removal has been proven (Zalakeviciute et al., 2018). $PM_{2.5}$ dispersion was greater in the north-south direction in QA and QB under the influence of westerly winds, while it was the lowest in the east-west direction in QC with a windward position. Therefore, $PM_{2.5}$ concentrations in the leeward zone are higher than those in the windward zone under vertical airflow. These results are consistent with the distribution of concentrations in street canyons under different wind flow directions (vertical, parallel, and inclined) (Abhijith et al., 2017). The greater contribution of mixed vegetation plantation to air quality in summer by decreasing $PM_{2.5}$ pollution has been confirmed (Lixin Chen et al., 2016). This finding reasonably explains the generally $PM_{2.5}$ concentration in T3 and the fluctuating high and low concentrations in T4 pattern (Figure 5.16 and 5.17). Additionally, evergreen tree plantation (T2) effectively reduced pollution in different weather conditions. In T0, deciduous *Cornus florida* (LAD=1) trees, which are 3 m tall, were planted as the main street trees. In T2, the evergreen camphorwood (LAD=1) trees, which are ~9 m tall, were planted as the main street trees. In T3, Japanese pagoda trees (LAD=1), which are ~11.93 m tall, were planted as the main street trees. Finally, in T4, a mix of evergreen camphorwood and deciduous *Cornus florida* trees were planted at intervals as the main street trees. In August, when the LAD of trees was the same, taller trees with a larger canopy produced a stronger $PM_{2.5}$ removal effect. Meanwhile, the composition grass integrated with Japanese pagoda trees achieved optimal performance in terms of $PM_{2.5}$ removal under different weather conditions, particularly on August 31, when the mean $PM_{2.5}$ removal concentration reached the maximum of $9 \mu\text{g}/\text{m}^3$ (Table 5.8). Similarly, the T4 pattern positively affected $PM_{2.5}$ removal (maximum reduction of $10 \mu\text{g}/\text{m}^3$). Overall, our simulation results demonstrated that complex canopy structures combined with changes in meteorological conditions are more effective in $PM_{2.5}$ removal.

5.9 Conclusions

A well-regulated thermal environment improves airflow through the urban canopy to alter the distribution of atmospheric pollutants. Moreover, it reduces the energy consumption of buildings and improves the thermal comfort of pedestrians. Simultaneously, an appropriate green space configuration reduces traffic noise and improves air quality. The present study explored idealized scenarios of mitigation strategies using the ENVI-met V5 model to assess the links between microclimate, thermal comfort, and air quality in a large-scale homogenous urban context. A comparative study of the cooling, aerodynamic, and air pollution mitigation effects of different space configuration patterns in the summer was successfully implemented in a typical Japanese station square area. The present study focused on the regulation of thermal environment and PM_{2.5} abatement using green strategies (vegetation structure, tree species, and combinations) within the same context. Except the multi-level (with additional evergreen trees) and no vegetation structures, the rest of the idealized scenarios produced cooling effects through integrated vegetation structure and tree species at the same number of trees. However, the best cooling effect on the thermal environment was confirmed in the structure composed solely of evergreen trees ($R_g=0$), with the maximum reduction of 0.6 °C. More interestingly, a multi-layer structure with deciduous and evergreen trees ($R_g=1.2$) produced the same optimal cooling effect as the former pattern.

The aspect ratios of three small-scale squares were complexly associated with the characteristics of green space configuration. Specifically, the aspect ratio affected the overall urban canopy airflow pattern to regulate microclimatic conditions and PM_{2.5} concentrations. The canyon square was windward on two days, with a high aspect ratio, which was conducive to thermal comfort and pollution mitigation during the summer. Meanwhile, the block and courtyard squares were disadvantageous in terms of thermal regulation and PM_{2.5} capture, as they were located close to traffic emission sources and in the leeward direction. Based on the results of the present study, the most effective composite configuration for the overall environment depends on the selection of tree species and the configuration characteristics of tree height and structural composition, leading to an ideal local green design that integrates heat stress reduction and pollution removal. In the present study, the single-layer, composite layer, and multi-layer structures created a better microclimate under different weather conditions than the original structure, enabling the regulation of cooling, humidification, ventilation, and radiation. Specifically, the composite layer structure of Japanese pagoda trees and grass was more effective in improving thermal comfort by reducing PET by 5.2 °C at 14:00 pm and the mean PET by 3 °C on typical summer days. Similarly, under different weather conditions, this green configuration patterns led to the maximum PM_{2.5} reduction of approximately 9 µg/m³. Therefore, this composite layer structure is an optimal design for achieving the threefold environmental benefits of microclimate, thermal comfort, and air quality. The proposed green configuration pattern can serve as a reference for decision-making in the future realization of TOD in urban station planning in Japan and contributing to the creation a comfortable and sustainable station environment. Moreover, this pattern can serve as a greening mitigation strategy for the development of sustainable and land-intensive stations to respond to summer heatwaves and HUI. Further, re-examination of building morphology and green space configuration by careful selection of vegetation structure and tree species can offer pedestrians with environmental benefits of outdoor station spaces.

Finally, there are some limitations in the present study using ENVI-met modeling. In simulation validation, we only tested the performance for T_a while neglecting the validation for other parameters. Moreover, the green configuration patterns focused on the regulatory effects of trees on the thermal environment and air quality, with a limited emphasis on the mitigation effects of other vegetation types, such as grasses or shrubs. Nonetheless, the present study is distinct from previous works on thermal comfort and microclimate in squares, which focused on the concentration distribution and thermal environment within the same square morphology. In addition, the present study addressed only a single type of pollutant without collectively considering multiple sources. ENVI-met can potentially overestimate or underestimate the concentration distribution of gaseous pollutants during simulation. Future studies should focus on different heights and canopy sizes in ENVI-met parametric modeling to assess how more specific vegetation characteristics affect thermal mitigation and pollution for implementing more refined designs with better mitigation performance and multiple impact factors in complexity analysis. In addition, future simulations should include more tree species and examine multiple pollutant types in seasonal variation.

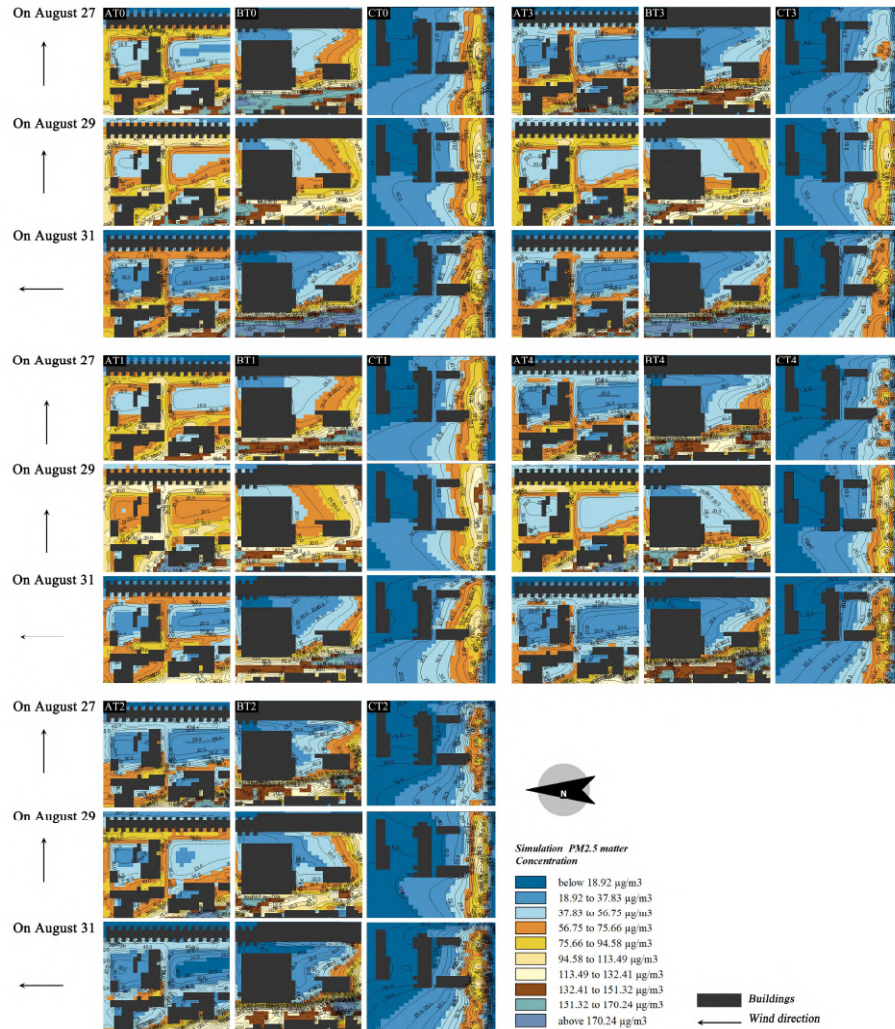


Figure 5.17 PM_{2.5} distribution 2.5 m height in a green configuration space under different wind directions (150 m × 150 m grid) in a heterogeneous building context on August 27, 29, and 31, 2021 (at 16:00 pm).

Table 5.8 Mean PM_{2.5} distribution at 2.5 m height with different green configurations in a homogeneous building context on August 27, 29, and 31, 2021.

Pattern/Date	Mean PM _{2.5} (µg/m ³)		
	08.27	08.29	08.31
T0	25.1	25.3	25.4
T1	26.7	27.0	18.5
T2	22.1	24.3	22.4
T3	23.9	23.4	16.3
T4	29.2	22.9	15.7

Chapter 6 Discussion

6.1 Climate-sensitive Design Principles Achieved in NSs and USRs

Buildings are prime contributors to global warming in the urban space. One obvious approach to mitigating climate change involves designing low or no-energy buildings. However, this study focuses on the ability of urban green infrastructure (UGI) in green spaces to regulate the climate environment. A key challenge for urban design involves developing climate-sensitive design strategies for cities, where climate change impacted designers and planners to reconsider the rationality of urban design, especially the design of green spaces and elements like urban parks, squares, and street trees. In contrast, these green spaces and design elements are termed UGI and provide corresponding environmental benefits through ecosystem services (Klemm et al., 2017). The redesign of the UGI promotes an optimal design to set a comfortable outdoor public space based on green building, which considers seasonality, ventilation, scale variations, natural shadows of the surrounding terrain, and weather and climatic zone characteristics (e.g., wind, rainfall, humidity). UGI is increasingly recognized for reducing urban heat levels to benefit citizens' health, well-being, and thermal comfort. The positive effects of UGI on thermal conditions have been described at different urban scales and targeted at different vegetation structures. In addition to enhancing physiological and thermal conditions, UGI has improved human thermal perception (Lenzholzer et al., 2018). Thermal comfort is one of the performances that characterize the quality of green spaces and significantly affects the time and activities people spend in public spaces. The cooling effect of UGI has been widely accepted by urban planners and researchers (Cui et al., 2021).

This study was conducted using the CFD and thermodynamics-based ENVI-met software to understand how designs could better integrate with local climate and site-specific microclimate features. The NS_s considers a proactive strategy for systematically optimizing the challenges of extreme cold and hot climates in the humid subtropical climate of the Hokuriku region and developing a synergistic optimization mechanism to regulate the future construction of Komatsu Station following climate-sensitive design principles. Thermal comfort and microclimate regulation involve considering complex parameters in a station space with a high density of people. Strategic landscape design can ameliorate local thermal stress and enhance climate resilience in urban areas. Densely populated station squares are particularly important outdoor activity areas that require more mitigation of thermal conditions during extreme weather. The traditional station square design focuses on the transport system and lacks the regulation of landscape services (e.g., climate change, scale, and element configuration). Thus, holistic optimal design strategies are still deficient in the station.

In the NSs, this study examines how thermal comfort is positively affected by various landscape layout patterns, the configuration ratio of deciduous to evergreen trees, and vegetation structure. We selected a typical station square of the Hokuriku region and measured a landscape microclimate environment in winter and summer during extremely cold and hot days. The thermal comfort performance represented by the PMV thermal index was compared using the ENVI-met simulation to reproduce the original case and new landscape design scenarios. The results indicated that planting trees in an array layout pattern with low PMV distributions improved thermal performance at 14:00 (0.3 PMV increase in winter and 1.3 PMV decrease in summer). The

tree configuration ratio is a critical greening indicator that regulates thermal comfort during the day and night. The optimal scenarios can be used as a guide for urban station square design to mitigate thermal comfort issues and promote station square planning, complying with adaptive-climate design strategies to construct sustainable cities.

In the USRs, the relationship between buildings and green space configuration is considered simultaneously, comparing green parameters such as vegetation structure, quantity, combination, and number ratios in the same building context. The assessment of microclimate, thermal comfort, and air quality is jointly regulated by the differences in scale and weather conditions. The removal of $PM_{2.5}$ and the thermal environment optimization are realized to respond to the problems of summer thermal stress and pollution concentrations to deal with the different thermal conditions in summer and building morphology. Station squares play exemplary roles in the design of urban landscapes, contributing to the mitigation of the UHI and atmospheric pollution dispersion effects. A vibrant station space is constructed by considering the various environmental benefits in its optimal design. However, the co-optimization strategies for building green spaces with station renaissance remain unclear. Therefore, we investigated a station square area in Komatsu City, Japan, taking on-site measurements and ENVI-met V5 simulations to reproduce three building morphologies (block, courtyard, and canyon) integrated with five green space configurations-T0 (original structure), T1 (no vegetation), T2 single-layer structure (evergreen trees), T3 composite layer structure (deciduous trees and grass), and T4 multi-layer structure (deciduous trees and evergreen trees). The ENVI-met V5 model was applied to simulate scenarios for optimizing green space patterns on hot summer days based on the PET index and environmental indicators of microclimate conditions, thermal comfort, and atmospheric $PM_{2.5}$ distribution. Simulations revealed that the deciduous trees (Japanese pagoda) and grass co-mitigated the local thermal environment (maximum reduction in mean PET of 3 °C) and $PM_{2.5}$ emission (maximum removal of 9 $\mu g/m^3$). Coincidentally, the T2 and T4 patterns exhibited the same cooling potential (maximum T_a reduction of 0.6 °C).

Moreover, the ratio of number of deciduous and evergreen trees was identified as a key green indicator for reducing thermal stress. Canyon square obtained greater environmental benefits in the windward direction in a high H/W. These results indicated that spatial configuration patterns and thermodynamic conditions are important factors for improving thermal comfort and air quality. The proposed optimal design can serve as a vital decision-making guideline for Japanese urban planning to develop a city radiating effect and climate responsive design within station squares.

6.2 The Challenges of Setting a Comfortable Station Square

Traffic congestion and air pollution have become serious problems in cities because of population and economic growth and people's reliance on cars. TOD is an effective way to address these problems and improve urban sustainability. It is a station-oriented urban development based on taking advantage of public transport systems integrated with station and city development. TOD has been used for over a century for urban development constructed around railways as one of Japan's strengths. The following aspects must be addressed to mitigate the environmental challenges in the station to create a comfortable environment.

Firstly, these challenges arise from the effective use of space at transport nodes and the efficient use of land

resources. In the Komatsu Station square area, some grey spaces face the reality of lacked function or abandonment. The configuration of small items, the functional positioning, and the articulation of the spatial configuration with the traffic nodes are mainly addressed to utilize space effectively.

For example, some grey spaces lack sufficient sunlight and have been abandoned in the canyon under the viaduct and between the station. The transformation of the viaduct space into a parking space for bicycles and vehicles must be accompanied by an efficient connection between transport and convenience, avoiding traffic jams to develop a cycle of functional spaces guided by traffic (Figure 6.1).

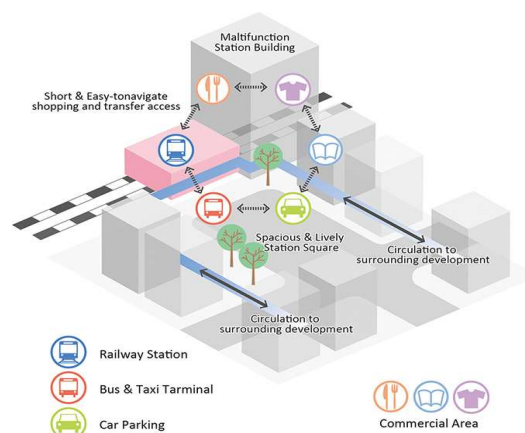


Figure 6.1 Transport-oriented development (TOD) of functional spatial cycles (Source from: https://www.nikken.co.jp/en/expertise/civil_engineering/planning_and_design_of_railway).

Secondly, Komatsu Station square lacks a public space to rejuvenate the city. The station square design limited innovative thinking for green space configuration, landscape, and site functions. As surrounding residents are keen on extreme skateboarding and cycling, there is a lack of consideration for the habits of people living on the site. The Komatsu Station Park to the east of the station is not effectively linked to the station square design to achieve a functional transition and connection. Thus, the integrated advantages of the comfortable station design achieved in the context of the building layout must meet the design objectives of functional connection, rational configuration, efficient operation, climate regulation, and air quality optimization.

Thirdly, the symbolic design of the station square is a city landmark and a postcard for the local area. It is challenging to incorporate the distinctive local traditional culture of Komatsu into the station square design. Creating an urban square with a sense of culture and history will increase the city's inhabitants' sense of well-being and belonging to emphasize its role as the city center.

Fourthly, the overall design will ensure the seismic reinforcement role and safeguard fire and flood safety in the station square area.

6.3 New Implementations Effective for Station Square

This study's new implementations in the NSs involved the redesign of landscape layouts and the quantitative analysis of tree configuration ratios for landscape mitigation mechanisms to regulate the spatial scale of the inner and outer rings in the station square. In implementations of the USRs, the case studies involved the

analogy of small-scale spaces (block, courtyards, canyon) around station squares, the regulation of multiple environmental considerations (thermal environment, microclimate environment, ambient air quality) by universal greening patterns, and the ratio of number of trees quantified the cooling the ambient environment. These new implementations respond to the specific application and reference of climate-sensitive design strategies for station squares and can be applied to new design scenarios for the future construction of homogeneous station squares and climatic conditions in the Hokuriku regions.

6.3.1 Effective in NSs-A New Synergistic Strategy

(1) New landscape layouts

In the new landscape design strategy of Chapter 4, the three landscape layouts are original in analogy to the perimeter, array, and scatter, and proposed co-adaptation responses for very cold and very hot climates. In new landscape layouts, the array layout is effective in resisting cold winds in winter, with a maximum reduction of 1.0m/s compared to the perimeter layout of on-site, especially for large-scale scenarios (L2-2a, L2-2b, L2-2c). In comparison, the scattered layout is less effective in reducing cold winds, with a maximum reduction of 0.65m/s. The L2-1 scenario can effectively be solved by changing the landscape design layout into an array layout (L1-1, L2-1, L3-1) with similar Q_A and G_A . The L2-1 scenario can effectively solve the cold wind prevailing in the human body for improving pedestrians' mobility in winter, which results in inconvenience and cold stress. Meanwhile, the array layout planted with trees can increase winter T_a and T_{mrt} regulation of surrounding thermal conditions. Correspondingly, the array layout of planted trees also effectively addresses the extremely hot conditions of August within the station square, reducing the T_a by a maximum of 1.0 °C to mitigate the persistent climate change of high temperatures.

(2) New greening indicator-tree configuration ratio

The new greening indicator was proposed to primarily fill the gap in the performance analysis of outdoor microclimate and the thermal environment by the configuration ratio of trees (deciduous trees vs. evergreen trees). Moreover, it was demonstrated in the microclimate simulations that the relationship between the different types of tree configuration influences seasonal climate change, spatial scale variation, and duration variation. In particular, the adjustment of tree configuration ratios in the same QB and GB scenarios directly determined the mitigation of extreme cold and hot phenomena in winter and summer, optimizing climate change on the outdoor environment and pedestrian trips in the greatest possible way. Evergreen trees are the main urban trees in the station square area for mitigating existing problems in the local landscape (①-⑤,⑦-⑧) and follow the capture of characteristic climatic conditions.

(3) Scale effect for station square

Optimizing the thermal environment by scale adjustment can improve the overall Komatsu urban plan to renew and increase the resilience of outdoor public spaces, providing new design guidelines for creating a more comfortable and sustainable habitat. In the NSs, the focus is on the core site of the station square and the overall thermal comfort of the inner and outer ring of street spaces. The small-scale (inner ring space) and large-scale (inner and outer ring environment) implementations include changed landscape design elements and indicators, with the large-scale adaptation strategy being the most beneficial for the station environment.

(4) Synergy optimization mechanism

The synergistic optimization mechanism has proposed a new landscape design implementation plan to achieve a holistic control of vegetation, scale, season, and duration in the horizontal and vertical structures. The mechanism realizes a holistic grasp of station space's inner and outer ring. The optimal design has the reference value for constructing station spaces with the same structural feature form throughout the central city of the HoKuriku region. This mechanism is also consistent with the urban planning goals of the SDGs, TOD, and climate-sensitive design can reduce the risk of exposure and health problems for pedestrians.

6.3.2 Effective in USRs-Urban Space Regulation Strategy

(1) An analogy of small-scale spaces in the station square area

In the regulation strategy of Chapter 5, the analogy with the building morphology of the station square area (block, courtyard, canyon) is mainly reflected in the typology of the spatial structure. The station square is orthogonally connected to the main parallel street, forming a small-scale typology of spaces commonly observed at Japanese stations. The block represents the outer ring where the external traffic space meets the square, and the canopy forms the courtyard that surrounds the internal ring of the station square. The surrounding building streets form the canyon space. The street type ($H/W=0.3-0.5$) has the worst microclimate conditions in the building context. In contrast, the courtyard type ($H/W=0.2-0.5$) has the most significant improvement in T_a and RH. In contrast, the canyon type ($H/W=0.5-1.0$) has the lowest T_{mrt} , indicating that variations in the building morphologies facilitate changes in the microclimate environment. Correspondingly, the canyon type significantly reached $5.0 \mu\text{g}/\text{m}^3$ in removing $\text{PM}_{2.5}$ from the station, mainly related to the distance from the station square where vehicle emissions are gathered and the wind environment.

(2) A universal landscape configuration pattern

The results of a universal landscape configuration pattern, comparing different configurations of native trees (*Corrus florida*, Camphorwood, Japanese pagoda) in response to thermal conditions and air pollution, showed that the composite pattern of Japanese pagoda and grass was the best vegetation structure in thermal mitigation (reduction of PET up to 3°C) and removal $\text{PM}_{2.5}$ (up to $9\mu\text{g}/\text{m}^3$). These results have wide applicability in all building types and can mitigate the potential risk of the UHI phenomena (e.g., vegetation structure, choice of urban street trees, excessive hard paving) in the existing station square area (QA, QB, QC). The specific problems are described in section 3.1.1, and this universal landscape configuration pattern has solved these problems by jointly regulating the internal heat exchange and traffic pollution in the station square.

(3) The new greening indicator - the ratio of the number of trees

The new greening indicator - the ratio of the number of trees (deciduous trees vs. evergreen trees) is mainly related to the issue of planting trees in urban streets of the station square central area. The cooling effect of evergreen trees with the same R_g reduced T_a by up to 0.6°C . The comprehensive study found that planting evergreen trees have a better thermal comfort regulation in summer than deciduous trees, which is verified by the simulation results in Chapter 5.

This study from the perspective of landscape design on the horizontal and vertical structure of the relationship between the space configuration to adapt to the thermal environment as follows: Chapter 4

proposed the control of tree configuration ratio for mitigating the extremely climates; and Chapter 5 used control of universal green configuration patterns for the mitigation of multiple environmental benefits. The main progress is promoting the analysis of the modeled performance of ENVI-met in evergreen and deciduous trees and testing its effect on thermal mitigation and pollutant removal.

6.4 How do you manage the gap between simulation and realistic scenarios?

6.4.1 Microclimate Model of ENVI-met Update

The vegetation modeling has evolved significantly with the continuous progress of ENVI-met (Figure 6.2). In ENVI-met V3, the vegetation model is mainly a simple model which cannot characterize the specific shape of the tree (Huttner, 2012). In ENVI-met V4, the vegetation modeling has been modified into simple and 3D vegetation models. The former is similar to the 1D vegetation model in V3, while the latter digitizes the LAD and RAD to get a more detailed vegetation modeling technique. In ENVI-metV5, the new user interface has been updated while refining the initial configuration settings concerning force modes in simple and full simulation modes. Python is the first to be integrated into the ENVI-met system for effective visualization and analysis. Realistic tree modeling is essential to accurately simulate vegetation's impact in producing urban environments. In previous versions, ENVI-met supported simple plants such as grasses and generic 3D plants representing different tree forms.

With the help of the next generation MiPSS (Microscale Plant Simulation System), ENVI-met V5 can model trees down to the high-resolution size of branches and leaves at the level of detail. It is also possible to define specific species and simulate their characteristics according to wind protection, solar protection, or transpiration. The new tree model is the basis of the Tree Pass, which will allow detailed simulations of tree mechanics and wind risks updated in 2022. ENVI-met V5 is a major step in simulating the highly complex interactions between different surfaces, materials, and structures to make the environment more realistic. Indexed View Sphere (IVS) uses intelligent light-tracking algorithms to scan the environment and visualize a part of the structure exchange radiation with the surrounding structure.

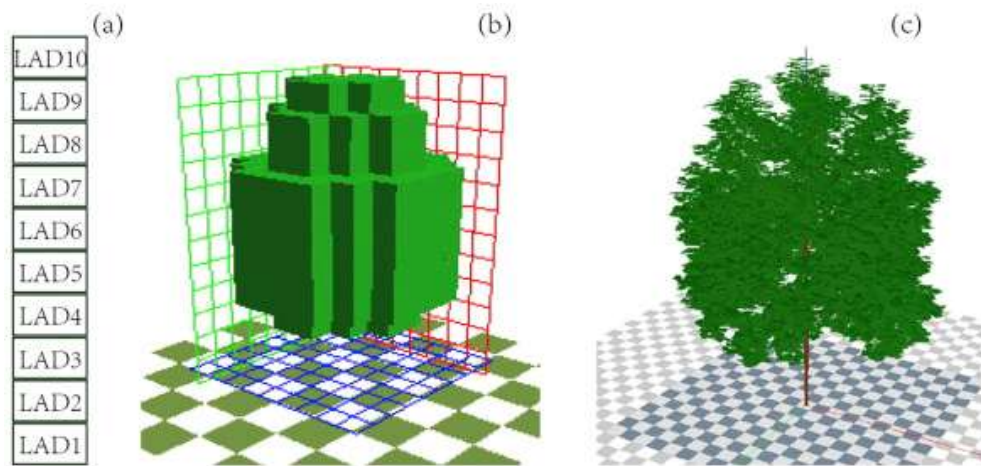


Figure 6.2 ENVI-met's tree models: (a) simple plants, (b) 3D plants, and (c) the model using the Lindenmayer-System in an ENVI-met V5 (Liu et al., 2021).

ENVI-met can assess physiological vegetation processes and represent vegetation in great detail, enabling a wide range of scenarios that would not be possible in the real world with a high spatial resolution (Koc et al., 2018). In reviewing previous ENVI-met studies on the optimal design of urban thermal environments, the studies usually follow a three-step research process of modeling, validation, and scenario simulation, which is widely applicable and common in numerical simulations. Model validation provides feedback on the microclimatic conditions of the restored site and how to capture the gap between the simulation and the realistic scenario. The main data sources are vegetation, materials, and reliable meteorological data capture. Where the output height of the meteorological data is kept at a steady state with the collection height to ensure the simulation results' accuracy, the forcing model choice is also an important means of ensuring the gap between simulation and reality. For ENVI-met to reduce errors and obtain more accurate results, it is advisable to conduct detailed on-site investigations to get better information on previous projects, especially on the technical and structural aspects of wall construction, vegetation albedo, and the LAI coefficients. In addition, validating the variable parameters with multiple statistical indices focuses more on the radiation aspects. The simulation scenario setting related to the research hypothesis allows us to validate and assess the environmental benefits from the areas and policies we are concerned with and simultaneously on a multidimensional basis, either in terms of climate zone distinctions, weather variations, seasonal variation or in synergy with multidimensional indicators in blue-green infrastructure design.

6.4.2 Progress of ENVI-met Software

Although the relevant ENVI-met simulations integrate the conventional three-step research process and have a solid physical basis, the simulation results are not representative of realistic scenarios but only on-site approximations. Some simple vegetation models in ENVI-met lack an integrated consideration of thermal radiation from evaporation and evapotranspiration. More than 50% of the relevant ENVI-met studies investigated the modeled performance of T_a , nearly 15% of the empirical validation of RH, while T_{mrt} only reached about 7%. Little validation has been carried out involving surface temperature, WS, long-wave

radiation, and short-wave radiation (Liu et al., 2021). Thus, there are still some limitations in the ENVI-met simulation, as follows:

- 1) Cloud and wind speed settings remain static under simple forcing, while the dynamic forcing process is ignored.
- 2) Building and vegetation modeling limitations of a detailed database to model materials and vegetation types. Lack of investigation of building and vegetation properties using sophisticated instruments, e.g., heat transfer properties of buildings (e.g., emissivity and thermal conductivity) and vegetation properties (albedo and LAD distribution).
- 3) ENVI-met's simulation scenarios were designed by making hypotheses about the conditions from the basic model, and only building geometry modeling does not have detailed building shapes.
- 4) ENVI-met lacks the consideration of heat as dynamic heat transfer, especially in vehicles and refrigeration appliances.
- 5) The blue infrastructure design ignores the issue of introducing multiple ways of water body design in small spaces, such as hand washing bowls, water walls, mirrored water bodies, and other forms of setting. The setting of fountain installations involves setting height and source geometries, but the time issue is not detailed.
- 6) The vegetation types are divided into deciduous and coniferous types, but setting the characteristic properties of evergreen trees are ignored. There is a lack of systematic consideration of the classification of vegetation systems. Creating new models for the 3D vegetation model lacked guidance and details for self-creation in ENVI-met V5.
- 7) Meteorological data is collected from different weather stations and meteorological equipment, and there is a lack of guidance and monitoring of scientific instruments to reduce simulation errors.
- 8) An actual measurement of vegetation canopy, leaf shape, and specific LAD characteristics lacks guidance on measurement techniques and methods.
- 9) Microscale terrain setting requires sophisticated remote sensing technology to support, which is difficult to obtain terrain data settings.

ENVI-met identifies some limitations, but updated numerical modeling techniques can improve the understanding and study of the mechanisms of complex environments. In addition to validating environmental goals such as microclimate and thermal comfort, future research is more concerned with integrating with air quality, visual environment, sound environment, emotional assessment, and gaining support from remote sensing techniques and Rhino software to obtain detail modeling and complexity mitigation strategy assessment.

6.5 Contributions to Knowledge Science

Knowledge science is an important new discipline that has emerged from the knowledge economy and information reform demands. The Knowledge Science at Japan Advanced Institute of Science and Technology (JAIST) is a field of study that integrates the humanities, social sciences, and natural sciences at the forefront

of “knowledge creation,” intending to discover mechanisms for creating, accumulating, and utilizing knowledge and generating ideas in the design of future societies. In knowledge science, modeling the knowledge creation process addresses the collection, synthesis, coordination, and creation of knowledge. Before proceeding to knowledge creation, knowledge is defined as “reasonable and true beliefs” that enable organized and effective action (Brix, 2017). As a systematic and multi-layered concept, organizational knowledge requires four related sub-processes: intuition, interpretation, integration, and institutionalization. In interpreting and integrating knowledge, knowledge innovation develops and builds a portfolio of new products and services that are essential for future survival. The process of assembling and innovating knowledge involves the contribution of individuals, groups, and organizations to knowledge, and they can create new strategies for specific contexts through their interactions (Figure 6.3).

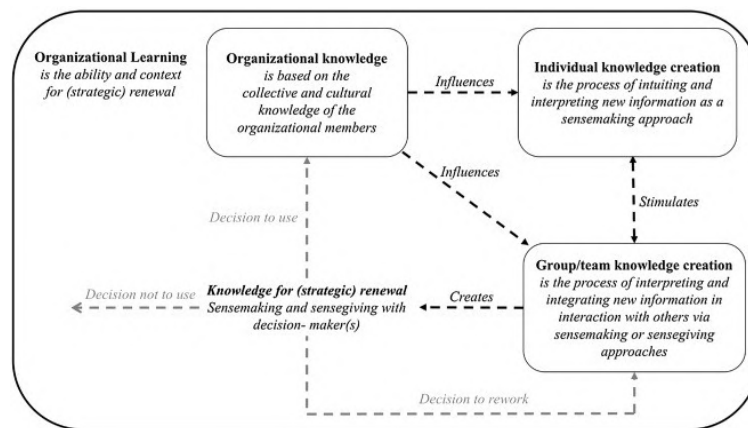


Figure 6.3 An integrated framework for organizational learning and knowledge creation (Brix, 2017).

Knowledge science is a problem-oriented and interdisciplinary field. The theme is the modeling of knowledge creation processes and applications. It is studied in disciplines in knowledge management and management science. JAIST’s science of knowledge was first created and provided an important academic contribution to the integrated approach to knowledge science and the theory of building systems. The book “Knowledge Science - Modeling the Knowledge Creation Process” presents the first mechanisms of knowledge integration and application for the process of knowledge creation and discovery (Nakamori, 2011). Combined with the theory of knowledge science, this study focuses on the intersection and application of multidisciplinary knowledge to form two optimal design strategies for system optimization. The NSs of Chapter 4 involved optimizing the spatial structure of horizontal and vertical landscapes from the landscape design theory and analysis of the time and space to assess the thermal comfort and microclimate environment adapted to the local central area of Komatsu Station Square. This study also integrates the environmental benefits of thermal comfort, microclimate, and air quality in the USRs of Chapter 5. It considers the integrated impact of green spaces to facilitate the city’s influence on the overall environmental benefits of microclimate simulation. The overall benefits of the spatial layout are analyzed singly and bi-directionally from the perspective of building morphological characteristics and vegetation configuration characteristics.

From the aspect of human life design, this study considers some aspects (i.e., climate, environment, urban

design, urban development) that affect the human living environment and sustainable development. From a social contribution perspective, the evaluation and simulation results of the two strategies provide optimal outdoor space to reduce urban construction costs and energy consumption. It provides a more comfortable and environmentally friendly optimal design of station squares and reduces the risk of pedestrian mobility. From an ecological perspective, the configuration studies in green design show that a reasonable configuration ratio and a ratio of the number of trees are key indicators of the impact on the thermal environment. New strategic research fields are formed by knowledge of urban climate, design planning, and microclimate assessment. This cross-discipline brings new strategies and thinking of knowledge and organizational learning (Figure 6.4).

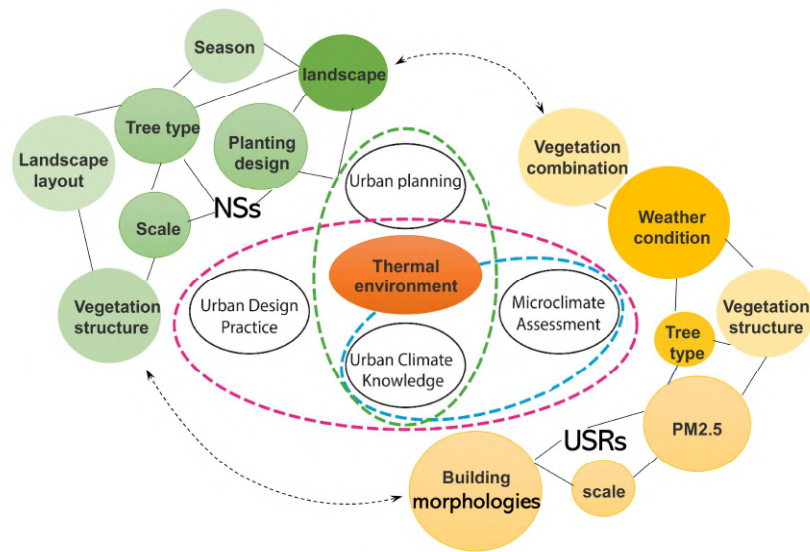


Figure 6.4 The intersection of new strategies and urban climate knowledge.

Chapter 7 Conclusion and Future Work

7.1 Conclusion

This study investigates how to optimize the design of station square areas to provide more comfortable public spaces for pedestrian activity in Komatsu City, seeking to improve the microclimate and taking into account human thermal comfort and air quality to achieve multiple environmental benefits. Implementing the NSs and USRs within a climate-sensitive design concept using ENVI-met microclimate simulations provides a new system to optimize station design solutions and co-regulate multiple environmental benefits in a universal greening pattern. Answers to RQ1 and RQ2 are specifically based on studies in Chapter 4 and Chapter 5. How these two key questions were specifically carried out is as follows.

RQ1: How to integrate climate characteristics, scales, and seasonal changes through a landscape design approach to achieve a synergistic design strategy for optimizing and regulating station squares?

The NS_s is more of a synergistic consideration of various influencing parameters such as landscape layout pattern, vegetation structure, tree configuration ratio, scale, and seasonal changes of a typical station square in the Hokuriku region. It is judged from the perspective of landscape design theory. The optimal performance of different tree configurations is considered in a landscape design system from horizontal to vertical structures, where specific optimal design solutions are balanced in time and space. The specific implementation methods are as follows:

- 1) Starting from the landscape layout was rearranged, changing the irregular layout of the original station square into an array and scattering with rectangular and circular shapes to quantify the similar green ratio from a horizontal structure. The landscape layout pattern improved thermal comfort and microclimate conditions, which were found to have weak performance in optimizing the thermal environment.
- 2) A new design scenario of small-scale tree configuration ratios for the array versus scattered layout scenario from the relationship of deciduous to evergreen tree configurations in the station square, in which it can be found that tree configuration ratios affect thermal comfort and microclimate changes in winter and summer.
- 3) The three synergistic approaches of landscape layout, tree configuration ratio, and vegetation structure were found to obtain the best small-scale design pattern for tree planting structures in the array layout.
- 4) The large-scale tree configuration ratios are based on the small-scale optimal design pattern to re-examine the regulation of the thermal environment. Large-scale tree configuration ratios were important greening indicators for co-regulating thermal comfort in winter and summer, both during the day and night.

RQ2: How to achieve a strategy for the regulation of station squares in microclimatic conditions, thermal comfort, and air quality for multiple types of spaces, considering both the building and the green environment configuration?

The USR_s corresponds to a strategy that emphasizes the relationship between the configuration of buildings

and green space to realize multiple environmental benefits. In the context of the urban canopy of Komatsu city, macro-scale and micro-scale investigations were carried out on three square types with different building form layouts. The optimal design pattern was finally obtained in the ENVI-met simulation scenario by considering various factors such as vegetation structure, combination, quantity, weather, and tree species. These influencing factors are in line with the local climatic characteristics, summer weather variations, and optimal configuration patterns. At the same time, the USRs analogized a universal greening pattern for the spatial configuration of greening patterns in the same urban morphology for the regulation of microclimate, thermal comfort, and atmospheric PM_{2.5}. The specific implementation approaches are as follows in several ways.

- 1) Five greening patterns were developed on the vegetation structure, with a similar sum of deciduous and evergreen tree numbers, based on which the tree design was adjusted. The results found that the ratio of the number of deciduous to evergreen trees was the key greening indicator for the cooling effect.
- 2) Through environmental assessment and analysis of microclimatic conditions, thermal indices, and PM_{2.5} atmospheric indicators, the composite layer structure - deciduous trees (Japanese pagoda) and grass became the universal greening configuration form for the three small-scale squares in different summer weather conditions, which achieved the threefold environmental benefit.
- 3) In the analogy of the different building morphologies, it was finally found that the canyon square is more optimized with the windward orientation and higher aspect ratio.
- 4) This study compares typical tree plantings in the area where tall and large trees are beneficial for PM_{2.5} removal in summer.

Various synergistic approaches exist in reviewing previous ENVI-met simulations performed to verify compliance with climate-sensitive design strategies. Recent research directions have shifted from focusing on the physical aspects of greening, buildings, and materials to integrating the physiological responses of human sight and sound. They are increasingly focused on the intersection of microclimate, thermal comfort, and air pollutant emissions (PM_{2.5}, PM₁₀, NO, NO₂, etc.). There has been a change from a strong focus on air temperature and humidity to concern thermal radiation and wind environments.

7.2 Future Work

This thesis focuses on the simulation results in the simple force mode of ENVI-met; based on this, I will be paid more attention to the full force mode in future simulation work. The model performance will be improved by comparing the two modes to reduce simulation errors. Moreover, numerical simulations focused on the deposition of multiple pollutants by a wider range of tree species types and vegetation, and practical validation results have been obtained through related field design projects. The consistency and heterogeneity of the results from realistic and ENVI-met simulations are summarized by comparing and analyzing the effects of climate regulation and adaptation before and after site improvements and reporting on realistic spatial assessments by users. This allows future numerical simulation studies to directly link to design and planning projects to obtain more favorable site optimization designs.

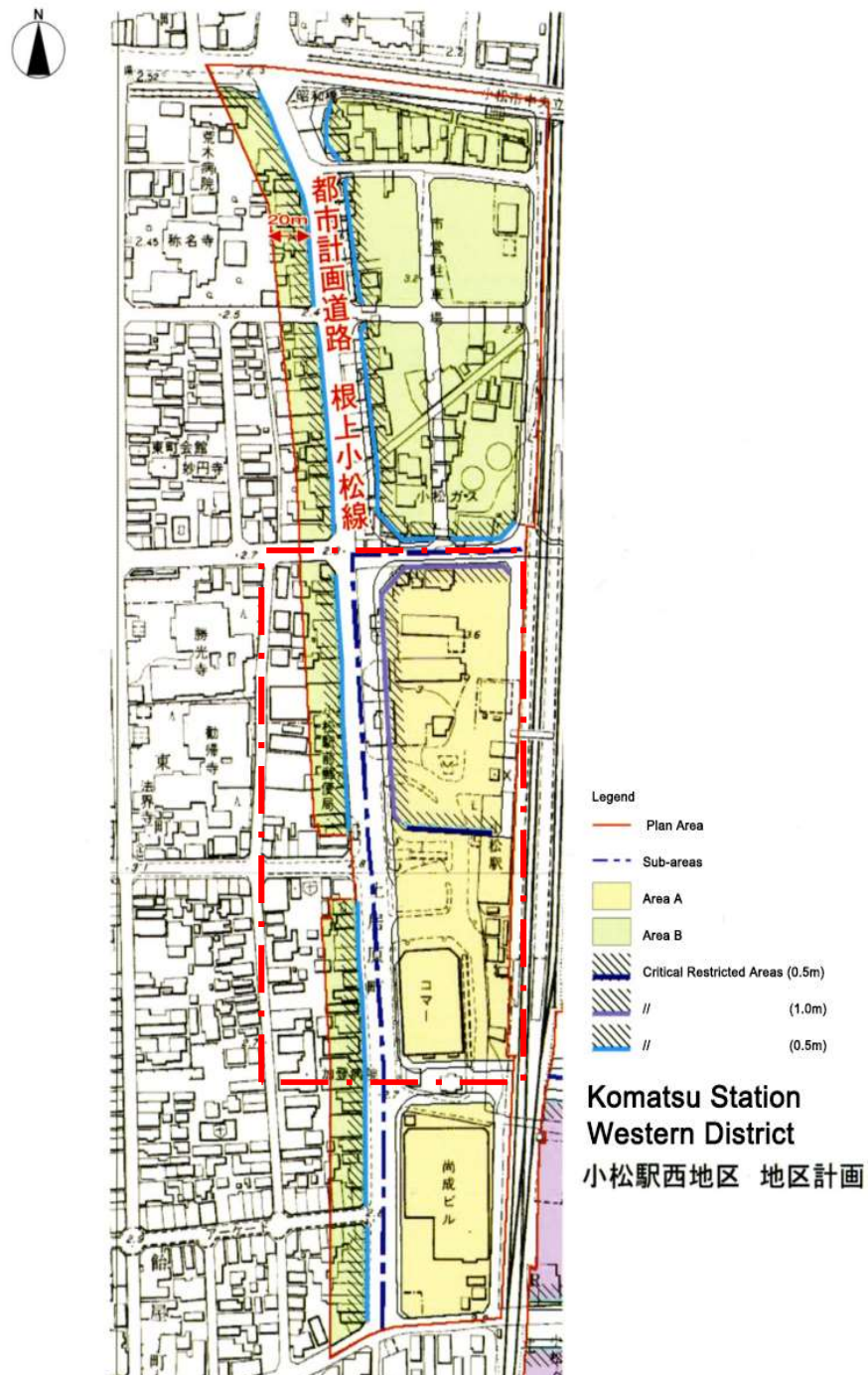
Following the Komatsu City Plan in 2040, the overall vision and planning guidelines address land use, urban street renovation, transport infrastructure renovation, landscape design, and urban disaster prevention. The United Nations have identified Komatsu as a key city for developing the SDGs, which focus on economic, social, and environmental synergy. However, Komatsu Station square as the core regeneration area of Komatsu has a radiating effect on the synergistic development of the city as a whole. The climate-sensitive design strategy for Komatsu Station square promotes the regeneration of various urban functions, revitalizing the overall urban area, and enhancing the overall environment with greater utilization and accessibility. With Intelligent Traffic Control (ITC), intelligent urban transport requires more efficient station nodes linking industrialization, ecology, communication, and low carbon. In addition, with the operation of the Hokuriku Shinkansen in Komatsu in 2025, the regeneration of the station surroundings and the reorganization of the streetscape will facilitate daily travel, communication, and activities of the residents and contribute to the construction of an environmentally friendly, circular and decarbonized town that will form an important direction in Japan's TOD urban development plans. The station square is orthogonally connected to the main parallel street, a typical typology of station squares in the Hokuriku region. The environmental improvement of the Komatsu station provides a good climate-sensitive design reference for the renewal of station squares in other central cities in the Hokuriku region.

Komatsu Station square adds a new boost to the construction and renewal of the urban complex as the central area of the urban master plan. With the opening of the Hokuriku Shinkansen at Komatsu Station imminent in 2023, the main future task is to rationalize urban environmental issues in the selection of urban street trees, interface treatment (paving, water bodies, walls, roofs), integration of history and culture, design of gray spaces with viaducts, and layout of rest areas. These issues will be addressed by climate-sensitive design strategies to improve the resilience of the central landscape to the urban climate, air quality, and a sense of urban comfort. The future station square area tries to overcome excessive hard paving in parking areas and blocks, and appropriately introduce rain gardens, permeable concrete, green roofs, and green walls. The application of these strategies in the environmental optimization performance can be effectively evaluated via ENVI-met in compliance with the Komatsu City 2040 Urban Master Plan goal to complete the renewal plan of the central urban station square.

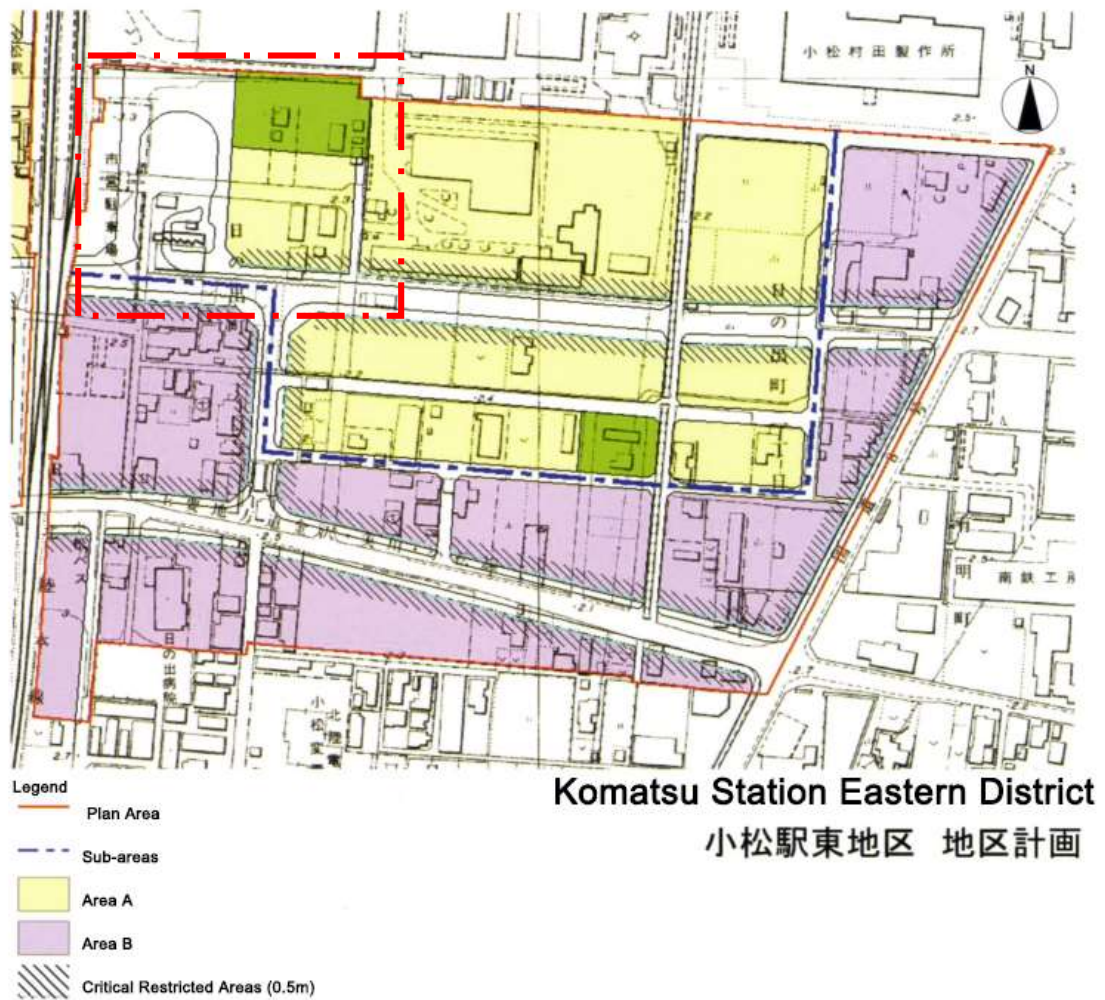
Appendix A

Komatsu Station Square Area Developing Planning

(1) Komatsu Station of western district planning (Source from: <https://www.city.komatsu.lg.jp/>)



(2) Komatsu Station of eastern district planning (Source from: <https://www.city.komatsu.lg.jp/>)



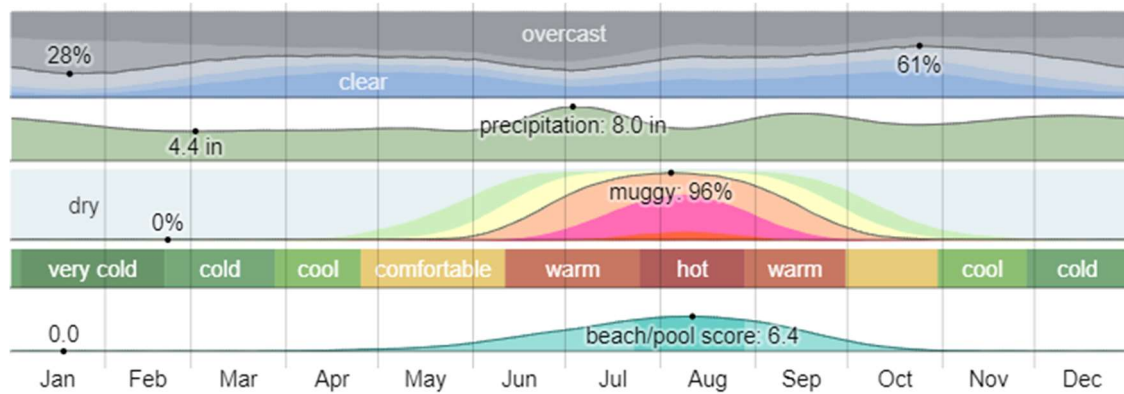
This study involved site scope



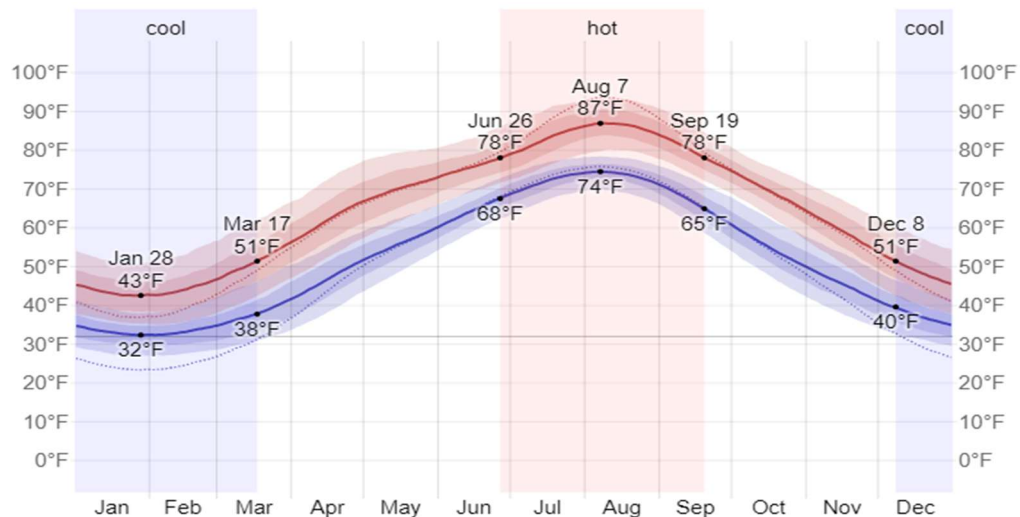
Appendix B

Climate and Average Annual Weather Characteristics of Komatsu, Japan

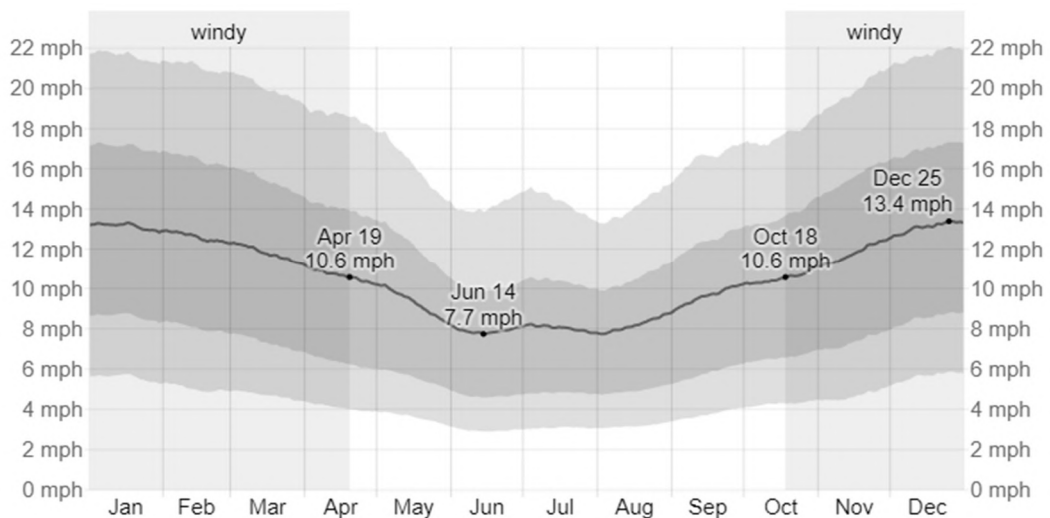
(1) Climate characteristics of Komatsu (Source from:<https://zh.weatherspark.com>)



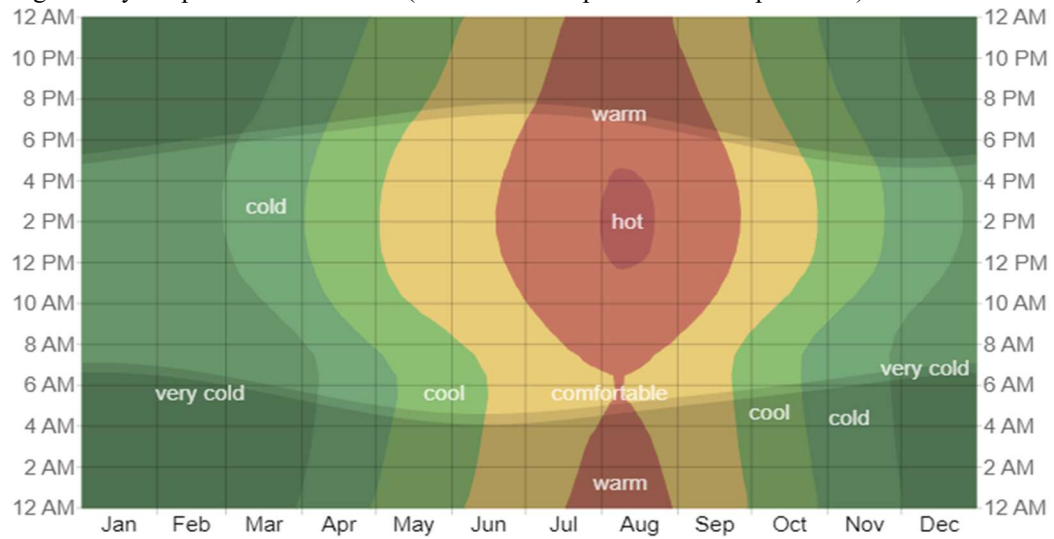
(2) Average high and low temperature in Komatsu (Source from:<https://zh.weatherspark.com>)



(3) Average wind speed in Komatsu (Source from:<https://zh.weatherspark.com>)



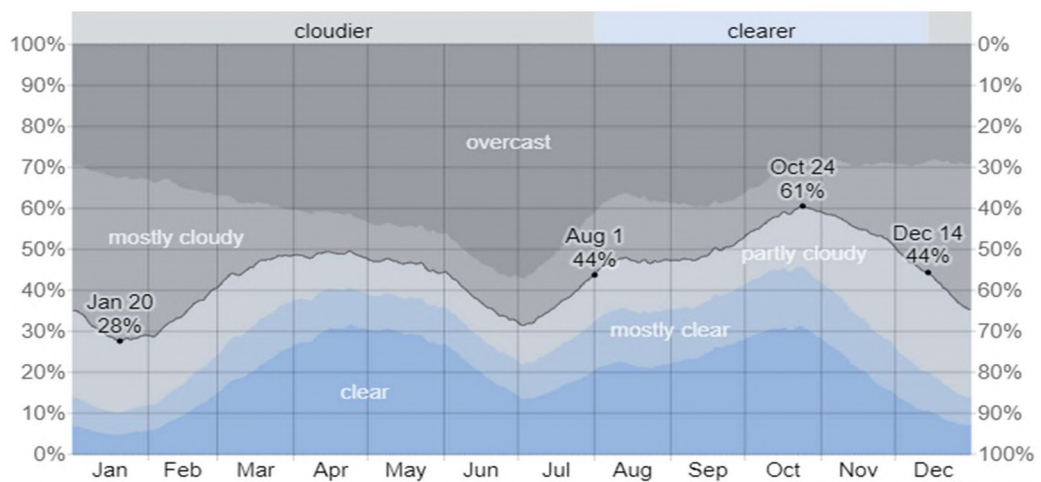
(4) Average hourly temperature in Komatsu (Source from:<https://zh.weatherspark.com>)



(5) Daily chance of precipitation in Komatsu (Source from:<https://zh.weatherspark.com>)



(6) Cloud cover categories in Komatsu (Source from:<https://zh.weatherspark.com>)



Appendix C

Site Analysis

(1) Location analysis

Hokuriku Region

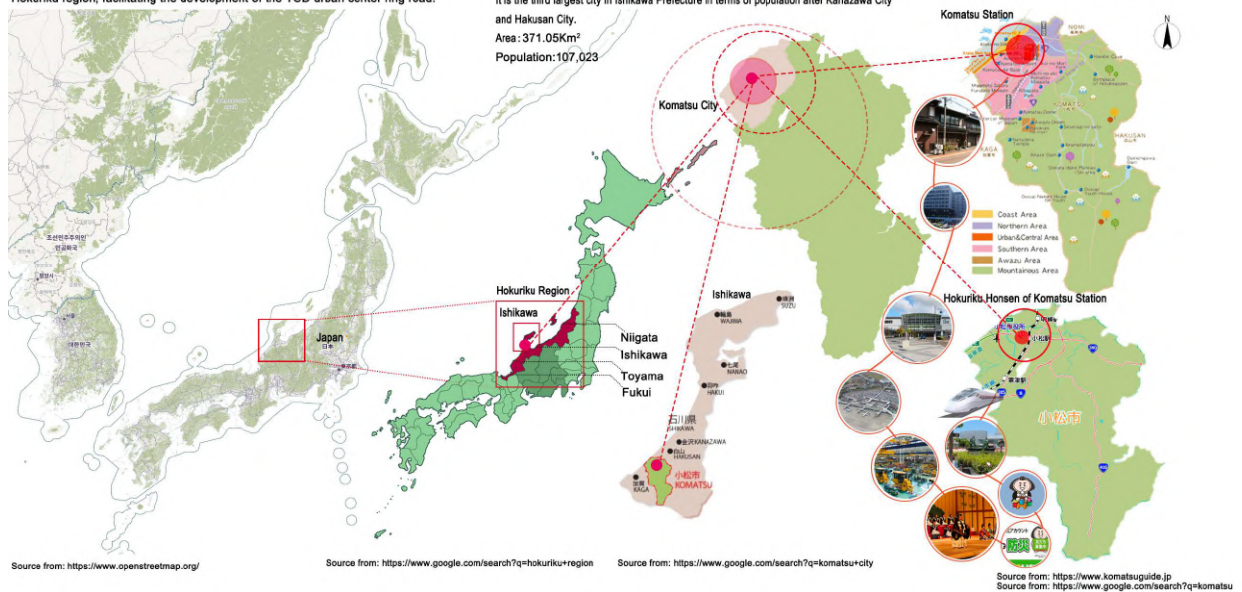
The Hokuriku region includes the four prefectures of Ishikawa, Fukui, Niigata and Toyama. The Hokuriku Shinkansen runs through the entire central city of the Hokuriku region, facilitating the development of the TOD urban center ring road.

Komatsu City

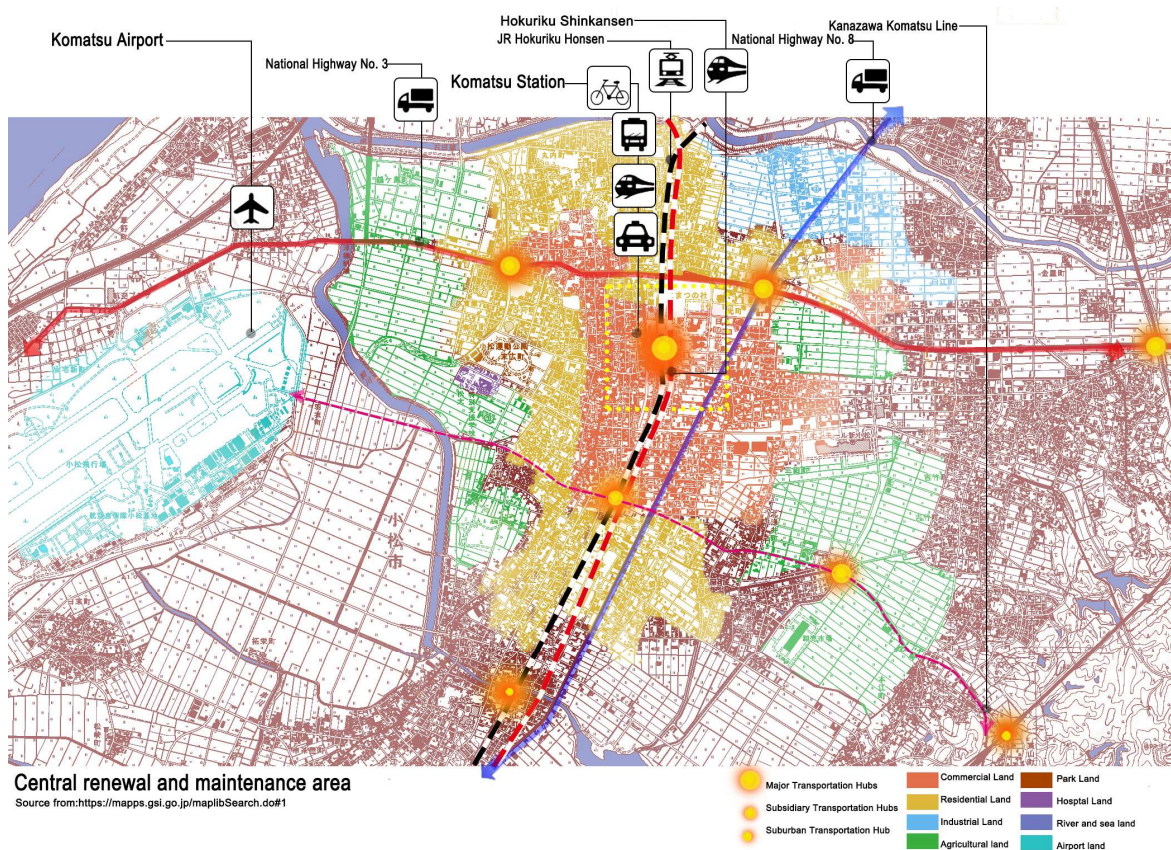
Location: It is an administrative division located in the southern part of Ishikawa Prefecture, Japan, bordered by the Sea of Japan to the west. It is the third largest city in Ishikawa Prefecture in terms of population after Kanazawa City and Hakusan City. Area: 371.05Km² Population: 107,023

Komatsu Station

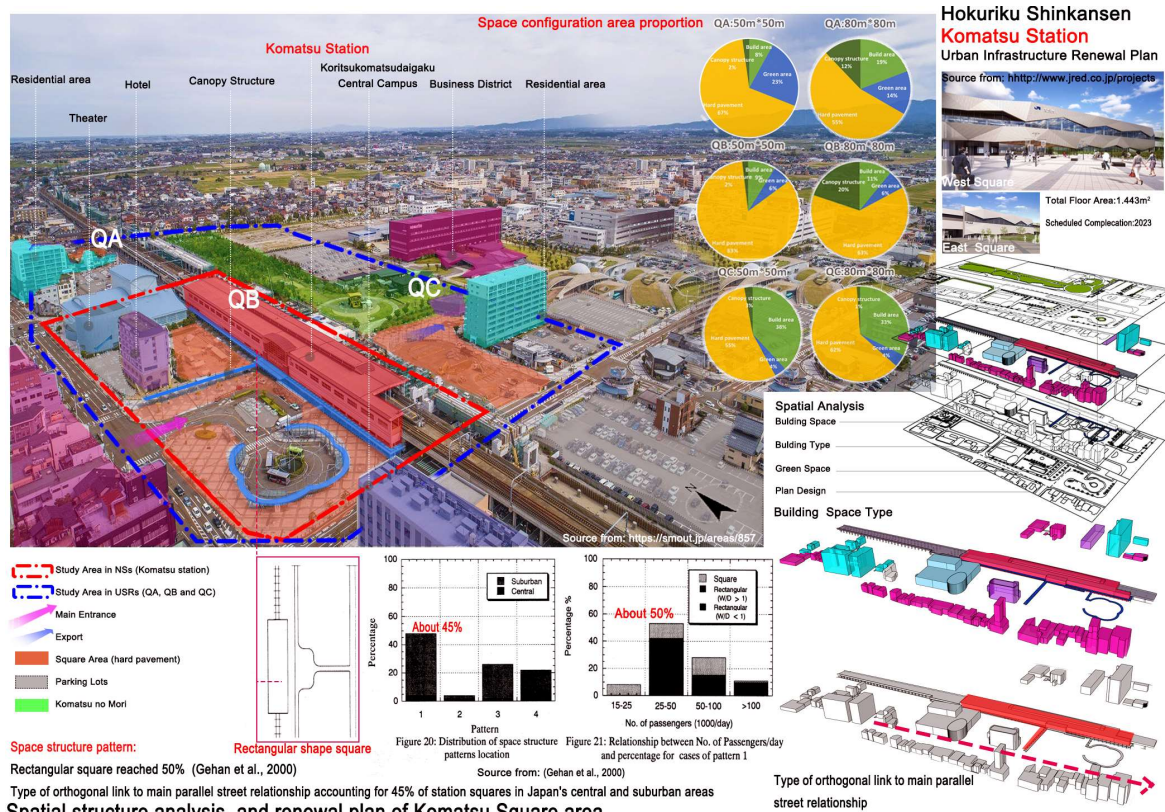
Central renewal and maintenance area from an urban master plan for the next 2040



(2) Transportation analysis



(3) Spatial structure analysis

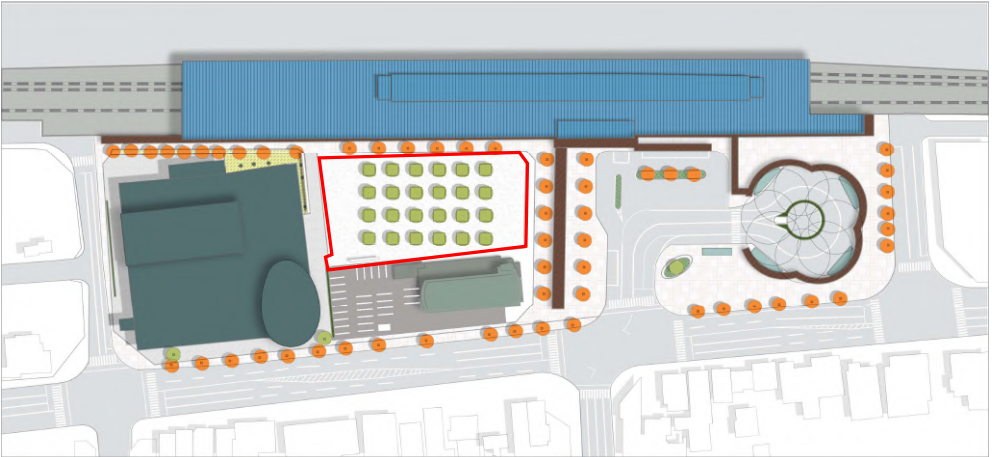
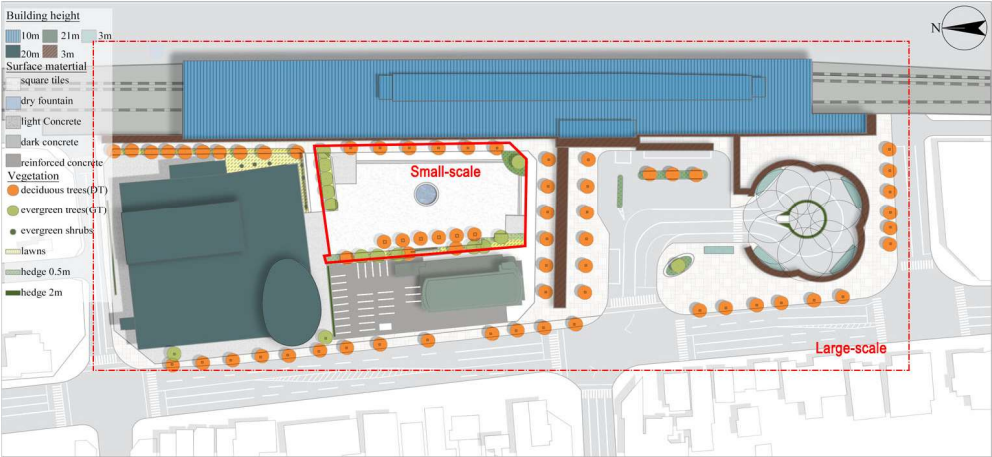
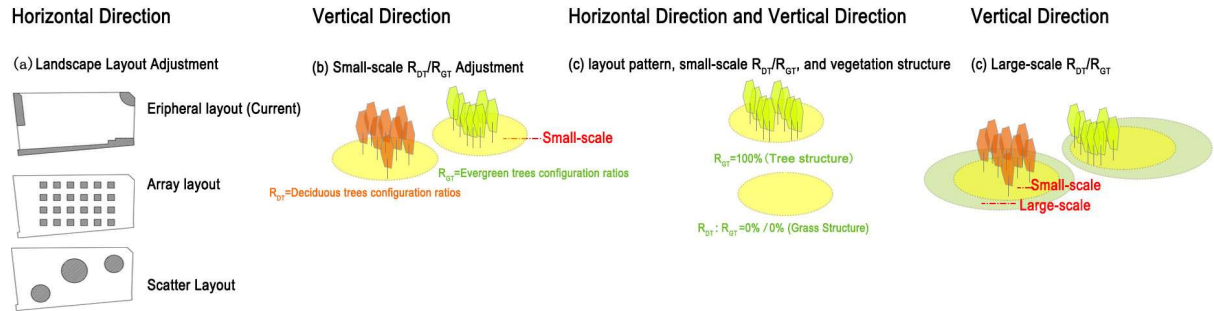


(4) Landscape environment analysis

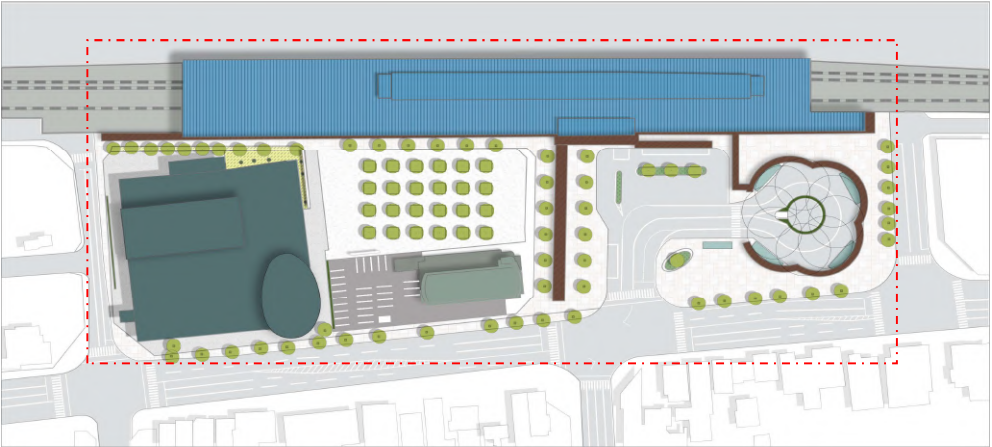


Local landscape design status and environmental issues

(5) Landscape design strategy analysis



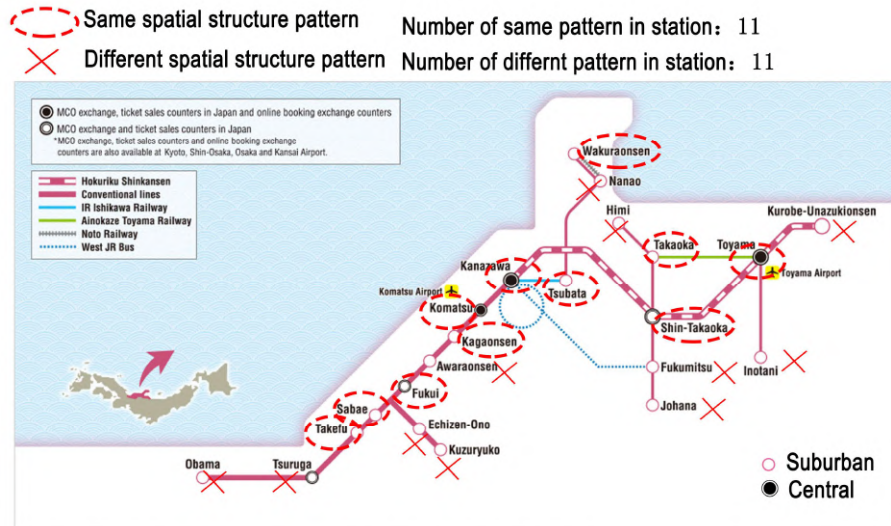
L2-2



L2-2c

Appendix D

Survey on the Same Spatial Structure Pattern of Train Stations in the Hokuriku Region



Source from: <https://www.his.com.sg/optional-2/jr-west-passes/>

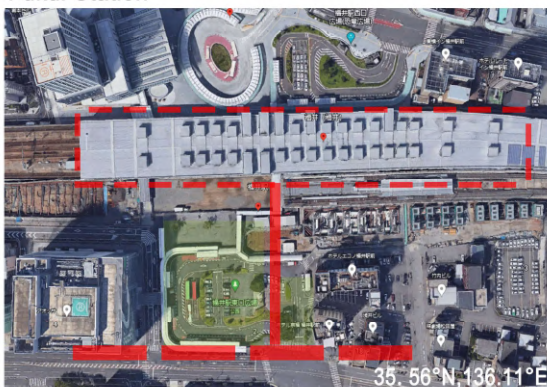
Komatsu Station



Takefu Station



Fukui Station



Tsubata Station



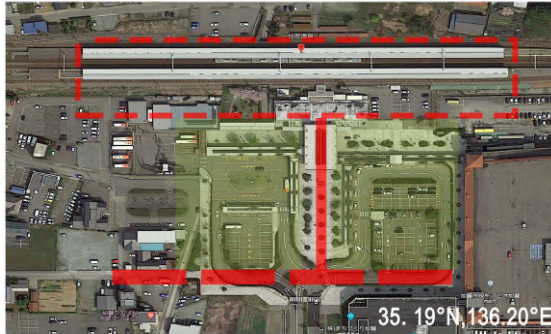
Takaoka Station



Structure Legend

- Train station
- | Orthogonally connected
- Square area
- Main parallel street

Kagaonsen Station



Wakuraonsen Station



Kanazawa Station



Shin-Takaoka Station



Toyama Station



Sabae Station



(Map from: <https://earth.google.com>)

Appendix E

Related Landscape (Green) Strategies Effect on Urban Square Microclimate and Thermal Comfort Studies

Author	Types	City	Seasons	Research objects	Research methods	Evaluation index
F. Gómez, L. Gil, J. Jabaloyes (2004)	Public space (square, road, street, garden)	Valencia, Spain	Spring, Summer, Autumn, Winter	Green area	Environment measurement, Survey visit	ID, PE, WBGT
M. Robitu, M. Musy, C. Inard, D. Groleau (2006)	Town square	Nantes, France	Summer	Landscape elements, Water pond	SOLENE software, FLUENT model	PMV
I. Knez, S. Thorsson (2006)	Public square	Göteborg, Sweden	Spring	Culture, Environmental attitude	RayMan, Field surveys, Psychological measures	PET
M. Nikolopoulou, S. Lykoudis (2007)	Neighborhood square	Matsudo, Japan Athens, Greece	Spring, Summer, Autumn, Winter	Spatial use preference, Meteorology	Environmental monitor, Interviews	-
I. Eliasson, I. Knez, U. Westerberg, S. Thorsson, F. Lindberg (2007)	Public space (square, courtyard, park, waterfront)	Gothenburg, Sweden	Spring, Summer, Autumn, Winter	Sensitive climate, Place-related attendance	Micrometeorological measurements, Structured interviews	-
S. Thorsson, T. Honjo, F. Lindberg, I. Eliasson, E. M. Lim (2007)	Public places (park, station square)	Tokyo, Japan	Spring, Summer	Outdoor activity, Thermal condition	Structured interviews, Observations, Measurements	PET
J. Spangenberg, P. Shinzato, E. Johansson, D. Duarte (2008)	Public space (park, square, street, canyon)	São Paulo, Brazil	Winter	Urban vegetation	On-site measurements, Thermal comfort surveys, ENVI-met	PET
S. Kariminia, S. Sh. Ahmad (2013)	Urban square	Esfahan, Iran	Summer, Winter	Landscape elements	Environment measurement,	PET

S. Stocco, M.A. Cantón, E.N. Correa (2015)	Urban square	Mendoza, Argentina	Summer	Vegetation structure	Questionnaire, RayMan Environment measurement, Monitor	-
A. Chatzidimitriou, S. Yannas (2015)	Urban space (squares, parks, courtyards)	Thessaloniki, Greece	Summer	Shading, Vegetation, Water, Material, Form	Environment measurement, Monitor	PMV, PET
J. Lindén, P. Fonti, J. Esper (2016)	Public space (park, courtyard, garden, street, square)	Mainz, Germany	Summer	Urban tree	Environment measurement, Monitor	-
A. Moser, M.A. Rahman, H. Pretzsch, S. Pauleit, T. Rötzer (2016)	Public square	Munich, Germany	Summer, Autumn	Urban tree	Environment measurement, Dendrometer, Dendrochronology	-
M.A. Rahman, A. Moser, A. Gold, T. Rötzer, S. Pauleit (2018)	Urban square	Munich, Germany	Summer	Urban tree, Street canyon	Environment measurement, Sap flux density calculation	-
J. Gaspari, K. Fabbri, M. Lucchi (2018)	Urban square	Cesena, Italy	Summer	Tree	ENVI-met	PET
G. Battista, R. de Lieto Vollaro, M. Zinzi (2019)	Urban square	Rome, Italy	Autumn	Urban vegetation, canopy, water stretches, material	ENVI-met	UTCI
T. Zölch, M.A. Rahman, E. Pfleiderer, G. Wagner, S. Pauleit (2019)	Public square	Munich, Germany	Summer	Green infrastructure (tree and grass)	ENVI-met V4	PET
N.A. Marçal, R.M. da Silva, C.A.G. Santos, J.S. dos Santos (2019)	Public square	Paraíba state, Brazil	Summer, Winter	Green area	Questionnaire, Climatic variable measurement	
S. Stocco, M.A. Cantón, E.N. Correa (2020)	Urban square	Mendoza, Argentina	Summer	Proportion and distribution of woodlot and sealed	ENVI-met V3.1	-

References

- Abdi, B., Hami, A., & Zarehaghi, D. (2020a). Impact of small-scale tree planting patterns on outdoor cooling and thermal comfort. *Sustainable Cities and Society*, 56, 102085. <https://doi.org/10.1016/J.SCS.2020.102085>
- Abhijith, K. V., Kumar, P., Gallagher, J., McNabola, A., Baldauf, R., Pilla, F., Broderick, B., Di Sabatino, S., & Pulvirenti, B. (2017). Air pollution abatement performances of green infrastructure in open road and built-up street canyon environments – A review. *Atmospheric Environment*, 162, 71–86. <https://doi.org/10.1016/J.ATMOSENV.2017.05.014>
- Aboelata, A., & Sodoudi, S. (2019). Evaluating urban vegetation scenarios to mitigate urban heat island and reduce buildings' energy in dense built-up areas in Cairo. *Building and Environment*, 166. <https://doi.org/10.1016/j.buildenv.2019.106407>
- Air Mobility Command. (1999). *Landscape Design Guide (AMC) | WBDG - Whole Building Design Guide*. Air Mobility Command. <https://www.wbdg.org/ffc/af-afcec/design-guides-standards/landscape-design>
- Amorim, J. H., Rodrigues, V., Tavares, R., Valente, J., & Borrego, C. (2013). CFD modelling of the aerodynamic effect of trees on urban air pollution dispersion. *Science of The Total Environment*, 461–462, 541–551. <https://doi.org/10.1016/J.SCITOTENV.2013.05.031>
- Anne VernezMoudon. (1994). Article review on getting to know the built landscape - Typomorphology.
- Aram, F., Higuera García, E., Solgi, E., & Mansournia, S. (2019). Urban green space cooling effect in cities. *Heliyon*, 5(4), e01339. <https://doi.org/10.1016/J.HELİYON.2019.E01339>
- Asanobu, K. (2004). *Digital Typhoon: AMeDAS Statistics : KOMATSU (56276)*. National Institute of Informatics (NII). <http://agora.ex.nii.ac.jp>
- Asghari, M., Teimori, G., Abbasinia, M., Shakeri, F., Tajik, R., Ghannadzadeh, M. J., & Ghalhari, G. F. (2019). Thermal discomfort analysis using UTCI and MEMI (PET and PMV) in outdoor environments: case study of two climates in Iran (Arak & Bandar Abbas). *Weather*, 74(S1), S57–S64. <https://doi.org/10.1002/WEA.3612>
- Battista, G., de Lieto Vollaro, R., & Zinzi, M. (2019). Assessment of urban overheating mitigation strategies in a square in Rome, Italy. *Solar Energy*, 180, 608–621. <https://doi.org/10.1016/j.solener.2019.01.074>
- Bowles Wyer. (2012). When is a garden designer a landscape designer? Indeed, when is a garden a landscape – or vice-versa? Blog. <http://www.bowleswyer.co.uk/blog/?p=541>
- Brix, J. (2017). Exploring knowledge creation processes as a source of organizational learning: A longitudinal case study of a public innovation project. *Scandinavian Journal of Management*, 33(2), 113–127. <https://doi.org/10.1016/J.SCAMAN.2017.05.001>
- Bruse, M. (2021). *ENVI-met*. ENVI-Met Website. <https://www.envi-met.com/zh-hans/>
- Buccolieri, R., Santiago, J. L., Rivas, E., & Sanchez, B. (2018). Review on urban tree modelling in CFD simulations: Aerodynamic, deposition and thermal effects. *Urban Forestry & Urban Greening*, 31, 212–220. <https://doi.org/10.1016/J.UFUG.2018.03.003>
- Carmona, M. (2021). Public places urban spaces: The dimensions of urban design. *Routledge*. <https://doi.org/10.4324/9781315158457/PUBLIC-PLACES-URBAN-SPACES-MATTHEW-CARMONA>
- Chatzidimitriou, A., & Yannas, S. (2015). Microclimate development in open urban spaces: The influence of form and materials. *Energy and Buildings*, 108, 156–174. <https://doi.org/10.1016/j.enbuild.2015.08.048>

- Chen, Liang, & Ng, E. (2012a). Outdoor thermal comfort and outdoor activities: A review of research in the past decade. *Cities*, 29(2), 118–125. <https://doi.org/10.1016/j.cities.2011.08.006>
- Chen, Lixin, Liu, C., Zou, R., Yang, M., & Zhang, Z. (2016). Experimental examination of effectiveness of vegetation as bio-filter of particulate matters in the urban environment. *Environmental Pollution*, 208, 198–208. <https://doi.org/10.1016/J.ENVPOL.2015.09.006>
- Cohen, A. J., Brauer, M., Burnett, R., Anderson, H. R., Frostad, J., Estep, K., Balakrishnan, K., Brunekreef, B., Dandona, L., Dandona, R., Feigin, V., Freedman, G., Hubbell, B., Jobling, A., Kan, H., Knibbs, L., Liu, Y., Martin, R., Morawska, L., ... Forouzanfar, M. H. (2017). Estimates and 25-year trends of the global burden of disease attributable to ambient air pollution: an analysis of data from the Global Burden of Diseases Study 2015. *The Lancet*, 389(10082), 1907–1918. [https://doi.org/10.1016/S0140-6736\(17\)30505-6](https://doi.org/10.1016/S0140-6736(17)30505-6)
- Cui, L., Rupprecht, C. D. D., & Shibata, S. (2021). Climate-responsive green-space design inspired by traditional gardens: Microclimate and human thermal comfort of Japanese gardens. *Sustainability*, 13(5), 2736. <https://doi.org/10.3390/SU13052736>
- d'Ambrosio Alfano, F. R., Palella, B. I., & Riccio, G. (2011). The role of measurement accuracy on the thermal environment assessment by means of PMV index. *Building and Environment*, 46(7), 1361–1369. <https://doi.org/10.1016/J.BUILDENV.2011.01.001>
- Dimoudi, A., & Nikolopoulou, M. (2003). Vegetation in the urban environment: microclimatic analysis and benefits. *Energy and Buildings*, 35(1), 69–76. [https://doi.org/10.1016/S0378-7788\(02\)00081-6](https://doi.org/10.1016/S0378-7788(02)00081-6)
- El-Bardisy, W. M., Fahmy, M., & El-Gohary, G. F. (2016). Climatic sensitive landscape design: Towards a better microclimate through plantation in public schools, Cairo, Egypt. *Procedia - Social and Behavioral Sciences*, 216, 206–216. <https://doi.org/10.1016/j.sbspro.2015.12.029>
- Eliasson, I. È. (2000). *The use of climate knowledge in urban planning*. [https://doi.org/10.1016/S0169-2046\(00\)00034-7](https://doi.org/10.1016/S0169-2046(00)00034-7)
- Eliasson, I., Knez, I., Westerberg, U., Thorsson, S., & Lindberg, F. (2007a). Climate and behaviour in a Nordic city. *Landscape and Urban Planning*, 82(1–2), 72–84. <https://doi.org/10.1016/j.landurbplan.2007.01.020>
- Erell, E., Pearlmutter, D., & Williamson, T. (2011). Urban microclimate: designing the spaces between buildings.
- Fabbri, K., Ugolini, A., Iacovella, A., & Bianchi, A. P. (2020). The effect of vegetation in outdoor thermal comfort in archaeological area in urban context. *Building and Environment*, 175, 106816. <https://doi.org/10.1016/J.BUILDENV.2020.106816>
- Fanger, P. O. (1970). Thermal comfort. Analysis and applications in environmental engineering. *Cabdirect.Org*. <https://www.cabdirect.org/cabdirect/abstract/19722700268>
- Freer-Smith, P. H., Beckett, K. P., & Taylor, G. (2005). Deposition velocities to Sorbus aria, Acer campestre, Populus deltoides × trichocarpa 'Beaupré', Pinus nigra and × Cupressocyparis leylandii for coarse, fine and ultra-fine particles in the urban environment. *Environmental Pollution*, 133(1), 157–167. <https://doi.org/10.1016/J.ENVPOL.2004.03.031>
- G. Mills. (2008). Luke howard and the climate of london. *Regionalclimateperspectives.Com*, 63(6). <http://www.regionalclimateperspectives.com/uploads/4/4/2/5/44250401/post6lukehoward.pdf>
- Galal, O. M., Mahmoud, H., & Sailor, D. (2020). Impact of evolving building morphology on microclimate in a hot arid climate. *Sustainable Cities and Society*, 54, 102011. <https://doi.org/10.1016/J.SCS.2019.102011>
- Gallagher, J., Baldauf, R., Fuller, C. H., Kumar, P., Gill, L. W., & McNabola, A. (2015). Passive methods for improving air quality in the built environment: A review of porous and solid barriers. *Atmospheric Environment*, 120, 61–70. <https://doi.org/10.1016/J.ATMOSENV.2015.08.075>

- Gaspari, J., Fabbri, K., & Lucchi, M. (2018). The use of outdoor microclimate analysis to support decision making process: Case study of Bufalini square in Cesena. *Sustainable Cities and Society*, 42, 206–215. <https://doi.org/10.1016/J.SCS.2018.07.015>
- Gatto, E., Buccolieri, R., Aarrevaara, E., Ippolito, F., Emmanuel, R., Perronace, L., & Santiago, J. L. (2020). Impact of urban vegetation on outdoor thermal comfort: comparison between a Mediterranean City (Lecce, Italy) and a Northern European City (Lahti, Finland). *Forests*, 11(2), 228. <https://doi.org/10.3390/F11020228>
- Gehan, E., KUBOTA, Y., & FUKAHORI, K. (2000). Visual geometrical analysis of outdoor space structure around railway station buildings. *Infrastructure Planning Review*, 17, 481–490. <https://doi.org/10.2208/JOURNALIP.17.481>
- Ghaffarianhoseini, A., Berardi, U., & Ghaffarianhoseini, A. (2015a). Thermal performance characteristics of unshaded courtyards in hot and humid climates. *Building and Environment*, 87, 154–168. <https://doi.org/10.1016/j.buildenv.2015.02.001>
- Gilani, S. I. U. H., Khan, M. H., & Pao, W. (2015). Thermal comfort analysis of PMV model prediction in air conditioned and naturally ventilated buildings. *Energy Procedia*, 75, 1373–1379. <https://doi.org/10.1016/J.EGYPRO.2015.07.218>
- Gómez, Francisco, Gil, L., & Jabaloyes, J. (2004). Experimental investigation on the thermal comfort in the city: relationship with the green areas, interaction with the urban microclimate. *Building and Environment*, 39(9), 1077–1086. <https://doi.org/10.1016/J.BUILDENV.2004.02.001>
- Gorka, D. (2021). *Number of passengers carried via JR transport in Japan FY 2010-2019*. Statista 2022. <https://www.statista.com/statistics/627142/japan-number-jr-passengers/>
- Gromke, C., Blocken, B., Janssen, W., Merema, B., van Hooff, T., & Timmermans, H. (2015). CFD analysis of transpirational cooling by vegetation: Case study for specific meteorological conditions during a heat wave in Arnhem, Netherlands. *Building and Environment*, 83, 11–26. <https://doi.org/10.1016/J.BUILDENV.2014.04.022>
- Hong, B., & Lin, B. (2015). Numerical studies of the outdoor wind environment and thermal comfort at pedestrian level in housing blocks with different building layout patterns and trees arrangement. *Renewable Energy*, 73, 18–27. <https://doi.org/10.1016/J.RENENE.2014.05.060>
- Hong, B., Lin, B., & Qin, H. (2017). Numerical investigation on the coupled effects of building-tree arrangements on fine particulate matter (PM_{2.5}) dispersion in housing blocks. *Sustainable Cities and Society*, 34, 358–370. <https://doi.org/10.1016/J.SCS.2017.07.005>
- Honjo, T., & Takakura, T. (1990). Simulation of thermal effects of urban green areas on their surrounding areas. *Energy and Buildings*, 15(3–4), 443–446. [https://doi.org/10.1016/0378-7788\(90\)90019-F](https://doi.org/10.1016/0378-7788(90)90019-F)
- Höppe, P. (1999). The physiological equivalent temperature - A universal index for the biometeorological assessment of the thermal environment. *International Journal of Biometeorology*, 43(2), 71–75. <https://doi.org/10.1007/s004840050118>
- Höppe, P. (2002). Different aspects of assessing indoor and outdoor thermal comfort. *Energy and Buildings*, 34(6), 661–665. [https://doi.org/10.1016/S0378-7788\(02\)00017-8](https://doi.org/10.1016/S0378-7788(02)00017-8)
- Houghten, F. C. (1923). Determining lines of equal comfort. *ASHVE Transactions*, 29, 163–176. <https://ci.nii.ac.jp/naid/10017481853/>
- Howard, L. (1833). The climate of London: deduced from meteorological observations made in the metropolis and at various places around it.
- Huang, H., & Peng, M. (2020a). The outdoor thermal comfort of urban square: A field study in a cold season in Chongqing. *IOP Conference Series: Earth and Environmental Science*, 467(1), 012215. <https://doi.org/10.1088/1755-1315/467/1/012215>
- Huttner, S. (2012). *Further development and application of the 3D microclimate simulation ENVI-met*. <https://doi.org/http://doi.org/10.25358/openscience-2022>

- Jamei, E., Rajagopalan, P., Seyedmahmoudian, M., & Jamei, Y. (2016). Review on the impact of urban geometry and pedestrian level greening on outdoor thermal comfort. *Renewable and Sustainable Energy Reviews*, 54, 1002–1017. <https://doi.org/10.1016/J.RSER.2015.10.104>
- Japan Automobile Manufacturers Association (JAMA). (2011). <http://www.jama.org/>
- Japan Meteorological Agency. (2007). Japan Meteorological Agency (JMA). <https://www.data.jma.go.jp/risk/obsdl/index.php>
- Karakounos, I., Dimoudi, A., & Zoras, S. (2018). The influence of bioclimatic urban redevelopment on outdoor thermal comfort. *Energy and Buildings*, 158, 1266–1274. <https://doi.org/10.1016/J.ENBUILD.2017.11.035>
- Kariminia, S., & Ahmad, S. S. (2013). Dependence of visitors' thermal sensations on built environments at an urban square. *Procedia - Social and Behavioral Sciences*, 85, 523–534. <https://doi.org/10.1016/j.sbspro.2013.08.381>
- Kariminia, S., Ahmad, S. S., & Saberi, A. (2015). Microclimatic conditions of an urban square: Role of built environment and geometry. *Procedia - Social and Behavioral Sciences*, 170, 718–727. <https://doi.org/10.1016/J.SBSPRO.2015.01.074>
- Kido, E. M. (2005). Aesthetic aspects of railway stations in Japan and Europe, as a part of “context sensitive design for railways.” *Journal of the Eastern Asia Society for Transportation Studies*, 6, 4381–4396. <https://doi.org/10.11175/EASTS.6.4381>
- Kidokoro, T. (2020). Transit oriented development (TOD) policies and station area development in Asian Cities. *IOP Conference Series: Earth and Environmental Science*, 532(1), 012001. <https://doi.org/10.1088/1755-1315/532/1/012001>
- Kleerekoper, L., Van Esch, M., & Salcedo, T. B. (2012). How to make a city climate-proof, addressing the urban heat island effect. *Resources, Conservation and Recycling*, 64, 30–38. <https://doi.org/10.1016/j.resconrec.2011.06.004>
- Klemm, W., Lenzholzer, S., & Van Den Brink, A. (2017). Developing green infrastructure design guidelines for urban climate adaptation. *Journal of Landscape Architecture*, 12(3), 60–71. <https://doi.org/10.1080/18626033.2017.1425320>
- Knaus, M., & Haase, D. (2020). Green roof effects on daytime heat in a prefabricated residential neighbourhood in Berlin, Germany. *Urban Forestry & Urban Greening*, 53, 126738. <https://doi.org/10.1016/J.UFUG.2020.126738>
- Koc, C., Osmond, P., Energy, & Peters, A. (2018). Evaluating the cooling effects of green infrastructure: A systematic review of methods, indicators and data sources. *Solar Energy*, 166, 486–508. <https://doi.org/10.1016/j.solener.2018.03.008>
- Kong, L., Lau, K. K. L., Yuan, C., Chen, Y., Xu, Y., Ren, C., & Ng, E. (2017). Regulation of outdoor thermal comfort by trees in Hong Kong. *Sustainable Cities and Society*, 31, 12–25. <https://doi.org/10.1016/J.SCS.2017.01.018>
- Koppe, C., Kovats, S., Jendritzky, G., Menne, B., Baumüller, J., Bitan, A., Díaz Jiménez, J., Ebi, K. L., Havenith, G., Santiago, L., Michelozzi, P., Nicol, F., Matzarakis, A., McGregor, G., Nogueira, P. J., Sheridan, S., & Wolf, T. (2004). *Health and Global Environmental Change Heat-waves: risks and responses*. <http://www.euro.who.int/globalchange>
- Kottek, M., Grieser, J., Beck, C., Rudolf, B., & Rubel, F. (2006). World map of the Köppen-Geiger climate classification updated. *Meteorologische Zeitschrift*, 15(3), 259–263. <https://doi.org/10.1127/0941-2948/2006/0130>
- Krier, R., & Rowe, C. (1979). *Urban space*. https://www.academia.edu/download/59711490/Krier__Rob_-_Urban_Space20190613-53582-75xfm4.pdf

- Krüger, E. L., Minella, F. O., & Rasia, F. (2011). Impact of urban geometry on outdoor thermal comfort and air quality from field measurements in Curitiba, Brazil. *Building and Environment*, 46(3), 621–634. <https://doi.org/10.1016/J.BUILDENV.2010.09.006>
- L. J. Battan. (1973). Radar observation of the atmosphere. *Quarterly Journal of the Royal Meteorological Society*, 99(422), 793–793. <https://doi.org/10.1002/QJ.49709942229>
- Lai, D., Liu, W., Gan, T., Liu, K., & Chen, Q. (2019). A review of mitigating strategies to improve the thermal environment and thermal comfort in urban outdoor spaces. *Science of The Total Environment*, 661, 337–353. <https://doi.org/10.1016/J.SCITOTENV.2019.01.062>
- Lalic, B., & Mihailovic, D. (2004). An empirical relation describing leaf-area density inside the forest for environmental modeling. *Journal of Applied Meteorology*, 43(4), 641–645. [https://doi.org/10.1175/1520-0450\(2004\)043%3C0641:AERDLD%3E2.0.CO;2](https://doi.org/10.1175/1520-0450(2004)043%3C0641:AERDLD%3E2.0.CO;2)
- Lenzholzer, S., Klemm, W., & Vasilikou, C. (2018). Qualitative methods to explore thermo-spatial perception in outdoor urban spaces. *Urban Climate*, 23, 231–249. <https://doi.org/10.1016/J.UCLIM.2016.10.003>
- Li, Jianwei, & Liu, N. (2020). The perception, optimization strategies and prospects of outdoor thermal comfort in China: A review. *Building and Environment*, 170, 106614. <https://doi.org/10.1016/J.BUILDENV.2019.106614>
- Li, Jiaying, You, W., & Ding, W. (2022). Exploring urban space quantitative indicators associated with outdoor ventilation potential. *Sustainable Cities and Society*, 79, 103696. <https://doi.org/10.1016/J.SCS.2022.103696>
- Li, Y., & Song, Y. (2019). Optimization of vegetation arrangement to improve microclimate and thermal comfort in an urban park. *International Review for Spatial Planning and Sustainable Development*, 7(1). https://doi.org/10.14246/irspsd.7.1_18
- Lin, B., Li, X., Zhu, Y., & Qin, Y. (2008). Numerical simulation studies of the different vegetation patterns' effects on outdoor pedestrian thermal comfort. *Journal of Wind Engineering and Industrial Aerodynamics*, 96(10–11), 1707–1718. <https://doi.org/10.1016/j.jweia.2008.02.006>
- Lin, T. P., & Matzarakis, A. (2008). Tourism climate and thermal comfort in Sun Moon Lake, Taiwan. *International Journal of Biometeorology*, 52(4), 281–290. <https://doi.org/10.1007/S00484-007-0122-7/FIGURES/11>
- Lindén, J., Fonti, P., & Esper, J. (2016). Temporal variations in microclimate cooling induced by urban trees in Mainz, Germany. *Urban Forestry & Urban Greening*, 20, 198–209. <https://doi.org/10.1016/J.UFUG.2016.09.001>
- Liu, W., Zhang, Y., & Deng, Q. (2016). The effects of urban microclimate on outdoor thermal sensation and neutral temperature in hot-summer and cold-winter climate. *Energy and Buildings*, 128, 190–197. <https://doi.org/10.1016/j.enbuild.2016.06.086>
- Liu, Z., Cheng, W., Jim, C. Y., Morakinyo, T. E., Shi, Y., & Ng, E. (2021). Heat mitigation benefits of urban green and blue infrastructures: A systematic review of modeling techniques, validation and scenario simulation in ENVI-met V4. *Building and Environment*, 200, 107939. <https://doi.org/10.1016/J.BUILDENV.2021.107939>
- Liu, Z., Zheng, S., & Zhao, L. (2018). Evaluation of the ENVI-Met vegetation model of four common tree species in a subtropical hot-humid area. *Atmosphere*, 9(5), 198. <https://doi.org/10.3390/ATMOS9050198>
- López-Cabeza, V. P., Galán-Marín, C., Rivera-Gómez, C., & Roa-Fernández, J. (2018). Courtyard microclimate ENVI-met outputs deviation from the experimental data. *Building and Environment*, 144, 129–141. <https://doi.org/10.1016/j.buildenv.2018.08.013>
- Magic, V. (2015). *WeatherSpark website*. Inc. <https://weatherspark.com/>
- Marçal, N. A., da Silva, R. M., Santos, C. A. G., & Santos, J. S. dos. (2019). Analysis of the environmental thermal comfort conditions in public squares in the semiarid region of northeastern

- Brazil. *Building and Environment*, 152, 145–159. <https://doi.org/10.1016/J.BUILDENV.2019.02.016>
- Marcus, C., & Francis, C. (1997). *People places: design guidelines for urban open space*. John Wiley & Sons.
- Matzarakis, A., & Amelung, B. (2008). Physiological equivalent temperature as indicator for impacts of climate change on thermal comfort of humans. *Advances in Global Change Research*, 30, 161–172. https://doi.org/10.1007/978-1-4020-6877-5_10
- Matzarakis, A., Mayer, H., & Iziomon, M. G. (1999). Applications of a universal thermal index: physiological equivalent temperature. *International Journal of Biometeorology*, 43(2), 76–84. <https://doi.org/10.1007/S004840050119>
- Mills, G. (2014). Urban climatology: History, status and prospects. *Urban Climate*, 10(P3), 479–489. <https://doi.org/10.1016/J.UCLIM.2014.06.004>
- Mirzaei, P., Environment, F. H.-B. and, & 2010, U. (2010). Approaches to study urban heat island–abilities and limitations. *Building and Environment*, 45(10), 2192–2201. <https://doi.org/10.1016/j.buildenv.2010.04.001>
- Moonen, P., Defraeye, T., Dorer, V., Blocken, B., & Carmeliet, J. (2012). Urban physics: Effect of the micro-climate on comfort, health and energy demand. *Frontiers of Architectural Research*, 1(3), 197–228. <https://doi.org/10.1016/J.FOAR.2012.05.002>
- Morakinyo, T. E., & Lam, Y. F. (2016a). Simulation study on the impact of tree-configuration, planting pattern and wind condition on street-canyon’s micro-climate and thermal comfort. *Building and Environment*, 103, 262–275. <https://doi.org/10.1016/j.buildenv.2016.04.025>
- Moser, A., Rahman, M. A., Pretzsch, H., Pauleit, S., & Rötzer, T. (2016). Inter- and intraannual growth patterns of urban small-leaved lime (*Tilia cordata* mill.) at two public squares with contrasting microclimatic conditions. *International Journal of Biometeorology*, 61(6), 1095–1107. <https://doi.org/10.1007/S00484-016-1290-0>
- Moughtin, C. (2007). Urban design: street and square. *Routledge*, 1–300. <https://doi.org/10.4324/9780080520278/URBAN-DESIGN-STREET-SQUARE-CLIFF-MOUGHTIN>
- Muniz-Gäal, L. P., Pezzuto, C. C., Carvalho, M. F. H. de, & Mota, L. T. M. (2020). Urban geometry and the microclimate of street canyons in tropical climate. *Building and Environment*, 169, 106547. <https://doi.org/10.1016/J.BUILDENV.2019.106547>
- Nakamori, Y. (2011). Knowledge science: Modeling the knowledge creation process.
- Ng, E., Chen, L., Wang, Y., & Yuan, C. (2012). A study on the cooling effects of greening in a high-density city: An experience from Hong Kong. *Building and Environment*, 47(1), 256–271. <https://doi.org/10.1016/J.BUILDENV.2011.07.014>
- Nikolopoulou, M., & Lykoudis, S. (2007). Use of outdoor spaces and microclimate in a Mediterranean urban area. *Building and Environment*, 42(10), 3691–3707. <https://doi.org/10.1016/j.buildenv.2006.09.008>
- Oke, T. R. (1981). Canyon geometry and the nocturnal urban heat island: Comparison of scale model and field observations. *Journal of Climatology*, 1(3), 237–254. <https://doi.org/10.1002/JOC.3370010304>
- Oliveira, S., Andrade, H., & Vaz, T. (2011). The cooling effect of green spaces as a contribution to the mitigation of urban heat: A case study in Lisbon. *Building and Environment*, 46(11), 2186–2194. <https://doi.org/10.1016/j.buildenv.2011.04.034>
- Oreskes, N. (2003). The role of quantitative models in science Naomi Oreskes. In *Canham, CD, Cole, JJ, and Lauenroth, WK*.
- Ould-Dada, Z. (2002). Dry deposition profile of small particles within a model spruce canopy. *Science of The Total Environment*, 286(1–3), 83–96. [https://doi.org/10.1016/S0048-9697\(01\)00965-2](https://doi.org/10.1016/S0048-9697(01)00965-2)

- Ouyang, W., Morakinyo, T. E., Ren, C., & Ng, E. (2020). The cooling efficiency of variable greenery coverage ratios in different urban densities: A study in a subtropical climate. *Building and Environment*, 174, 106772. <https://doi.org/10.1016/J.BUILDENV.2020.106772>
- Ozdemir, H. (2019). Mitigation impact of roadside trees on fine particle pollution. *Science of The Total Environment*, 659, 1176–1185. <https://doi.org/10.1016/J.SCITOTENV.2018.12.262>
- Page, J. K. (1976). Application of building climatology to the problems of housing and building for human settlements (WMO No. 441). Technical Note No. 150, 64.
- Palladio, A. (2002). *The four books on architecture*. Mit Press.
- Perini, K., Chokhachian, A., & Auer, T. (2018). Green streets to enhance outdoor comfort. *Nature Based Strategies for Urban and Building Sustainability*, 119–129. <https://doi.org/10.1016/B978-0-12-812150-4.00011-2>
- PM_{2.5} Annual Report. (n.d.). *Air quality status in Ishikawa Prefecture*. Ishikawa Prefecture. Retrieved April 7, 2022, from <http://ishikawa-taiki.jp>
- Potchter, O., Cohen, P., Lin, T. P., & Matzarakis, A. (2018). Outdoor human thermal perception in various climates: A comprehensive review of approaches, methods and quantification. *Science of the Total Environment*, 631, 390–406. <https://doi.org/10.1016/j.scitotenv.2018.02.276>
- Qin, H., Hong, B., Jiang, R., Yan, S., & Zhou, Y. (2019). The effect of vegetation enhancement on particulate pollution Reduction: CFD simulations in an urban park. *Forests*, 10(5), 373. <https://doi.org/10.3390/F10050373>
- Rahman, M. A., Moser, A., Gold, A., Rötzer, T., & Pauleit, S. (2018). Vertical air temperature gradients under the shade of two contrasting urban tree species during different types of summer days. *Science of the Total Environment*, 633, 100–111. <https://doi.org/10.1016/j.scitotenv.2018.03.168>
- Rahman, M. A., Moser, A., Rötzer, T., & Pauleit, S. (2017). Microclimatic differences and their influence on transpirational cooling of *Tilia cordata* in two contrasting street canyons in Munich, Germany. *Agricultural and Forest Meteorology*, 232, 443–456. <https://doi.org/10.1016/J.AGRFORMET.2016.10.006>
- Robitu, M., Musy, M., Inard, C., & Groleau, D. (2006a). Modeling the influence of vegetation and water pond on urban microclimate. *Solar Energy*, 80(4), 435–447. <https://doi.org/10.1016/j.solener.2005.06.015>
- Rui, L., Buccolieri, R., Gao, Z., Ding, W., & Shen, J. (2018). The impact of green space layouts on microclimate and air quality in residential districts of Nanjing, China. *Forests*, 9(4). <https://doi.org/10.3390/f9040224>
- Rui, L., Buccolieri, R., Gao, Z., Gatto, E., & Ding, W. (2019). Study of the effect of green quantity and structure on thermal comfort and air quality in an urban-like residential district by ENVI-met modelling. *Building Simulation*, 12(2), 183–194. <https://doi.org/10.1007/s12273-018-0498-9>
- S. Huttner, M.B. (2009). Numerical modeling of the urban climate—a preview on ENVI-met 4.0. *Citeseer*. <https://citeseerx.ist.psu.edu/viewdoc/download?doi=10.1.1.556.2976&rep=rep1&type=pdf>
- Saito, K., Said, I., & Shinozaki, M. (2017). Evidence-based neighborhood greening and concomitant improvement of urban heat environment in the context of a world heritage site-Malacca, Malaysia. *Computers, Environment and Urban Systems*, 64, 356–372. <https://www.sciencedirect.com/science/article/pii/S0198971516303386>
- Salata, F., Golasi, I., de Lieto Vollaro, R., & de Lieto Vollaro, A. (2016). Urban microclimate and outdoor thermal comfort. A proper procedure to fit ENVI-met simulation outputs to experimental data. *Sustainable Cities and Society*, 26, 318–343. <https://doi.org/10.1016/j.scs.2016.07.005>
- Salata, F., Golasi, I., Petitti, D., de Lieto Vollaro, E., Coppi, M., & de Lieto Vollaro, A. (2017). Relating microclimate, human thermal comfort and health during heat waves: An analysis of heat island mitigation strategies through a case study in an urban outdoor environment. *Sustainable Cities and Society*, 30, 79–96. <https://doi.org/10.1016/J.SCS.2017.01.006>

- Salmond, J. A., Williams, D. E., Laing, G., Kingham, S., Dirks, K., Longley, I., & Henshaw, G. S. (2013). The influence of vegetation on the horizontal and vertical distribution of pollutants in a street canyon. *Science of The Total Environment*, 443, 287–298. <https://doi.org/10.1016/J.SCITOTENV.2012.10.101>
- Sanborn, E. (2017). Integrating climate sensitive design principles in municipal processes: A case study of Edmonton's winter patios. <https://www.diva-portal.org/smash/record.jsf?pid=diva2:1150414>
- Santamouris, M., & Asimakopoulos, D. (1996). *Passive cooling of buildings*.
- Schaefer, M., Ebrahimi Salari, H., Köckler, H., & Thinh, N. X. (2021). Assessing local heat stress and air quality with the use of remote sensing and pedestrian perception in urban microclimate simulations. *Science of The Total Environment*, 794, 148709. <https://doi.org/10.1016/J.SCITOTENV.2021.148709>
- Seposo, X., Kondo, M., Ueda, K., Honda, Y., Michikawa, T., Yamazaki, S., & Nitta, H. (2018). Health impact assessment of PM_{2.5}-related mitigation scenarios using local risk coefficient estimates in 9 Japanese cities. *Environment International*, 120, 525–534. <https://doi.org/10.1016/J.ENVINT.2018.08.037>
- Shahidan, M. F., Jones, P. J., Gwilliam, J., & Salleh, E. (2012). An evaluation of outdoor and building environment cooling achieved through combination modification of trees with ground materials. *Building and Environment*, 58, 245–257. <https://doi.org/10.1016/j.buildenv.2012.07.012>
- Shinichi, S. (2021). *Strength of Japan's TOD*. Ministry of Land, Infrastructure, Transport and Tourism (MLIT). <https://www.mlit.go.jp/common/001398605.pdf>
- Simon, H., Sinsel, T., & Bruse, M. (2020). Introduction of fractal-based tree digitalization and accurate in-Canopy radiation transfer modelling to the microclimate model ENVI-met. *Forests*, 11(8), 869. <https://doi.org/10.3390/F11080869>
- Sodoudi, S., Zhang, H., Chi, X., Müller, F., & Li, H. (2018). The influence of spatial configuration of green areas on microclimate and thermal comfort. *Urban Forestry & Urban Greening*, 34, 85–96. <https://doi.org/10.1016/J.UFUG.2018.06.002>
- Spangenberg, J., Shinzato, P., Johansson, E., & Duarte, D. (2008). Simualtion of the infuence of vegetation on microclimate and thermal comfort in the city of SÃO PAULO. *Revista Da Sociedade Brasileira de Arborização Urbana*, 3(2), 1–19. <https://doi.org/10.5380/REVSBAU.V3I2.66265>
- Srivanit, M., & Hokao, K. (2013). Evaluating the cooling effects of greening for improving the outdoor thermal environment at an institutional campus in the summer. *Building and Environment*, 66, 158–172. <https://doi.org/10.1016/J.BUILDENV.2013.04.012>
- Starke, B., & Simonds, J. (2013). *Landscape architecture: a manual of environmental planning and design*. <https://library.wur.nl/WebQuery/titel/2057233>
- Stocco, S., Cantón, M. A., & Correa, E. (2021). Evaluation of design schemes for urban squares in arid climate cities, Mendoza, Argentina. *Building Simulation*, 14(3), 763–777. <https://doi.org/10.1007/s12273-020-0691-5>
- Stocco, S., Cantón, M. A., & Correa, E. N. (2015). Design of urban green square in dry areas: Thermal performance and comfort. *Urban Forestry & Urban Greening*, 14(2), 323–335. <https://doi.org/10.1016/J.UFUG.2015.03.001>
- Stojanovski, T., & Axelsson, Ö. (2019). *Typo-morphology and environmental perception of urban space*. <http://elib.sfu-kras.ru/handle/2311/111758>
- T. Kidokoro. (2019). Transit-oriented pevelopment policies and station area development in Asian cities. <http://119.78.100.173/C666/handle/2XK7JSWQ/237614>
- Taleghani, M., Clark, A., Swan, W., & Mohegh, A. (2020). Air pollution in a microclimate; the impact of different green barriers on the dispersion. *Science of The Total Environment*, 711, 134649. <https://doi.org/10.1016/J.SCITOTENV.2019.134649>

- Tan, Z., Lau, K. K. L., & Ng, E. (2016). Urban tree design approaches for mitigating daytime urban heat island effects in a high-density urban environment. *Energy and Buildings*, 114, 265–274. <https://doi.org/10.1016/J.ENBUILD.2015.06.031>
- Taylor, L., & Hochuli, D. F. (2017). Defining greenspace: Multiple uses across multiple disciplines. *Landscape and Urban Planning*, 158, 25–38. <https://doi.org/10.1016/J.LANDURBPLAN.2016.09.024>
- Thorsson, S., Honjo, T., Lindberg, F., Eliasson, I., & Lim, E.-M. (2007). Thermal comfort and outdoor activity in Japanese urban public places. *Environment and Behavior*, 39(5), 660–684. <https://doi.org/10.1177/0013916506294937>
- Transport and Environment in Japan. (2019). In *Eco-Mo Foundation*. <http://www.ecomo.or.jp/english/tej.html>
- Tsoka, S., Tsikaloudaki, A., & Theodosiou, T. (2018). Analyzing the ENVI-met microclimate model's performance and assessing cool materials and urban vegetation applications—A review. In *Sustainable Cities and Society*, 43, 55–76. Elsevier Ltd. <https://doi.org/10.1016/j.scs.2018.08.009>
- Tumini, I. (2015). The urban microclimate in open space. Case studies in Madrid. *Cuadernos de Investigación Urbanística*, 96. <https://doi.org/10.20868/CIUR.2014.96.3022>
- Willmott C.J. (1982). Some comments on the evaluation of model performance. *Bulletin of the American Meteorological Society*, 63(11), 1309–1313. [https://doi.org/https://doi.org/10.1175/1520-0477\(1982\)063<1309:SCOTEO>2.0.CO;2](https://doi.org/https://doi.org/10.1175/1520-0477(1982)063<1309:SCOTEO>2.0.CO;2)
- Wu, J., Luo, K., Wang, Y., & Wang, Z. (2021). Urban road greenbelt configuration: The perspective of PM_{2.5} removal and air quality regulation. *Environment International*, 157, 106786. <https://doi.org/10.1016/J.ENVINT.2021.106786>
- Xiao, J., & Yuizono, T. (2022). Climate-adaptive landscape design: Microclimate and thermal comfort regulation of station square in the Hokuriku Region, Japan. *Building and Environment*, 212, 108813. <https://doi.org/10.1016/J.BUILDENV.2022.108813>
- Xie, C., Guo, J., Yan, L., Jiang, R., Liang, A., & Che, S. (2022). The influence of plant morphological structure characteristics on PM_{2.5} retention of leaves under different wind speeds. *Urban Forestry & Urban Greening*, 71, 127556. <https://doi.org/10.1016/J.UFUG.2022.127556>
- Yang, J., & Shi, X. (2019). The centre of city: Thermal environment and spatial morphology. *Springer Verlag, Singapor*, 1–229. <https://doi.org/10.1007/978-981-13-9706-6>
- Yang, Yujin, Gatto, E., Gao, Z., Buccolieri, R., Morakinyo, T. E., & Lan, H. (2019). The “plant evaluation model” for the assessment of the impact of vegetation on outdoor microclimate in the urban environment. *Building and Environment*, 159, 106151. <https://doi.org/10.1016/J.BUILDENV.2019.05.029>
- Yang, Yujun, Zhou, D., Gao, W., Zhang, Z., Chen, W., & Peng, W. (2018). Simulation on the impacts of the street tree pattern on built summer thermal comfort in cold region of China. *Sustainable Cities and Society*, 37, 563–580. <https://doi.org/10.1016/J.SCS.2017.09.033>
- Zalakeviciute, R., López-Villada, J., & Rybarczyk, Y. (2018). Contrasted effects of relative humidity and precipitation on urban PM_{2.5} pollution in high elevation urban areas. *Sustainability*, 10(6), 2064. <https://doi.org/10.3390/SU10062064>
- Zeka, B. (2011). The humanistic meaning of urban squares: the case of çayyolu urban square project. In *Middle East Technical University*. <https://open.metu.edu.tr/handle/11511/20466>
- Zhang, A., Bokel, R., van den Dobbelssteen, A., Sun, Y., Huang, Q., & Zhang, Q. (2017a). An integrated school and schoolyard design method for summer thermal comfort and energy efficiency in Northern China. *Building and Environment*, 124, 369–387. <https://doi.org/10.1016/j.buildenv.2017.08.024>

- Zhang, K., Dong, X., Liu, Z., Gao, W., Hu, Z., & Wu, G. (2019). Quantifying the effects of urban form on land surface temperature in subtropical high-density urban areas using machine learning. *Remote Sensing* 2019, Vol. 11, Page 959, 11(8), 959. <https://doi.org/10.3390/RS11080959>
- Zhang, L., Zhan, Q., & Lan, Y. (2018). Effects of the tree distribution and species on outdoor environment conditions in a hot summer and cold winter zone: A case study in Wuhan residential quarters. *Building and Environment*, 130, 27–39. <https://doi.org/10.1016/J.BUILDENV.2017.12.014>
- Zheng, S., Zhao, L., & Li, Q. (2016). Numerical simulation of the impact of different vegetation species on the outdoor thermal environment. *Urban Forestry and Urban Greening*, 18, 138–150. <https://doi.org/10.1016/j.ufug.2016.05.008>
- Zhong, J., Cai, X. M., & Bloss, W. J. (2016). Coupling dynamics and chemistry in the air pollution modelling of street canyons: A review. *Environmental Pollution*, 214, 690–704. <https://doi.org/10.1016/J.ENVPOL.2016.04.052>
- Zhongming, Z., Linong, L., Xiaona, Y., Wangqiang, Z., & Wei, L. (2019). *Landmark United in Science Report Informs Climate Action Summit*. <http://resp.llas.ac.cn/C666/handle/2XK7JSWQ/217616>
- Zölch, T., Rahman, M. A., Pfleiderer, E., Wagner, G., & Pauleit, S. (2019). Designing public squares with green infrastructure to optimize human thermal comfort. *Building and Environment*, 149, 640–654. <https://doi.org/10.1016/j.buildenv.2018.12.051>

Publication

Papers Published and Submitted in Journals

Xiao, J., & Yuizono, T. (2022). Climate-adaptive landscape design: Microclimate and Thermal Comfort Regulation of Station Square in the Hokuriku Region, Japan. *Building and Environment*, 212, 108813.

DOI: <https://doi.org/10.1016/j.buildenv.2022.108813>

This journal paper is the main content of Chapter 4 of my doctoral thesis.

Xiao, J., & Yuizono, T. (2022). Integrated Effects of Building Morphology and Green Space Configuration on Thermal Environment and Air Quality in a Station Square. *Sustainable Cities and Society*. (Submission)

This journal paper is the main content of Chapter 5 in my doctoral thesis.

International Conference Proceeding

Xiao, J., Yuizono, T., & Gokon, H. (2021, December). Numerical Simulation of Winter Microclimate and Thermal Comfort of an Asymmetric Canyon in the Urban Square Area. In 2021 5th International Conference on Vision, Image and Signal Processing (ICVISIP) (pp. 201-205). IEEE.

DOI: <https://doi.org/10.1109/ICVISIP54630.2021.00044>

Xiao, J., Yuizono (2022, July). Impact of Microclimate Landscape Design Updates on Thermal Comfort in a Community Park. 5th International Conference on Building Energy and Environment, 25th-29th July 2022 | Concordia University. (Acceptance)